

# Supporting Information

## Lignocellulose Conversion via Catalytic Transformations Yields Methoxyterephthalic Acid directly from Sawdust

Simon S. Pedersen<sup>a</sup>, Gabriel M. F. Batista<sup>a</sup>, Martin L. Henriksen<sup>b</sup>, Hans Christian D. Hammershøj<sup>a</sup>, Kathrin H. Hopmann<sup>c</sup>, and Troels Skrydstrup<sup>a\*</sup>

<sup>a</sup>Carbon Dioxide Activation Center (CADIAC), Interdisciplinary Nanoscience Center, Department of Chemistry, Aarhus University; Gustav Wieds Vej 14, 8000 Aarhus C, Denmark.

<sup>b</sup>Department of Biological and Chemical Engineering, Aarhus University; Aabogade 40, 8200 Aarhus N, Denmark.

<sup>c</sup>Department of Chemistry, UiT - The Arctic University of Norway, N-9037 Tromsø, Norway.

\*Email: ts@chem.au.dk

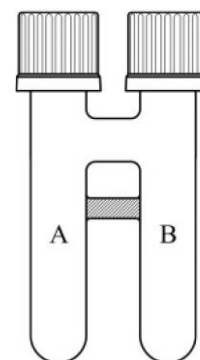
### Table of Contents

<b>General Information</b>	<b>S2</b>
<b>Setup for high-pressure reactions with H<sub>2</sub> or O<sub>2</sub></b>	<b>S3</b>
<b>Synthesis of Aryl Fluorosulfates</b>	<b>S4</b>
<b>Optimizations</b>	<b>S6</b>
<b>Lignin Content Determination</b>	<b>S9</b>
<b>General Procedures</b>	<b>S11</b>
<b>Synthesis of Aryl Nitriles</b>	<b>S12</b>
<b>Synthesis of Methoxyterephthalic Acid</b>	<b>S16</b>
<b>Polymerization of MTA with Ethylene Glycol</b>	<b>S18</b>
<b>Mechanistic Investigations (Experimental and DFT studies)</b>	<b>S20</b>
<b>X-ray crystallography</b>	<b>S34</b>
<b>References</b>	<b>S37</b>
<b>NMR Spectra</b>	<b>S39</b>

## General Information

**General Methods:** All purchased chemicals were used as received without further purification. Autoclaves were pressurized using a 5000 Multi Reactor System (Parr®) or a Berghof® BR-300 autoclave using hydrogen or oxygen (both 99.999% purity) from Air Liquide. The pressure vessels were heated in aluminum blocks specially designed to fit the vessels. Lignocellulose samples were obtained from a private local supplier near Aarhus, Denmark, and filtered coarsely then dried o/n in an oven at 120 °C before reactions. When necessary, solvents were dried according to standard procedures and degassed by bubbling with argon for minimum 30 minutes. Flash column chromatography was carried out on silica gel 60 (230-400 mesh). The <sup>1</sup>H-NMR spectra were recorded at 400 MHz, <sup>13</sup>C-NMR spectra were recorded at 101 MHz, <sup>19</sup>F-NMR spectra were recorded at 377 MHz, and <sup>31</sup>P-NMR were recorded at 162 MHz on a Bruker 400 spectrometer. The chemical shifts are reported in ppm, of which <sup>1</sup>H- and <sup>13</sup>C-NMR are reported relative to solvent residual peak. Coupling patterns in the NMR spectra are abbreviated as follows: s = singlet, d = doublet, t = triplet, q = quartet, quint = quintuplet, sext = sextet, sep = septet, m = multiplet, br = broad, dd = double doublet, dt = double triplet, ddd = double double doublet. NMR spectra are reported as follows: (multiplicity; coupling constant(s) in Hz; integration). HRMS spectra were recorded on a LC TOF (ES) apparatus. GC experiments were conducted using an Agilent 8890 GC System (Column: HP-5 5% Phenyl methyl siloxane, 30 m x 250 μm x 0.25 μm). Calibration curves for the quantification of phenol products was done with the use of dodecane as an internal standard.

**Handling of HCN and Sulfuryl Fluoride:** All reactions with HCN or Sulfuryl Fluoride were performed in a two-chamber system, in which gaseous HCN or SO<sub>2</sub>F<sub>2</sub> was released in chamber A and utilized in chamber B. The two-chamber system (COWare®) is depicted to the right and is composed of two glass vials (Chamber A and B) connected with a glass tube to allow gas-transfer (Total Volume = 20 mL.). Large scale reactions were conducted with an identical but larger two-chamber system (Total Volume = 210 mL). The chambers can be sealed with a screw cap and a Teflon® coated silicone seal. HCN gas was released from KCN in ethylene glycol diethyl ether with AcOH at rt,<sup>1</sup> while SO<sub>2</sub>F<sub>2</sub> gas was released from 1,1'-sulfonylbis(1*H*-imidazole) (SDI) and KF in TFA at rt.<sup>2</sup> Precise conditions are given in the general procedures.



**WARNING:** Glassware under pressure!

- Glass equipment should always be examined for damages to its surface, which may weaken its strength.
- One must abide to all laboratory safety procedures and always work behind a shield when working with glass equipment under pressure.
- COWare is pressure tested to 224 psi (15.4 bar) but should under no circumstances be operated above 60 psi (5 bar).

**Differential Scanning Calorimetry:** Differential Scanning Calorimetry (DSC) were obtained under nitrogen atmosphere in a DSC 8500 (PerkinElmer, USA) controlled by Pyris (v. 11.1.0.0488, PerkinElmer, USA). 5-10 mg sample are sealed (Universal Crimper Press, PerkinElmer, USA) into aluminum pans (Pans and covers type: 02190041) prior to measurement. All samples are run through the following program. 1) Heating from 20.0 °C to 300.0 °C at 10.0 °C min<sup>-1</sup>, 2) Cooling from 300.0 °C to 20.0 °C at 60.0 °C min<sup>-1</sup>, 3) Heating from 20.0 °C to 300.0 °C at 10.0 °C min<sup>-1</sup>, 4) Cooling from 300.0 °C to 0.0 °C at 60.0 °C min<sup>-1</sup>, 5) Holding for 1.0 min at 0.0 °C, 6) StepScan of step size 1.0 °C from 0.0 to 300.0 °C at 5.0 °C min<sup>-1</sup>. The reported *T<sub>g</sub>* is based on the Half CP method, *T<sub>m</sub>* is the peak maximum of the calculated specific heat based on the StepScan. When conducting DSC-analysis of a sample multiple times, the error was found to be ± 1.0 °C.

**Thermogravimetric Analysis:** Thermogravimetric Analysis (TGA) was obtained under nitrogen atmosphere in a TG 209 F1 Libra (Netzsch, GE). 5-10 mg samples are heated at  $10\text{ }^{\circ}\text{C min}^{-1}$  from  $35\text{ }^{\circ}\text{C}$  to  $500\text{ }^{\circ}\text{C}$ . The 5% mass loss temperature ( $T_{5\%}$ ) and the degradation temperature ( $T_d$ ) is reported. The derivative is found via a Savitzky-Golay filter (25 points average, 2<sup>nd</sup> order, 1<sup>st</sup> derivative) and the  $T_d$  is found as the derivative's apex. When conducting TGA-analysis of a sample multiple times, the error was found to be  $\pm 1.7\text{ }^{\circ}\text{C}$ .

**Fourier Transformed Infrared Spectroscopy:** Fourier Transformed Infrared Spectroscopy (FT-IR) of the samples were collected in an Attenuated Total Reflection (ATR) mode on an iS5 spectrophotometer (Thermo Fisher Scientific, USA) fitted with a ZnSe crystal (iD5, Thermo Fisher Scientific, USA). Background (n =16) and sample measurement (n =16) was measured with a resolution of  $2\text{ cm}^{-1}$ .

### Setup for high-pressure reactions with $\text{H}_2$ or $\text{O}_2$



**Figure S1.** Small-scale autoclave setup. Left picture, the assembled Parr® autoclave and the on-site made heating block. Right picture, a PTFE inlay (30 mL max.), the disassembled autoclave and the heating block.

All small-scale high pressure hydrogenolysis reactions with  $\text{H}_2$  (1 g of sawdust) and oxidation reactions with  $\text{O}_2$  were setup as depicted in Fig. S1 using a stir bar within the PTFE inlay. Special care must be taken to avoid risk of explosion, and a thorough examination of the equipment manual is advisable. Special precautions must be taken in the case of high-pressure oxidation reactions with  $\text{O}_2$ .

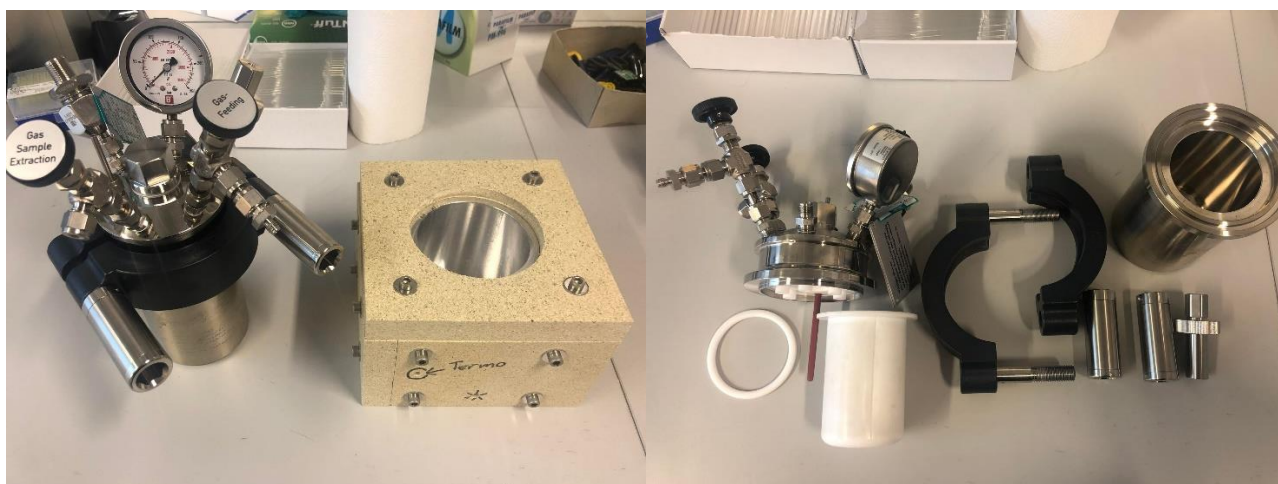
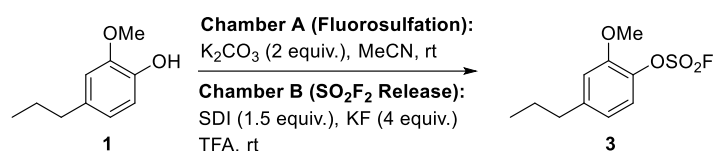


**Figure S2.** Large-scale autoclave setup. Left picture, the assembled Berghof® autoclave and the on-site made heating block. Right picture, a PTFE inlay (310 mL max.) and the disassembled autoclave.

All large-scale high pressure hydrogenolysis reactions with H<sub>2</sub> (20 g of sawdust) were setup as depicted in Fig. S2 using a stir bar within the PTFE inlay. Special care must be taken to avoid risk of explosion, and a thorough examination of the equipment manual is advisable.

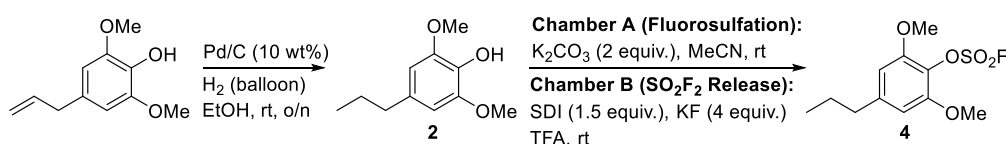
## Synthesis of Aryl Fluorosulfates

### 2-methoxy-4-propylphenyl sulfurofluoridate



To chamber A of a two-chamber reactor (210 mL total volume) was added 2-methoxy-4-propylphenol (1.6 mL, 10 mmol), K<sub>2</sub>CO<sub>3</sub> (2.77 g, 20.0 mmol, 2.0 equiv.) and MeCN (40 mL). The chamber was sealed with a screwcap fitted with a Teflon<sup>®</sup>-coated silicone seal. To chamber B of the two-chamber reactor was added 1,1'-sulfonylbis(1*H*-imidazole) (2.98 g, 15.0 mmol, 1.5 equiv.) and KF (2.33 g, 40.1 mmol, 4.0 equiv.). The chamber was sealed with a screwcap fitted with a pierceable Teflon<sup>®</sup>-coated silicone seal. Trifluoroacetic acid (20 mL) was then added to the closed chamber B *via* the pierceable Teflon<sup>®</sup>-coated silicone seal and sulfuryl fluoride release was observed within a minute. The reactor was stirred at room temperature for 16 hours, after which the reaction mixture was concentrated *in vacuo*, and then passed through a short silica dry column (5 cm silica) with CH<sub>2</sub>Cl<sub>2</sub>. Concentration *in vacuo*, yielded the product as a colorless liquid (2.43 g, 98%). <sup>1</sup>H-NMR (400 MHz, CDCl<sub>3</sub>) δ<sub>H</sub> (ppm) 7.20 (d, *J* = 8.3 Hz, 1H), 6.85 (d, *J* = 1.7 Hz, 1H), 6.79 (dd, *J*<sub>1</sub> = 8.3 Hz, *J*<sub>2</sub> = 1.9 Hz, 1H), 3.90 (s, 3H), 2.60 (t, *J* = 7.5 Hz, 2H), 1.65 (sext, *J* = 7.4 Hz, 2H), 0.96 (t, *J* = 7.3 Hz, 3H). <sup>13</sup>C-NMR (100 MHz, CDCl<sub>3</sub>) δ<sub>C</sub> (ppm) 150.9, 145.0, 137.2, 122.0, 120.8, 113.6, 56.2, 38.1, 24.6, 13.9. <sup>19</sup>F-NMR (376 MHz, CDCl<sub>3</sub>) δ<sub>F</sub> (ppm) -39.2. HRMS C<sub>10</sub>H<sub>14</sub>FO<sub>4</sub>S<sup>+</sup> [*M* + H<sup>+</sup>]: calcd 249.0591, found 249.0585.

### 2,6-dimethoxy-4-propylphenyl sulfurofluoridate

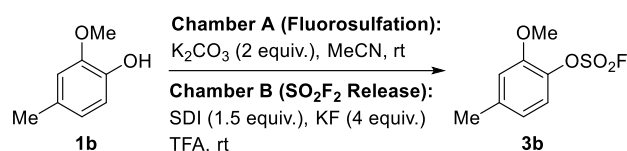


**Step 1 (Hydrogenation):** 4-allyl-2,6-dimethoxyphenol (1.8 mL, 10 mmol) and Pd/C (10 wt%, 106 mg) in EtOH (50 mL) was purged with H<sub>2</sub> and thereafter fitted with a balloon of H<sub>2</sub>. The reaction was stirred o/n, then filtered through celite to obtain the product as a black oil (1.96 g, 100%). <sup>1</sup>H-NMR (400 MHz, CDCl<sub>3</sub>) δ<sub>H</sub> (ppm) 6.40 (s, 2H), 5.35 (s, 1H), 3.88 (s, 6H), 2.51 (t, *J* = 7.5 Hz, 2H), 1.62 (sext, *J* = 7.4 Hz, 2H), 0.94 (t, *J* = 7.3 Hz, 3H). <sup>13</sup>C-NMR (100 MHz, CDCl<sub>3</sub>) δ<sub>C</sub> (ppm) 146.9 (2C), 133.9, 132.7, 105.0 (2C), 56.3 (2C), 38.3, 24.9, 13.9. HRMS C<sub>11</sub>H<sub>17</sub>O<sub>3</sub><sup>+</sup> [*M* + H<sup>+</sup>]: calcd 197.1172, found 197.1169.

**Step 2 (Fluorosulfation):** To chamber A of a two-chamber reactor (210 mL total volume) was added 2,6-dimethoxy-4-propylphenol (1.96 g, 10.0 mmol), K<sub>2</sub>CO<sub>3</sub> (2.77 g, 20.0 mmol, 2.0 equiv.) and MeCN (40 mL). The chamber was sealed with a screwcap fitted with a Teflon<sup>®</sup>-coated silicone seal. To chamber B of the two-chamber reactor was added 1,1'-sulfonylbis(1*H*-imidazole) (2.98 g, 15.0 mmol, 1.5 equiv.) and KF (2.33 g, 40.1 mmol, 4.0 equiv.). The chamber was sealed with a screwcap fitted with a pierceable Teflon<sup>®</sup>-coated silicone seal. Trifluoroacetic acid (20 mL) was then added to the closed chamber B *via* the pierceable Teflon<sup>®</sup>-coated silicone seal and sulfuryl fluoride release was observed within a minute. The reactor was stirred at room

temperature for 16 hours, after which the reaction mixture was concentrated *in vacuo*, and then passed through a short silica dry column (5 cm silica) with CH<sub>2</sub>Cl<sub>2</sub>. Concentration *in vacuo*, yielded the product as a white solid (2.71 g, 97%). <sup>1</sup>H-NMR (400 MHz, CDCl<sub>3</sub>) δ<sub>H</sub> (ppm) 6.43 (s, 2H), 3.88 (s, 3H), 2.56 (t, *J* = 7.6 Hz, 2H), 1.65 (sext, *J* = 7.4 Hz, 2H), 0.96 (t, *J* = 7.3 Hz, 3H). <sup>13</sup>C-NMR (100 MHz, CDCl<sub>3</sub>) δ<sub>C</sub> (ppm) 152.2, 144.4, 105.1 (4C), 56.4 (2C), 38.8, 24.6, 14.0. <sup>19</sup>F-NMR (376 MHz, CDCl<sub>3</sub>) δ<sub>F</sub> (ppm) -42.1. HRMS C<sub>11</sub>H<sub>16</sub>FO<sub>5</sub>S<sup>+</sup> [M + H<sup>+</sup>]: calcd 279.0697, found 279.0690.

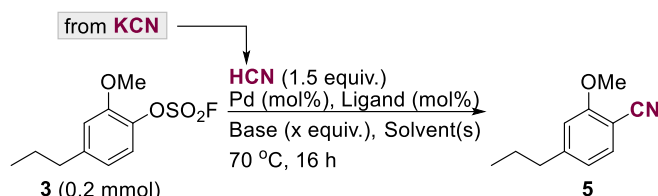
### 2-methoxy-4-methylphenyl sulfurofluoridate (3b)



To chamber A of a two-chamber reactor (210 mL total volume) was added 2-methoxy-4-methylphenol (691 mg, 5.00 mmol), K<sub>2</sub>CO<sub>3</sub> (1.38 g, 10.0 mmol, 2.0 equiv.) and MeCN (20 mL). The chamber was sealed with a screwcap fitted with a Teflon<sup>®</sup>-coated silicone seal. To chamber B of the two-chamber reactor was added 1,1'-sulfonylbis(1*H*-imidazole) (1.49 g, 7.50 mmol, 1.5 equiv.) and KF (1.16 g, 20.0 mmol, 4.0 equiv.). The chamber was sealed with a screwcap fitted with a pierceable Teflon<sup>®</sup>-coated silicone seal. Trifluoroacetic acid (10 mL) was then added to the closed chamber B *via* the pierceable Teflon<sup>®</sup>-coated silicone seal and sulfonyl fluoride release was observed within a minute. The reactor was stirred at room temperature for 16 hours, after which the reaction mixture was concentrated *in vacuo*, and then passed through a short silica dry column (5 cm silica) with CH<sub>2</sub>Cl<sub>2</sub>. Concentration *in vacuo*, yielded the product as a colorless liquid (991 mg, 90%). <sup>1</sup>H NMR (400 MHz, CDCl<sub>3</sub>) δ<sub>H</sub> (ppm) 7.18 (dd, *J* = 8.3, 1.4 Hz, 1H), 6.85 (m, 1H), 6.78 (m, 1H), 3.89 (s, 3H), 2.38 (s, 3H). <sup>13</sup>C NMR (101 MHz, CDCl<sub>3</sub>) δ<sub>H</sub> (ppm) 150.8, 140.2, 137.1, 137.1, 122.0, 121.4, 114.2, 56.2, 21.7. <sup>19</sup>F-NMR (376 MHz, CDCl<sub>3</sub>) δ<sub>F</sub> (ppm) -39.2.

## Optimization of the Palladium-Catalyzed Cyanation of Aryl Fluorosulfates

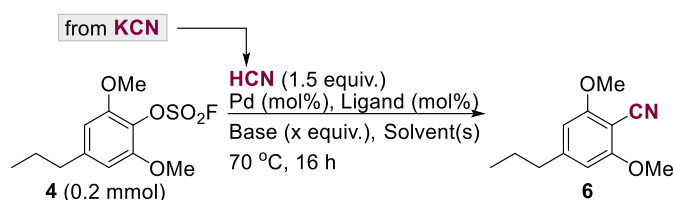
**General procedure for the cyanation optimization with 2-methoxy-4-propylphenyl sulfurofluoridate **3** and HCN:** In a glovebox, the specified reagents and solvent(s) were added to chamber A of a two-chamber system. The chamber was sealed with a screwcap fitted with a Teflon<sup>®</sup>-coated silicone seal. To chamber B of a two-chamber system was added KCN (1.5 equiv.), ethylene glycol diethyl ether (0.5 mL) and AcOH (9.0 equiv.) (**Beware! The AcOH must be added slowly on top of the glycol solvent, otherwise HCN release will occur before the chamber is sealed**). The chamber was sealed with a screwcap fitted with a Teflon<sup>®</sup>-coated silicone seal and then stirred at rt, while chamber A was stirred at 70 °C. The reaction was conducted for 16 hours in a well-ventilated fume-hood and upon completion, the two-chamber system was opened and left stirring for 20-30 min under good ventilation. The reaction mixture was then passed through celite and concentrated *in vacuo*. <sup>1</sup>H-NMR yields were obtained using 1,3,5-trimethoxybenzene as an internal standard. Purification by flash column chromatography (Pentane to Pentane/EtOAc 95:5) yielded 2-methoxy-4-propylbenzonitrile **5** as a colorless liquid. <sup>1</sup>H-NMR (400 MHz, CDCl<sub>3</sub>) δ<sub>H</sub> (ppm) 7.44 (d, *J* = 7.8 Hz, 1H), 6.81 (dd, *J*<sub>1</sub> = 7.8 Hz, *J*<sub>2</sub> = 1.3 Hz, 1H), 6.76 (s, 1H), 3.91 (s, 3H), 2.61 (t, *J* = 7.5 Hz, 2H), 1.65 (sext, *J* = 7.4 Hz, 2H), 0.94 (t, *J* = 7.3 Hz, 3H). <sup>13</sup>C-NMR (100 MHz, CDCl<sub>3</sub>) δ<sub>C</sub> (ppm) 161.4, 150.6, 133.5, 121.1, 117.0, 111.5, 99.1, 56.0, 38.7, 24.2, 13.8. HRMS C<sub>11</sub>H<sub>14</sub>NO<sup>+</sup> [*M* + *H*<sup>+</sup>]: calcd 176.1070, found 176.1082.



Entry	Pd (mol%) / Ligand (mol%)	Base (equiv.)	Solvent(s) (x mL)	T (°C)	Conv. (%) (HNMR)
1	Pd(OAc) <sub>2</sub> (5), dppp (5)	NEt <sub>3</sub> (2.0)	PhMe (1 mL)	70	0
2	Pd(OAc) <sub>2</sub> (5), Xantphos (5)	NEt <sub>3</sub> (2.0)	PhMe (1 mL)	70	25
3	Pd(OAc) <sub>2</sub> (5), <i>rac</i> -BINAP (5)	NEt <sub>3</sub> (2.0)	PhMe (1 mL)	70	32
4	Pd(OAc) <sub>2</sub> (5), dppf (5)	NEt <sub>3</sub> (2.0)	PhMe (1 mL)	70	Traces
5	Pd(OAc) <sub>2</sub> (5), PPh <sub>3</sub> (10)	NEt <sub>3</sub> (2.0)	PhMe (1 mL)	70	32
6	Pd(OAc) <sub>2</sub> (5), PCy <sub>3</sub> (10)	NEt <sub>3</sub> (2.0)	PhMe (1 mL)	70	0
7	Pd(OAc) <sub>2</sub> (5), PtBu <sub>3</sub> (10)	NEt <sub>3</sub> (2.0)	PhMe (1 mL)	70	0
8	Pd(OAc) <sub>2</sub> (5), DPEPhos (5)	NEt <sub>3</sub> (2.0)	PhMe (1 mL)	70	79
9	PEPSI-Pd-IPr (5)	NEt <sub>3</sub> (2.0)	PhMe (1 mL)	70	0
10	DPEPhos-Pd-G4 (5)	NEt <sub>3</sub> (2.0)	PhMe (1 mL)	70	55
11	Pd(OAc) <sub>2</sub> (5), XPhos (5)	NEt <sub>3</sub> (2.0)	PhMe (1 mL)	70	99
12	Pd(OAc) <sub>2</sub> (5), XPhos (5)	NEt <sub>3</sub> (2.0)	PhMe/MeCN (1:1, 1 mL)	70	99
13	XPhos-Pd-G4 (5)	NEt <sub>3</sub> (2.0)	PhMe/MeCN (1:1, 1 mL)	70	99
14	XPhos-Pd-G4 (5)	NEt <sub>3</sub> (1.5)	PhMe/MeCN (1:1, 1 mL)	70	99
15	XPhos-Pd-G4 (2)	NEt <sub>3</sub> (2.0)	PhMe/MeCN (1:1, 1 mL)	70	99
16	Pd/C (5)	NEt <sub>3</sub> (2.0)	PhMe/MeCN (1:1, 1 mL)	70	0
17	XPhos-Pd-G4 (2)	K <sub>2</sub> CO <sub>3</sub> (2.0)	2-MeTHF/MeCN (1:1, 1 mL)	70	100 [98] <sup>a,b</sup>

**Table S1.** Optimization of the cyanation of 2-methoxy-4-propylphenyl sulfurofluoridate **3** using HCN as the cyanide source. <sup>a</sup>Yields given in brackets were isolated by flash column chromatography. <sup>b</sup>The reaction was conducted on a 0.4 mmol scale.

**General procedure for the cyanation optimization with 2,6-dimethoxy-4-propylphenyl sulfurofluoridate **4** and HCN:** In a glovebox, the specified reagents and solvent(s) were added to chamber A of a two-chamber system. The chamber was sealed with a screwcap fitted with a Teflon<sup>®</sup>-coated silicone seal. To chamber B of a two-chamber system was added KCN (1.5 equiv.), ethylene glycol diethyl ether (0.5 mL) and AcOH (9.0 equiv.) (**Beware! The AcOH must be added slowly on top of the glycol solvent, otherwise HCN release will occur before the chamber is sealed**). The chamber was sealed with a screwcap fitted with a Teflon<sup>®</sup>-coated silicone seal and then stirred at rt, while chamber A was stirred at 70 °C. The reaction was conducted for 16 hours in a well-ventilated fume-hood and upon completion, the two-chamber system was opened and left stirring for 20-30 min under good ventilation. The reaction mixture was then passed through celite and concentrated *in vacuo*. <sup>1</sup>H-NMR yields were obtained using 1,3,5-trimethoxybenzene as an internal standard. Purification by flash column chromatography (Pentane/EtOAc 95:5 to 80:20) yielded 2,6-dimethoxy-4-propylbenzonitrile **6** as a white crystalline solid. <sup>1</sup>H-NMR (400 MHz, CDCl<sub>3</sub>) δ<sub>H</sub> (ppm) 6.36 (s, 2H), 3.88 (s, 6H), 2.58 (t, *J* = 7.5 Hz, 2H), 1.65 (sext, *J* = 7.4 Hz, 2H), 0.95 (t, *J* = 7.3 Hz, 3H). <sup>13</sup>C-NMR (100 MHz, CDCl<sub>3</sub>) δ<sub>C</sub> (ppm) 162.6 (2C), 151.1, 114.6, 103.8 (2C), 88.9, 56.2 (2C), 39.3, 24.3, 13.9. HRMS C<sub>12</sub>H<sub>16</sub>NO<sub>2</sub><sup>+</sup> [*M* + H<sup>+</sup>]: calcd 206.1176, found 206.1177.

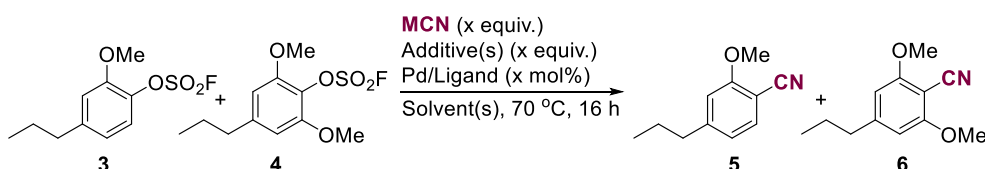


Entry	Pd (mol%) / Ligand (mol%)	Base (equiv.)	Solvent(s) (x mL)	T (°C)	Conv. (%) (HNMR)
1	XPhos-Pd-G4 (2)	NEt <sub>3</sub> (1.5)	PhMe/MeCN (1:1, 1 mL)	70	79
2	XPhos-Pd-G4 (2)	NEt <sub>3</sub> (1.5)	MeCN (1 mL)	70	61
3	XPhos-Pd-G4 (2), XPhos (4)	NEt <sub>3</sub> (1.5)	MeCN (1 mL)	70	65
4	<i>t</i> BuXPhos-Pd-G4 (5)	NEt <sub>3</sub> (1.5)	MeCN (1 mL)	70	17
5	Pd(OAc) <sub>2</sub> (5), SPhos (10)	NEt <sub>3</sub> (1.5)	MeCN (1 mL)	70	25
6	Pd(OAc) <sub>2</sub> (5), CyJohnPhos (10)	NEt <sub>3</sub> (1.5)	MeCN (1 mL)	70	0
7	Pd(OAc) <sub>2</sub> (5), JohnPhos (10)	NEt <sub>3</sub> (1.5)	MeCN (1 mL)	70	0
8	Pd(OAc) <sub>2</sub> (5), DavePhos (10)	NEt <sub>3</sub> (1.5)	MeCN (1 mL)	70	0
9	Pd(OAc) <sub>2</sub> (5), MePhos (10)	NEt <sub>3</sub> (1.5)	MeCN (1 mL)	70	0
10	Pd(OAc) <sub>2</sub> (5), RuPhos (10)	NEt <sub>3</sub> (1.5)	MeCN (1 mL)	70	7
11	Pd(OAc) <sub>2</sub> (5), BrettPhos (10)	NEt <sub>3</sub> (1.5)	MeCN (1 mL)	70	23
12	Pd(OAc) <sub>2</sub> (5), <i>t</i> BuBrettPhos (10)	NEt <sub>3</sub> (1.5)	MeCN (1 mL)	70	0
13	XPhos-Pd-G4 (2)	NEt <sub>3</sub> (1.5)	PrCN (1 mL)	90	74
14	XPhos-Pd-G4 (2)	TMG (1.5)	MeCN (1 mL)	70	0
15	XPhos-Pd-G4 (2)	NEt <sub>3</sub> (1.5)	MeCN/dioxane (1:1, 1 mL)	70	66
16	XPhos-Pd-G4 (2)	NEt <sub>3</sub> (1.5)	MeCN/CPME (1:1, 1 mL)	70	87
17	XPhos-Pd-G4 (2)	NEt <sub>3</sub> (1.5)	MeCN/2-MeTHF (1:1, 1 mL)	70	84
18	XPhos-Pd-G4 (2)	K <sub>2</sub> CO <sub>3</sub> (2.0)	MeCN (1 mL)	70	77
19	XPhos-Pd-G4 (2)	KOAc (2.0)	MeCN (1 mL)	70	54
20	XPhos-Pd-G4 (2)	K <sub>2</sub> HPO <sub>4</sub> (2.0)	MeCN (1 mL)	70	50
21	XPhos-Pd-G4 (2)	K <sub>3</sub> PO <sub>4</sub> (2.0)	MeCN (1 mL)	70	48
22	XPhos-Pd-G4 (2)	K <sub>2</sub> CO <sub>3</sub> (2.0)	MeCN/CPME (1:1, 1 mL)	70	100
23	XPhos-Pd-G4 (2)	K <sub>2</sub> CO <sub>3</sub> (2.0)	MeCN/2-MeTHF (1:1, 4 mL)	70	100 [96] <sup>a,b</sup>

24	XPhos-Pd-G4 (2)	K <sub>2</sub> CO <sub>3</sub> (2.0)	MeCN/2-MeTHF (1:1, 4 mL) (non-dried solvents)	70	61 <sup>b</sup>
25	XPhos-Pd-G4 (2)	K <sub>2</sub> CO <sub>3</sub> (2.0)	MeCN/2-MeTHF (1:1, 4 mL)	70	0 <sup>b,c</sup>
26	XPhos-Pd-G4 (2)	K <sub>2</sub> CO <sub>3</sub> (2.0)	2-MeTHF (4 mL)	70	0

**Table S2.** Optimization of the cyanation of 2,6-dimethoxy-4-propylphenyl sulfurofluoridate **3** using HCN as the cyanide source. <sup>a</sup>Yields given in brackets were isolated by flash column chromatography. <sup>b</sup>The reaction was conducted at a 0.4 mmol scale. <sup>c</sup>The reaction was set up and conducted under air.

**General procedure for the cyanation optimization with KCN using a 1:1 mixture of 2-methoxy-4-propylphenyl sulfurofluoridate **3** and 2,6-dimethoxy-4-propylphenyl sulfurofluoridate **4**:** In a glovebox, the specified reagents and solvent(s) were added to a pressure tube (9 mL total volume). The chamber was sealed with a screwcap fitted with a Teflon<sup>®</sup>-coated silicone seal and stirred at 70 °C for 16 hours. The reaction mixture was then passed through celite and concentrated *in vacuo*. <sup>1</sup>H-NMR yields were obtained using 1,3,5-trimethoxybenzene as an internal standard.



Entry	3, 4 or (3+4) (x mmol total)	Pd (mol%), Ligand (mol%)	KCN (equiv.)	Additives (equiv.)	Solvent(s) (x mL)	Conv. (%) (5/6) (HNMR)
1	4 - (0.4 mmol)	XPhos-Pd-G4 (2)	KCN (1.5)	K <sub>2</sub> CO <sub>3</sub> (2.0 equiv.)	MeCN/2-MeTHF (1:1, 4 mL)	99
2	4 - (0.4 mmol)	XPhos-Pd-G4 (2)	KCN (1.5)	K <sub>2</sub> CO <sub>3</sub> (0.04 equiv.)	MeCN/2-MeTHF (1:1, 4 mL)	99
3	4 - (0.4 mmol)	XPhos-Pd-G4 (2)	KCN (1.5)	-	MeCN/2-MeTHF (1:1, 4 mL)	99
4	3+4 (1:1) (0.4 mmol)	XPhos-Pd-G4 (2)	KCN (1.5)	-	MeCN/2-MeTHF (1:1, 4 mL)	94/98
5	3+4 (1:1) (0.4 mmol)	XPhos-Pd-G4 (2)	NaCN (1.5)	-	MeCN/2-MeTHF (1:1, 4 mL)	94/95
6	3+4 (1:1) (0.4 mmol)	XPhos-Pd-G4 (2)	KCN (3.0)	-	MeCN/2-MeTHF (1:1, 4 mL)	100/93
7	3+4 (1:1) (0.4 mmol)	XPhos-Pd-G4 (2)	KCN (6.0)	-	MeCN/2-MeTHF (1:1, 4 mL)	93/100
8	3+4 (1:1) (0.4 mmol)	XPhos-Pd-G4 (2)	KCN (1.5)	-	2-MeTHF (4 mL)	0/0
9	3+4 (1:1) (0.4 mmol)	XPhos-Pd-G4 (2)	KCN (1.5)	-	MeCN (4 mL)	7/0
10	3+4 (1:1) (0.4 mmol)	XPhos-Pd-G4 (1)	KCN (1.5)	-	MeCN/2-MeTHF (1:1, 4 mL)	100/100
11	3+4 (1:1) (0.4 mmol)	XPhos-Pd-G4 (0.5)	KCN (1.5)	-	MeCN/2-MeTHF (1:1, 4 mL)	99/72
12	3+4 (1:1) (0.4 mmol)	Pd(OAc) <sub>2</sub> (2) XPhos (4)	KCN (1.5)	-	MeCN/2-MeTHF (1:1, 4 mL)	100/51



13	3+4 (1:1) (0.4 mmol)	tBuXPhos-Pd-G4 (2)	KCN (1.5)	-	MeCN/2-MeTHF (1:1, 4 mL)	100/20
14	3+4 (1:1) (0.4 mmol)	XPhos-Pd-G4 (2)	KCN (1.5)	H <sub>2</sub> O (1 equiv.)	MeCN/2-MeTHF (1:1, 4 mL)	100/99
15	3+4 (1:1) (0.4 mmol)	XPhos-Pd-G4 (2)	KCN (1.5)	H <sub>2</sub> O (2 equiv.)	MeCN/2-MeTHF (1:1, 4 mL)	0/0
16	3+4 (1:1) (0.4 mmol)	XPhos-Pd-G4 (2)	KCN (1.5)	H <sub>2</sub> O (3 equiv.)	MeCN/2-MeTHF (1:1, 4 mL)	0/0
17	3+4 (1:1) (0.4 mmol)	XPhos-Pd-G4 (2)	KCN (1.5)	H <sub>2</sub> O (4 equiv.)	MeCN/2-MeTHF (1:1, 4 mL)	0/0
18	3+4 (1:1) (0.4 mmol)	XPhos-Pd-G4 (2)	KCN (1.5)	H <sub>2</sub> O (5 equiv.)	MeCN/2-MeTHF (1:1, 4 mL)	0/0
19	3+4 (1:1) (0.4 mmol)	XPhos-Pd-G4 (2)	KCN (1.5)	H <sub>2</sub> O (5 equiv.), K <sub>2</sub> CO <sub>3</sub> (3.0 equiv.)	MeCN/2-MeTHF (1:1, 4 mL)	100/99
20	3+4 (1:1) (0.4 mmol)	XPhos-Pd-G4 (2)	KCN (1.5)	H <sub>2</sub> O (5 equiv.), Na <sub>2</sub> SO <sub>4</sub> (3.0 equiv.)	MeCN/2-MeTHF (1:1, 4 mL)	0/0
21	3+4 (1:1) (0.4 mmol)	-	KCN (1.5)	-	MeCN/2-MeTHF (1:1, 4 mL)	0/0
22	3 (2 mmol)	XPhos-Pd-G4 (2)	KCN (1.5)	-	MeCN/2-MeTHF (1:1, 20 mL)	[99] <sup>a,b</sup>
23	3 (10 mmol)	XPhos-Pd-G4 (2)	KCN (1.5)	-	MeCN/2-MeTHF (1:1, 100 mL)	[96] <sup>a</sup>
24	3 (7.5 mmol)	XPhos-Pd-G4 (0.5)	KCN (1.5)	-	MeCN/2-MeTHF (1:1, 75 mL)	[98] <sup>c</sup>

**Table S3.** Optimization of the cyanation of 2-methoxy-4-propylphenyl sulfurofluoridate **3** and 2,6-dimethoxy-4-propylphenyl sulfurofluoridate **4** using KCN or NaCN as the cyanide source. <sup>a</sup>Yields given in brackets were isolated by flash column chromatography. <sup>b</sup>Was set up with a pressure tube (total volume = 50 mL). <sup>c</sup>Was set up with a pressure tube (total volume = 120 mL). <sup>d</sup>Was set up with a pressure tube (total volume = 250 mL).

## Determination of the Lignin Content in Lignocellulose Samples by the Klason

### Method<sup>3</sup>

The relevant sawdust was weighed out (2.5 g) into a cellulose thimble (22 x 80 mm) and was placed in a Soxhlet extraction setup that was allowed to extract overnight, using a Toluene/EtOH mixture (2:1, 150 mL) (See flow-chart, Fig. S3). Then, the extract was discarded, and the wet sawdust was allowed to dry for one day, covering the thimble with a perforated tin foil. The dried and extracted sawdust was then transferred to a pre-weighed beaker that was placed in an oven (120 °C) overnight. By evaluating the mass of the dried sawdust before and after Soxhlet extraction, the weight percentages of extractables can be found (see Table S4). The dried and extracted sawdust (1 g) was added aq. H<sub>2</sub>SO<sub>4</sub> (72%, 15 mL), and the slurry was stirred for 2 h at room temperature. Thereafter, the slurry was added to H<sub>2</sub>O (300 mL) in a 500 mL round-bottomed flask, and an additional H<sub>2</sub>O (60 mL) was used for rinsing the beaker, giving finally an aq. H<sub>2</sub>SO<sub>4</sub> concentration of 3%. The round bottomed flask was equipped with a condenser and a stir-bar, then refluxed for 4 h. The resulting slurry was filtered through a pre-weighed glass microfiber filter grade 691, and the filter, containing the Klason lignin, was afterwards dried o/n at 120 °C. The weight of the resulting dried Klason lignin can then be used to calculate lignin weight percentages for the individual sawdust samples (see Table S4).

Sample species

Extractables Average (% w/w)

Klason lignin Average (% w/w)

<b>Oak</b>	(2.2 ± 0.3)	(23 ± 0.7)
<b>Sycamore Maple</b>	(1.4 ± 0.4)	(28 ± 0.7)
<b>Hazel</b>	(1.4 ± 0.1)	(29 ± 1.5)
<b>Grandis fir</b>	(1.9 ± 0.4)	(36 ± 0.5)
<b>Birch</b>	(5.0 ± 0.2)	(25 ± 1.6)
<b>Noble fir</b>	(2.5 ± 0.1)	(34 ± 0.1)
<b>Willow</b>	(3.5 ± 0.4)	(24 ± 0.3)
<b>Spruce</b>	(0.8 ± 0.1)	(35 ± 0.1)

**Table S4.** Summary of the obtained results on extractables and Klason lignin wt% contents in each analyzed sample. Averages are obtained from triplicate results.

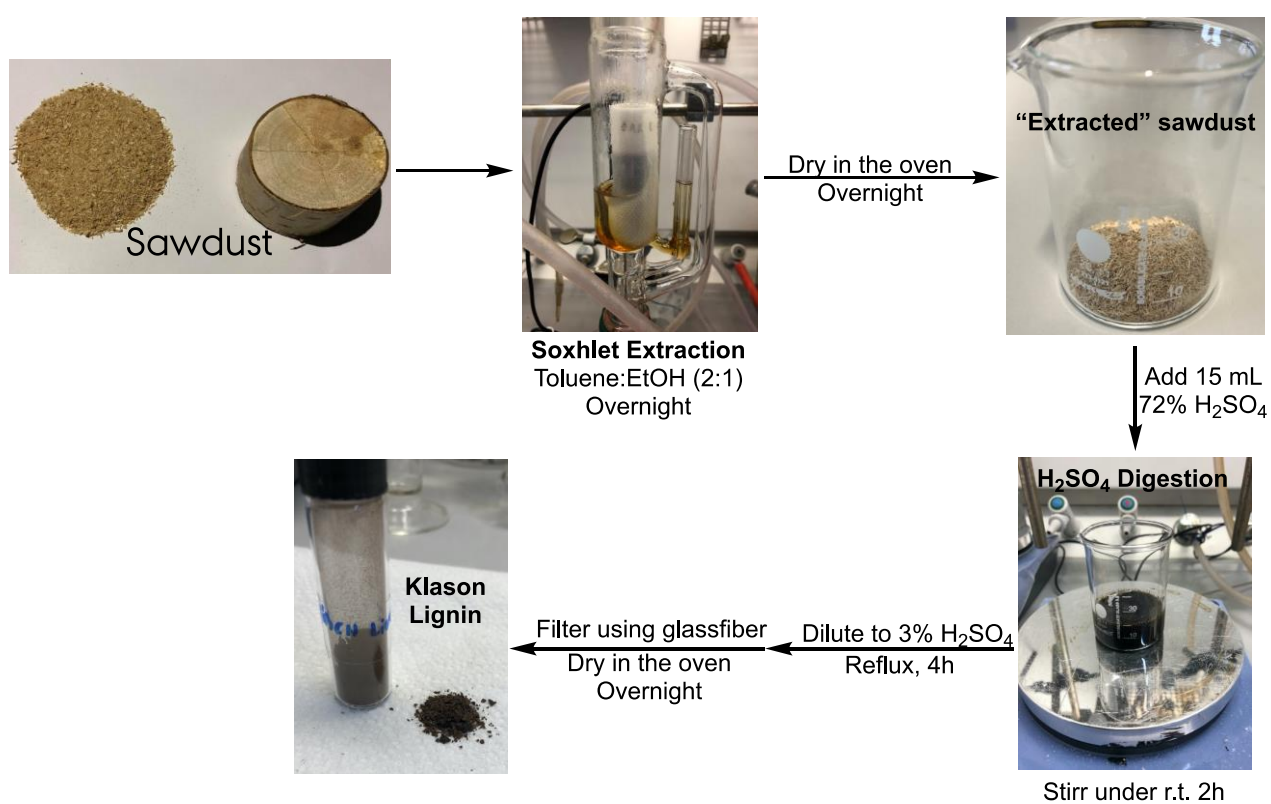


**Figure S3.** Flow-chart for the determination of Klason lignin percentages in sawdust samples.

## General Procedures

### General Procedure A for the three-step cyanation of lignocellulose samples (small-scale)

**Step I - Hydrogenolysis:** To each of two duplicate Parr autoclave reactors fitted with Teflon inlays (30 mL total volume) was added Ru/C (5 wt% Ru, 75 mg), the relevant lignocellulose sample (500 mg) and MeOH (10 mL). The reactors were closed, evacuated 5 times with H<sub>2</sub> and subjected to a H<sub>2</sub>-pressure of 30 bar at room temperature. The autoclaves were then stirred at 250 °C for 16 hours, and thereafter filtered through celite into a round-bottomed flask, rinsing with EtOAc, and concentrated *in vacuo*. The concentrate was added EtOAc (25 mL) and then sonicated for 5 min, added pentane (25 mL), whereafter the mixture was passed through a short silica dry column (5 cm silica), rinsing with EtOAc/Pentane (1:1, 50 mL) into a cone-shaped flask (100 mL). The concentrate was used in the subsequent step without further purification. The 2-methoxy-4-propylphenol and 2,6-dimethoxy-4-propylphenol products were quantified *via* GC-MS using dodecane as an internal standard, and their combined molar amount represents the scale for the subsequent reaction steps.

**Step II - Fluorosulfation:** To chamber A of a two-chamber reactor (20 mL total volume) was added K<sub>2</sub>CO<sub>3</sub> (3.0 equiv.) and the concentrate from step I, which was transferred with MeCN (4 x 1 mL). The chamber was sealed with a screwcap fitted with a Teflon<sup>®</sup>-coated silicone seal. To chamber B of the two-chamber reactor was added 1,1'-sulfonylbis(1*H*-imidazole) (3.0 equiv.) and KF (8.0 equiv.). The chamber was sealed with a screwcap fitted with a pierceable Teflon<sup>®</sup>-coated silicone seal. Trifluoroacetic acid (0.5 mL) was then added to the closed chamber B *via* the Teflon<sup>®</sup>-coated silicone seal and sulfonyl fluoride release was observed within a minute. The reactor was stirred at room temperature for 16 hours, after which the reaction mixture was passed through celite into a cone-shaped flask and concentrated *in vacuo*. The concentrate was used in the subsequent step without further purification.

**Step III - Cyanation:** In an argon glovebox, to a pressure tube (9 mL total volume) was added Pd-XPhos-G4 (5 mol%), K<sub>2</sub>CO<sub>3</sub> (3.0 equiv.), KCN (1.5 equiv.) and the concentrate from Step II, which was transferred with MeCN (2 x 1 mL) and 2-MeTHF (2 x 1 mL). The chamber was sealed with a screwcap fitted with a Teflon<sup>®</sup>-coated silicone seal and stirred at 70 °C for 16 hours. The reaction mixture was then evaporated onto celite and purified by flash column chromatography to yield the relevant nitrile product(s).

### General Procedure B for the three-step cyanation of lignocellulose samples (large scale)

**Step I - Hydrogenolysis:** To a Berghof autoclave reactor fitted with a Teflon inlay (310 mL total volume) was added Ru/C (5 wt% Ru, 3 g), the relevant lignocellulose sample (20 g) and MeOH (150 mL). The reactor was closed, purged with H<sub>2</sub> for 15 min and subjected to a H<sub>2</sub>-pressure of 30 bar at room temperature. The autoclave was then stirred at 230 °C for 16 hours, and thereafter filtered through celite into a round-bottomed flask, rinsing with EtOAc, and concentrated *in vacuo*. The concentrate was added EtOAc (100 mL) and then sonicated for 5 min, added pentane (100 mL), whereafter the mixture was passed through a short silica dry column (5 cm silica), rinsing with EtOAc/Pentane (1:1, 300 mL) into a round-bottomed flask (500 mL). The concentrate was used in the subsequent step without further purification. The 2-methoxy-4-propylphenol and 2,6-dimethoxy-4-propylphenol products were quantified *via* GC-MS using dodecane as an internal standard, and their combined molar amount represent the scale for the subsequent reactions.

**Step II - Fluorosulfation:** To chamber A of a two-chamber reactor was added K<sub>2</sub>CO<sub>3</sub> (3.0 equiv.) and the concentrate from step I, which was transferred with MeCN (4 x 5 mL). The chamber was sealed with a screwcap fitted with a Teflon<sup>®</sup>-coated silicone seal. To chamber B of the two-chamber reactor was added 1,1'-sulfonylbis(1*H*-imidazole) (3.0 equiv.) and KF (8.0 equiv.). The chamber was sealed with a screwcap fitted with a pierceable Teflon<sup>®</sup>-coated silicone seal. Trifluoroacetic acid (10 mL) was then added to the closed

chamber B *via* the pierceable Teflon<sup>®</sup>-coated silicone seal and sulfuryl fluoride release was observed within a minute. The reactor was stirred at room temperature for 16 hours, after which the reaction mixture was passed through celite into a cone-shaped flask and concentrated *in vacuo*. The concentrate was used in the subsequent step without further purification.

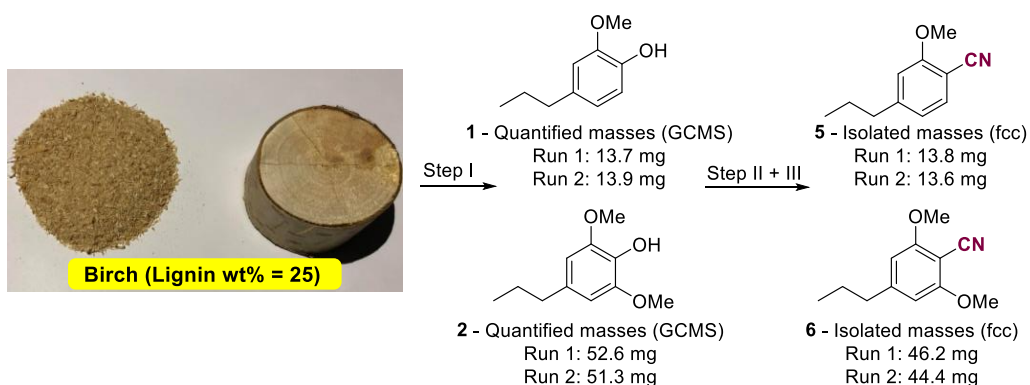
**Step III - Cyanation:** In an argon glovebox, to a pressure tube (120 mL total volume) was added Pd-XPhos-G4 (6.5 mol%), K<sub>2</sub>CO<sub>3</sub> (3.9 equiv.), KCN (2.0 equiv.) and the concentrate from Step II, which was transferred with MeCN (2 x 10.5 mL) and 2-MeTHF (2 x 10.5 mL). The chamber was sealed with a screwcap fitted with a Teflon<sup>®</sup>-coated silicone seal and stirred at 70 °C for 16 hours. The reaction mixture was then evaporated onto celite and purified by flash column chromatography to yield the relevant nitrile product(s).

## Synthesis of Aryl Nitriles from Lignocellulose Samples

In all cases, small amounts of 4-ethyl-2-methoxybenzonitrile and 4-ethyl-2,6-dimethoxybenzonitrile were found to co-elute when purifying the nitrile products **5** and **6** by flash column chromatography. Thus, all mass yields given for **5** and **6** in this section are corrected yields in order to account for the two co-eluting ethyl-substituted products. N.B. The masses of the phenol products **1** and **2** after step I were determined by GC-MS analysis and not weighed directly, thus an uncertainty can be expected with these numbers.

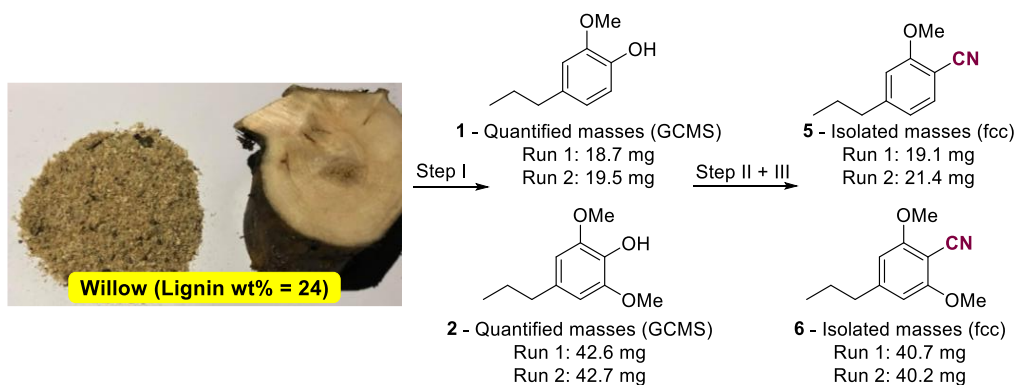
Two lignocellulose samples, namely Alder tree sawdust and sawdust from an unidentified white-painted piece of furniture were the only unsuccessful substrates with the General Procedure A. For these reactions, the phenol products **1** and **2** were observed after step 1, and full conversions to the corresponding aryl fluorosulfates **3** and **4** were also observed. The cyanation reaction step showed however no conversion of the aryl fluorosulfates, and we hypothesize that this could be due to catalyst deactivation either from the unknown additives that could be present in the furniture piece (including the white paint), or the high percentage of extractable compounds that were observed with the Alder tree species (6.3 ± 0.3 wt%). Isolation of the aryl fluorosulfates before the cyanation step is likely to be key for reactions such as these with unknown problematic additives or extractables.

### 2-methoxy-4-propylbenzonitrile **5** and 2,6-dimethoxy-4-propylbenzonitrile **6** from birch sawdust



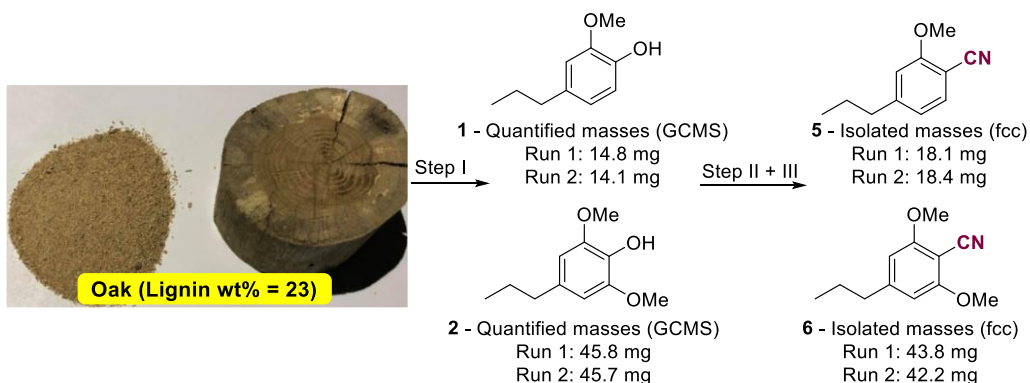
The title compounds were synthesized according to the General Procedure A. The quantified masses of 2-methoxy-4-propylphenol **1** and 2,6-dimethoxy-4-propylphenol **2** by GC-MS are given in the scheme above, and their combined molar amount sets the scale for the subsequent reaction steps at 0.350 mmol (Run 1) and 0.345 mmol (Run 2). Flash column chromatography (Pentane to Pentane/EtOAc 95:5, then Pentane/EtOAc 95:5 to 80:20) yielded 2-methoxy-4-propylbenzonitrile **5** as a colorless liquid (13.8 mg, 5.5 wt% (Run 1) and 13.6 mg, 5.4 wt% (Run 2)) and 2,6-dimethoxy-4-propylbenzonitrile **6** as a crystalline white solid (46.2 mg, 18 wt% (Run 1) and 44.4 mg, 18 wt% (Run 2)).

## 2-methoxy-4-propylbenzonitrile **5** and 2,6-dimethoxy-4-propylbenzonitrile **6** from willow sawdust



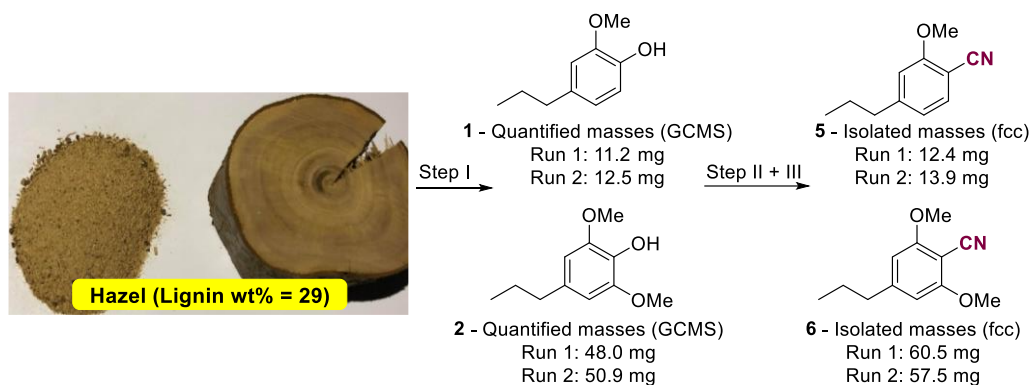
The title compounds were synthesized according to the General Procedure A. The quantified masses of 2-methoxy-4-propylphenol **1** and 2,6-dimethoxy-4-propylphenol **2** by GC-MS are given in the scheme above, and their combined molar amount sets the scale for the subsequent reaction steps at 0.330 mmol (Run 1) and 0.335 mmol (Run 2). Flash column chromatography (Pentane to Pentane/EtOAc 95:5, then Pentane/EtOAc 95:5 to 80:20) yielded 2-methoxy-4-propylbenzonitrile **5** as a colorless liquid (19.1 mg, 8.0 wt% (Run 1) and 21.4 mg, 8.9 wt% (Run 2)) and 2,6-dimethoxy-4-propylbenzonitrile **6** as a crystalline slightly yellow solid (40.7 mg, 17 wt% (Run 1) and 40.2 mg, 17 wt% (Run 2)).

## 2-methoxy-4-propylbenzonitrile **5** and 2,6-dimethoxy-4-propylbenzonitrile **6** from oak sawdust



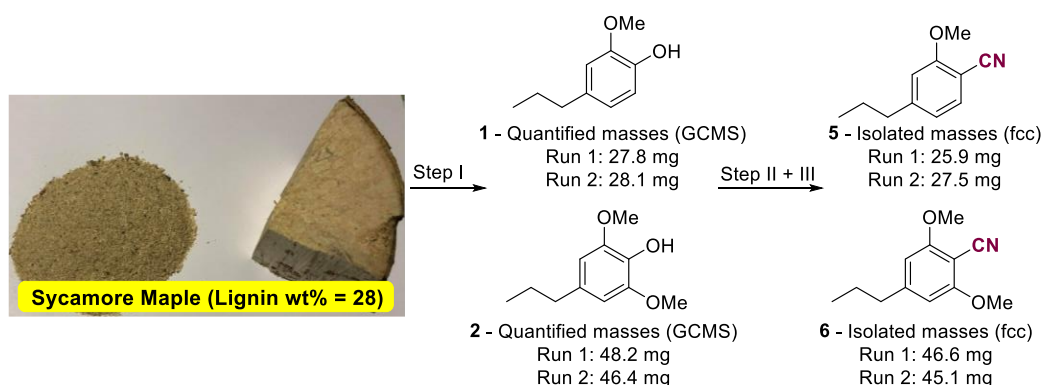
The title compounds were synthesized according to the General Procedure A. The quantified masses of 2-methoxy-4-propylphenol **1** and 2,6-dimethoxy-4-propylphenol **2** by GC-MS are given in the scheme above, and their combined molar amount sets the scale for the subsequent reaction steps at 0.322 mmol (Run 1) and 0.319 mmol (Run 2). Flash column chromatography (Pentane to Pentane/EtOAc 95:5, then Pentane/EtOAc 95:5 to 80:20) yielded 2-methoxy-4-propylbenzonitrile **5** as a colorless liquid (18.1 mg, 7.9 wt% (Run 1) and 18.4 mg, 8.0 wt% (Run 2)) and 2,6-dimethoxy-4-propylbenzonitrile **6** as a crystalline white solid (43.8 mg, 19 wt% (Run 1) and 42.2 mg, 18 wt% (Run 2)).

## 2-methoxy-4-propylbenzonitrile **5** and 2,6-dimethoxy-4-propylbenzonitrile **6** from hazel sawdust



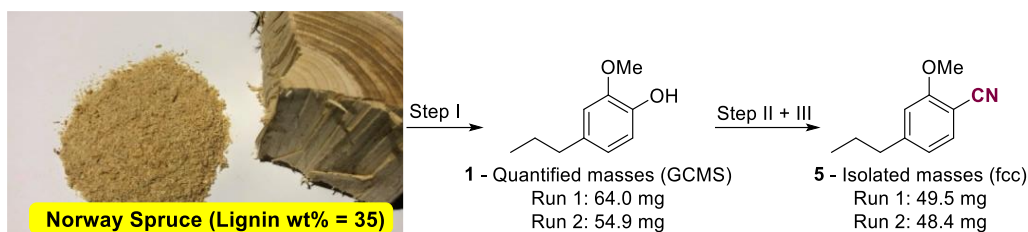
The title compounds were synthesized according to the General Procedure A. The quantified masses of 2-methoxy-4-propylphenol **1** and 2,6-dimethoxy-4-propylphenol **2** by GC-MS are given in the scheme above, and their combined molar amount sets the scale for the subsequent reaction steps at 0.312 mmol (Run 1) and 0.334 mmol (Run 2). Flash column chromatography (Pentane to Pentane/EtOAc 95:5, then Pentane/EtOAc 95:5 to 80:20) yielded 2-methoxy-4-propylbenzonitrile **5** as a colorless liquid (12.4 mg, 4.3 wt% (Run 1) and 13.9 mg, 4.8 wt% (Run 2)) and 2,6-dimethoxy-4-propylbenzonitrile **6** as a crystalline white solid (60.5 mg, 21 wt% (Run 1) and 57.5 mg, 20 wt% (Run 2)).

## 2-methoxy-4-propylbenzonitrile **5** and 2,6-dimethoxy-4-propylbenzonitrile **6** from sycamore maple sawdust



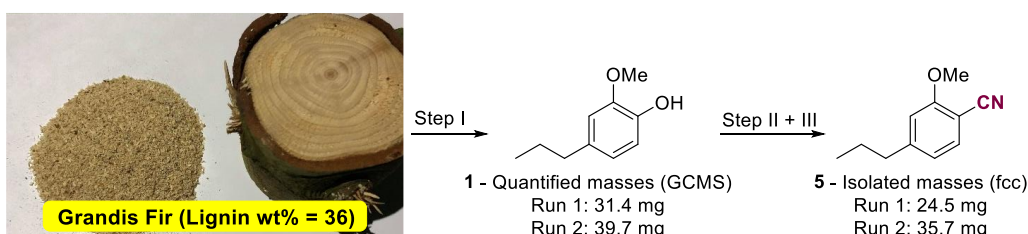
The title compounds were synthesized according to the General Procedure A. The quantified masses of 2-methoxy-4-propylphenol **1** and 2,6-dimethoxy-4-propylphenol **2** by GC-MS are given in the scheme above, and their combined molar amount sets the scale for the subsequent reaction steps at 0.413 mmol (Run 1) and 0.405 mmol (Run 2). Flash column chromatography (Pentane to Pentane/EtOAc 95:5, then Pentane/EtOAc 95:5 to 80:20) yielded 2-methoxy-4-propylbenzonitrile **5** as a colorless liquid (25.9 mg, 9.3 wt% (Run 1) and 27.5 mg, 9.8 wt% (Run 2)) and 2,6-dimethoxy-4-propylbenzonitrile **6** as a crystalline white solid (46.6 mg, 17 wt% (Run 1) and 45.1 mg, 16 wt% (Run 2)).

## 2-methoxy-4-propylbenzotrile 5 from Norway spruce sawdust



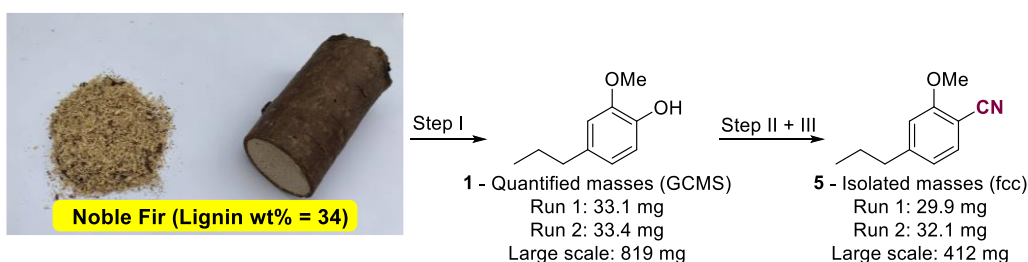
The title compound was synthesized according to the General Procedure A. The quantified mass of 2-methoxy-4-propylphenol **1** by GC-MS is given in the scheme above, and the molar amount sets the scale for the subsequent reaction steps at 0.385 mmol (Run 1) and 0.330 mmol (Run 2). Flash column chromatography (Pentane to Pentane/EtOAc 95:5) yielded 2-methoxy-4-propylbenzotrile **5** as a colorless liquid (49.5 mg, 14 wt% (Run 1) and 48.4 mg, 14 wt% (Run 2)).

## 2-methoxy-4-propylbenzotrile 5 from Grandis fir sawdust



The title compound was synthesized according to the General Procedure A. The quantified mass of 2-methoxy-4-propylphenol **1** by GC-MS is given in the scheme above, and the molar amount sets the scale for the subsequent reaction steps at 0.189 mmol (Run 1) and 0.239 mmol (Run 2). Flash column chromatography (Pentane to Pentane/EtOAc 95:5) yielded 2-methoxy-4-propylbenzotrile **5** as a colorless liquid (24.5 mg, 6.8 wt% (Run 1) and 35.7 mg, 9.9 wt% (Run 2)).

## 2-methoxy-4-propylbenzotrile 5 from Noble fir sawdust



*Small scale:* The title compound was synthesized according to the General Procedure A. The quantified mass of 2-methoxy-4-propylphenol **1** by GC-MS is given in the scheme above, and the molar amount sets the scale for the subsequent reaction steps at 0.199 mmol (Run 1) and 0.201 mmol (Run 2). Flash column chromatography (Pentane to Pentane/EtOAc 95:5) yielded 2-methoxy-4-propylbenzotrile **5** as a colorless liquid (29.9 mg, 8.8 wt% (Run 1) and 32.1 mg, 9.4 wt% (Run 2)).

*Large scale:* The title compound was synthesized according to the General Procedure B. The quantified mass of 2-methoxy-4-propylphenol **1** by GC-MS is given in the scheme above, and the molar amount sets the scale for the subsequent reaction steps at 3.30 mmol. Flash column chromatography (Pentane to Pentane/EtOAc 95:5) yielded 2-methoxy-4-propylbenzotrile **5** as a colorless liquid (412 mg, 6.1 wt%).

## Representative GC-MS Chromatograms for the General Procedure A with Birch Sawdust

Following the General Procedure A, GC-MS chromatograms were recorded for each step, showing the contents of the reaction mixture (Fig. S4). The chromatogram for step III is before purification with flash column chromatography. Near to quantitative conversions were observed for step II and III.

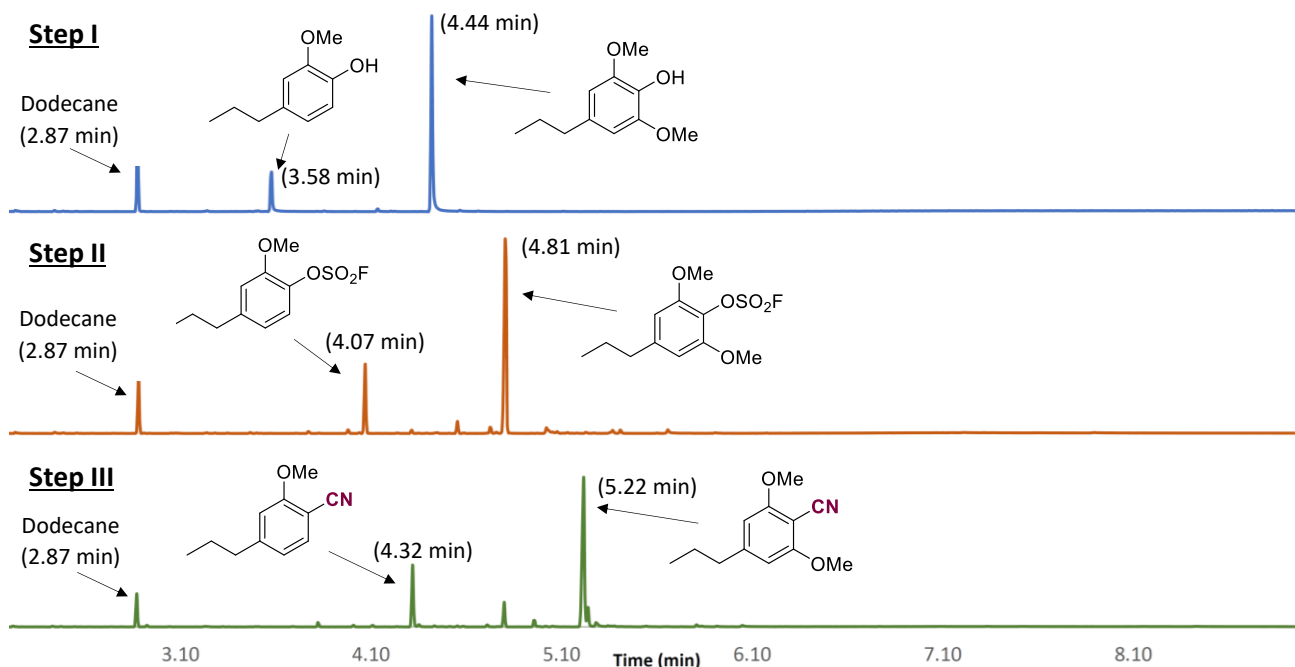
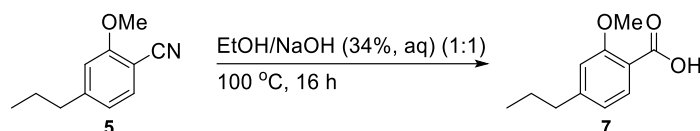


Figure S4. GC-MS TIC for each individual step of the General Procedure A with Birch sawdust.

## Synthesis of Methoxyterephthalic Acid

### 2-Methoxy-4-propylbenzoic acid *via* hydrolysis of 2-methoxy-4-propylbenzotrile



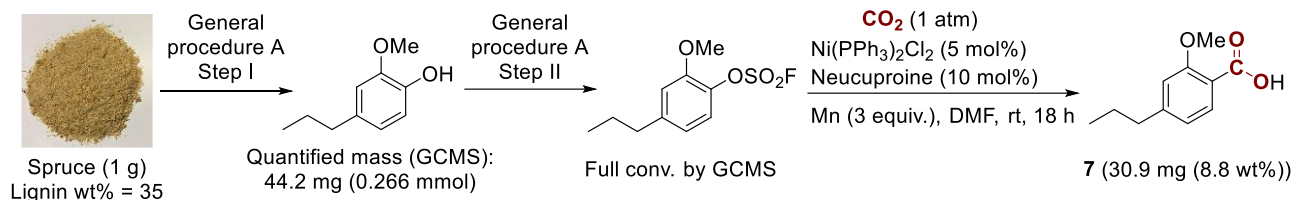
*Small scale procedure:* To a pressure tube (9 mL total volume) was added 2-methoxy-4-propylbenzotrile **5** (35.1 mg, 0.200 mmol (from petrochemical origin)), EtOH (2 mL) and aq. NaOH (34%, 2 mL). The tube was sealed with a screwcap fitted with a Teflon<sup>®</sup>-coated silicone seal, and then heated to 100 °C for 16 h. The reaction mixture was diluted with EtOAc (25 mL) and extracted with aq. NaOH (1 M, 2 x 25 mL). The combined aqueous phases were acidified carefully with conc. HCl (pH < 3) and then extracted with EtOAc (3 x 50 mL), after which the combined organic phases were dried over Na<sub>2</sub>SO<sub>4</sub>, filtered, and concentrated *in vacuo* to yield the product as an off-white solid (38.0 mg, 98%). The procedure was repeated with 2-methoxy-4-propylbenzotrile **5** (36.5 mg, 0.208 mmol) rendering the product as an off-white solid (40.0 mg, 99%), thus the average yield is 99% for small-scale. <sup>1</sup>H-NMR (400 MHz, Acetone-d<sub>6</sub>) δ<sub>H</sub> (ppm) 10.82 (br, 1H), 7.85 (d, *J* = 7.9 Hz, 1H), 7.09 (s, 1H), 6.94 (dd, *J*<sub>1</sub> = 7.9 Hz, *J*<sub>2</sub> = 1.5 Hz, 1H), 4.04 (s, 3H), 2.65 (t, *J* = 7.5 Hz, 2H), 1.67 (sext, *J* = 7.4 Hz, 2H), 0.94 (t, *J* = 7.3 Hz, 3H). <sup>13</sup>C-NMR (100 MHz, Acetone-d<sub>6</sub>) δ<sub>C</sub> (ppm) 166.1, 159.6, 151.1, 133.2, 122.0, 117.3, 113.2, 56.8, 38.7, 24.9, 14.0. HRMS C<sub>11</sub>H<sub>13</sub>O<sub>3</sub><sup>-</sup> [M - H<sup>+</sup>]: calcd 193.0870, found 193.0863.

*Large scale procedure:* To a pressure tube (120 mL total volume) was added 2-methoxy-4-propylbenzotrile **5** (412 mg, 2.35 mmol (from Noble fir)), EtOH (20 mL) and aq. NaOH (34%, 20 mL). The tube was sealed with



a screwcap fitted with a Teflon<sup>®</sup>-coated silicone seal, and then heated to 100 °C for 16 h. After the reaction, the EtOH was removed *in vacuo*, after which the concentrate was added EtOAc (100 mL) and extracted with aq. NaOH (1 M, 2 x 50 mL). The combined aqueous phases were acidified carefully with conc. aq. HCl until pH < 3 and was then extracted with EtOAc (3 x 100 mL), after which the combined organic phases were dried over Na<sub>2</sub>SO<sub>4</sub>, filtered, and concentrated *in vacuo* to yield the product as an off-white solid (430 mg, 94%).

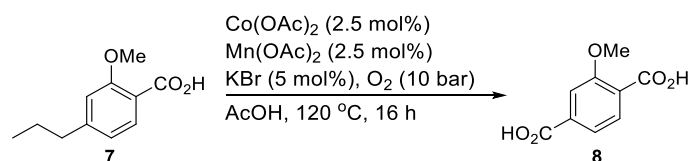
### 2-Methoxy-4-propylbenzoic acid *via* carboxylation of 2-methoxy-4-propylphenyl sulfurofluoridate



This step was applied to the concentrate obtained after Step I and II of the General Procedure A. The amount of quantified 2-methoxy-4-propylphenol after Step I was determined by GC-MS to be 44.2 mg (0.266 mmol) and represents the scale of this reaction.

In a glovebox, to a flame dried pressure tube (9 mL total volume) was added Ni(PPh<sub>3</sub>)<sub>2</sub>Cl<sub>2</sub> (5 mol%), neocuproine (10 mol%), manganese (3 equiv.) and the aryl fluorosulfate concentrate from step II of the General Procedure A, which was transferred with DMF (3 x 0.5 mL). The chamber was sealed with a screwcap fitted with a pierceable Teflon<sup>®</sup>-coated silicone seal. The reaction was taken outside the glovebox and the atmosphere was exchanged for CO<sub>2</sub> for 5 min. using a balloon to bubble through the solution, after which the reaction was fitted with a filled CO<sub>2</sub>-balloon and stirred at room temperature for 18 h. Thereafter, the reaction was quenched by aq. NaOH (1 M) and the aqueous phase was washed with CH<sub>2</sub>Cl<sub>2</sub> (x 2), followed by acidification with aq. HCl (4 M). The aqueous phase was then extracted with EtOAc (x 4), and the combined organic phases were dried over MgSO<sub>4</sub> and concentrated to yield **7** (30.9 mg, 8.8 wt%). <sup>1</sup>H NMR (400 MHz, CDCl<sub>3</sub>) δ<sub>H</sub> (ppm) 8.06 (d, *J* = 8.1 Hz, 1H), 6.94 (dd, *J* = 8.1, 1.6 Hz, 1H), 6.84 (s, 1H), 4.05 (s, 3H), 2.64 (t, *J* = 7.5 Hz, 2H), 1.66 (h, *J* = 7.4 Hz, 2H), 0.95 (t, *J* = 7.3 Hz, 3H). <sup>13</sup>C-NMR (101 MHz, CDCl<sub>3</sub>) δ<sub>C</sub> (ppm) 165.9, 158.2, 151.3, 133.8, 122.5, 115.1, 111.7, 56.7, 38.4, 24.2, 13.9.

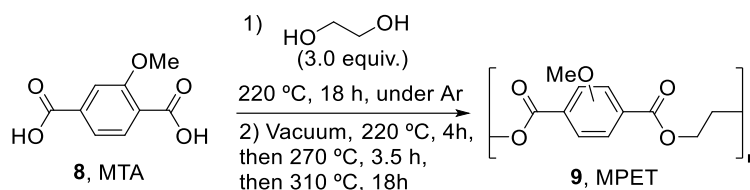
### Methoxyterephthalic acid



A suspension of 2-Methoxy-4-propylbenzoic acid **7** from Noble fir (430 mg, 2.21 mmol), Co(OAc)<sub>2</sub> (9.8 mg, 0.055 mmol, 2.5 mol%), Mn(OAc)<sub>2</sub> (9.6 mg, 0.055 mmol, 2.5 mol%) and KBr (13 mg, 0.11 mmol, 5.0 mol%) in AcOH (2 mL) was stirred in a vial and heated gently with a heat gun until homogeneous. The solution was transferred to a Paar autoclave reactor fitted with a Teflon inlay (30 mL total volume), rinsing with AcOH (1 mL), and was then closed, evacuated 10 times with O<sub>2</sub> at a pressure of 5 bar, and then pressurized to an O<sub>2</sub>-pressure of 10 bar at room temperature. The reaction was heated to 120 °C for 16 h under slow stirring (100 rpm), whereafter the reaction mixture was transferred to a round-bottomed flask, in which a white precipitate would form over time. The white precipitate was decanted with AcOH (8 mL), H<sub>2</sub>O (2 x 8 mL) and pentane (8 mL). The precipitate was dried *in vacuo* to yield the product as a white solid (289 mg, 67%). <sup>1</sup>H-NMR (400 MHz, DMSO-d<sub>6</sub>) δ<sub>H</sub> (ppm) 13.1 (br, 1H), 7.68 (d, *J* = 7.8 Hz, 1H), 7.58-7.53 (m, 2H), 3.86 (s, 3H). <sup>13</sup>C-

NMR (100 MHz, DMSO- $d_6$ )  $\delta_c$  (ppm) 166.9, 166.5, 157.4, 134.4, 130.3, 125.6, 120.9, 112.4, 55.8 (3C). HRMS  $C_9H_7O_5^-$  [ $M - H^+$ ]: calcd 195.0299, found 195.0296.

## Polymerization of Methoxyterephthalic acid with Ethylene Glycol



Methoxyterephthalic acid (obtained from a literature protocol)<sup>4</sup> (3.54 g, 18.1 mmol) was stirred in ethylene glycol (3.0 mL, 54 mmol, 3.0 equiv.) under Ar in a pressure tube (20 mL total volume) at 220 °C for 18 h, after which the reaction was subjected to vacuum heating at 220 °C for 4 h, then 270 °C for 3.5 h, and finally 310 °C for 18 h. The resulting polymer was isolated without further manipulation and characterized by IR-, TGA- and DSC-analysis (See Fig. S5-S7).

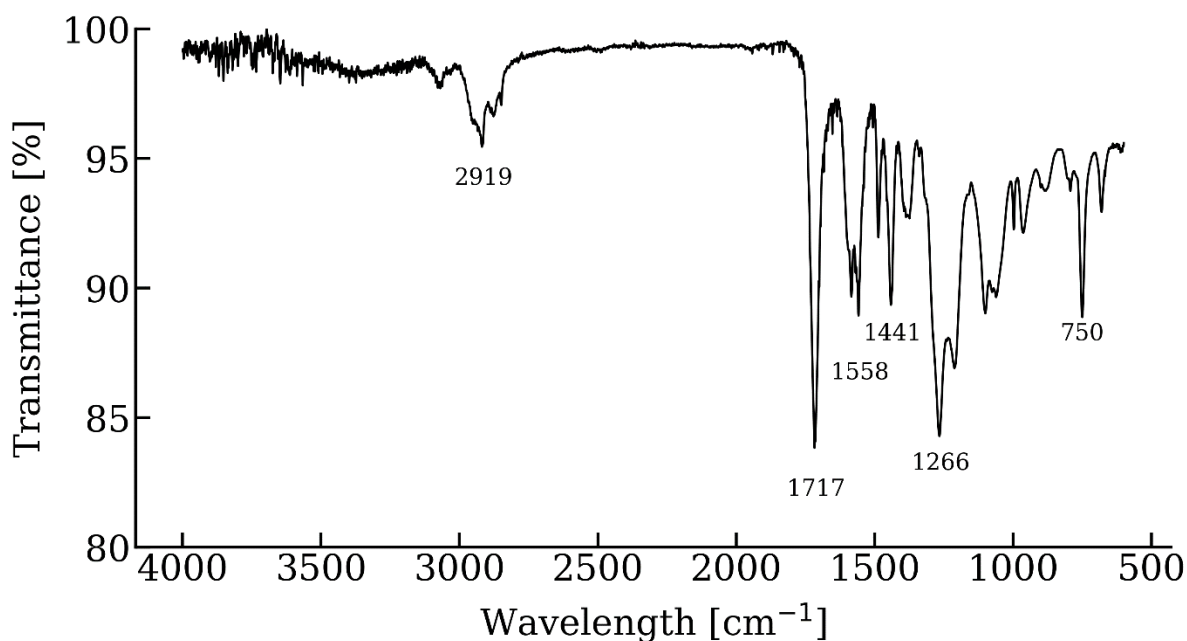


**Figure S5.** ATR-IR spectrum of methoxy-polyethylene terephthalate **9**. The carbonyl is found at 1717  $cm^{-1}$  together with asymmetric and symmetric C-O-C vibrations at 1266  $cm^{-1}$  and 1075  $cm^{-1}$ , respectively. The methoxy group is presented by the  $sp^3$  hybridized peaks found as a peak at 2919  $cm^{-1}$  with a shoulder at 2960  $cm^{-1}$  and the peak at 2856  $cm^{-1}$ . 1558  $cm^{-1}$  is assigned to the C=C in the 1,4-substituted aromatic ring.

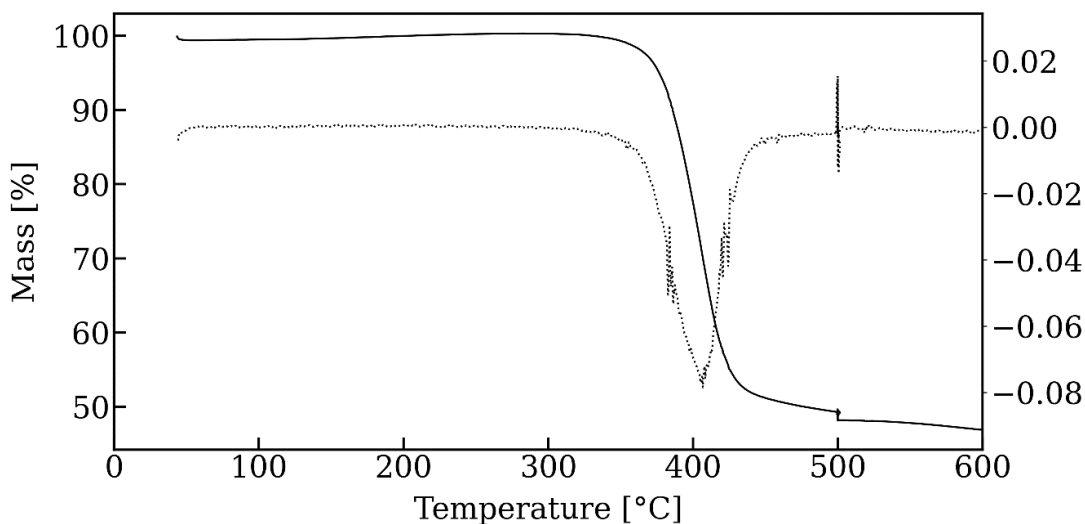


**Figure S6.** TGA spectrum of methoxy-polyethylene terephthalate **9**.  $T_d = 407\text{ }^\circ\text{C}$ ,  $T_{5\%} = 377\text{ }^\circ\text{C}$ .

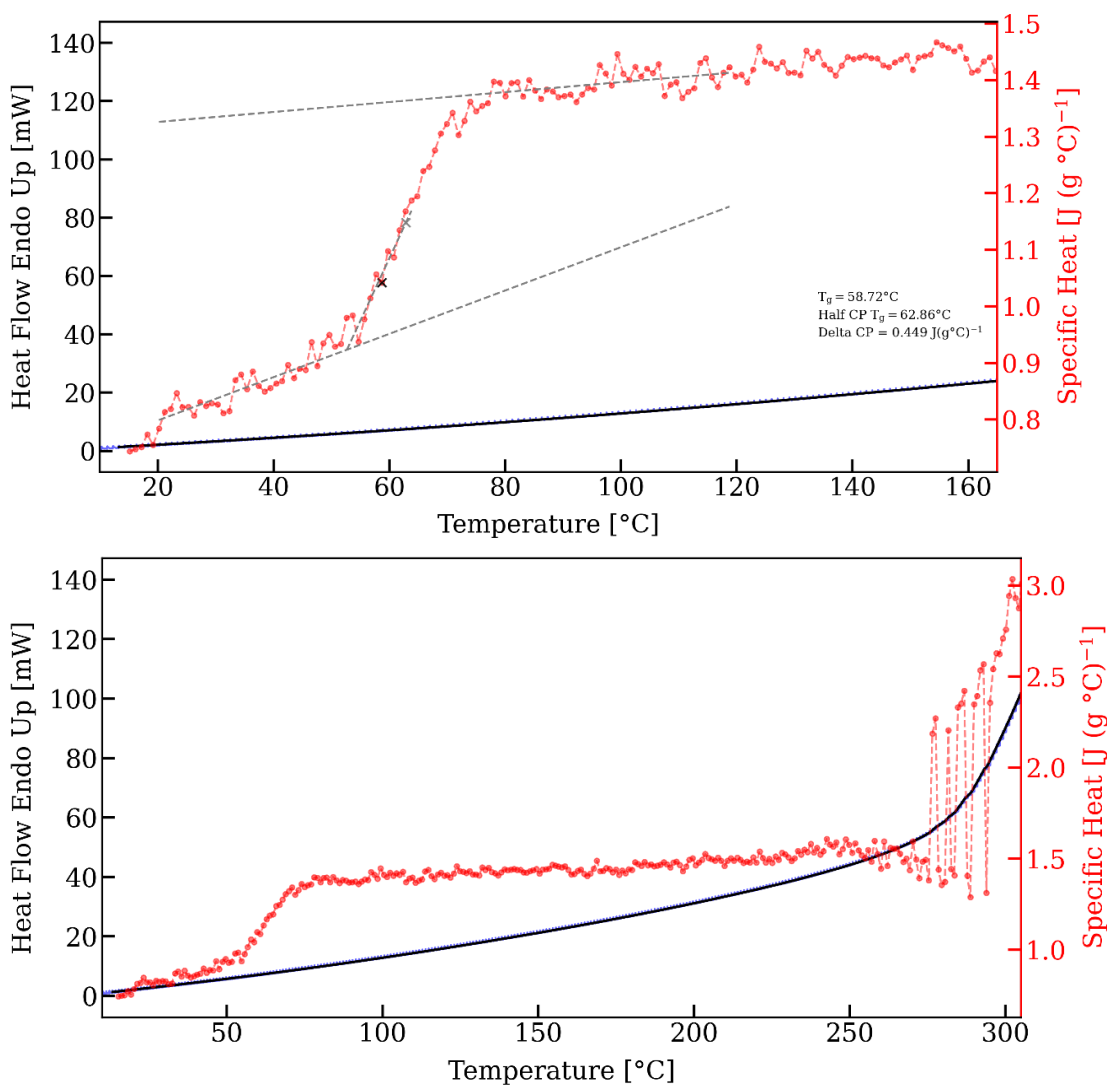
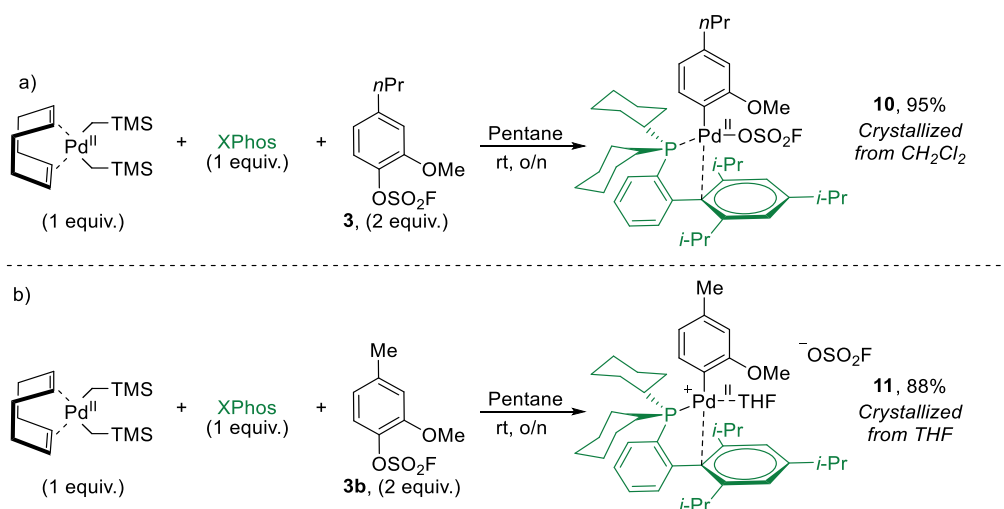


**Figure S7.** DSC spectra of methoxy-polyethylene terephthalate **9**.  $T_g = 59\text{ }^\circ\text{C}$ . There is no defined melting point  $T_m$ , which indicates an amorphous polymer.

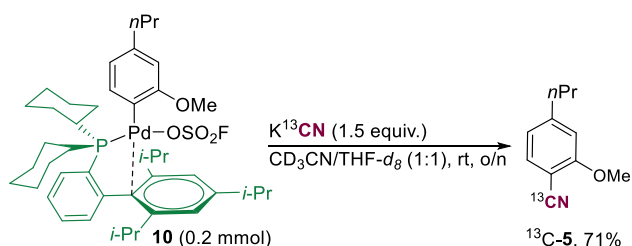
## Mechanistic Studies on the Pd-catalyzed cyanation of aryl fluorosulfates with KCN (DFT, stoichiometric experiments, and NMR studies)

To obtain insight into the reaction mechanism for the cyanation reaction, a series of experiments were conducted, such as NMR-experiments, stoichiometric reactions with XPhos-ligated palladium complexes, and DFT calculations. The synthesis of XPhos-ligated oxidative addition complexes with palladium has been shown before for aryl iodides and this method could be successfully applied for the aryl fluorosulfates **3** and **3b**.<sup>5</sup> The oxidative addition complexes, **10** and **11**, could be isolated in 95% and 88% yields, respectively, from the reaction with **3** or **3b** in pentane o/n, and the crystal structure was dependent on the solvent used for crystallization. With slow vapor diffusion of pentane into CH<sub>2</sub>Cl<sub>2</sub>, complex **10** was obtained, however exchanging CH<sub>2</sub>Cl<sub>2</sub> for THF, complex **11** was the resulting complex, where the fluorosulfate anion was displaced by a coordinating THF solvent molecule (Scheme S1).



**Scheme S1.** Synthesis of oxidative addition complexes **10** and **11**.

In the case of the reductive elimination step yielding the product nitrile, it has been previously reported by Hartwig and co-workers that aryl-Pd(II)L-CN complexes undergo reductive elimination even at low temperatures.<sup>6</sup> With complex **10** in hand, we subjected it to K<sup>13</sup>CN for an o/n reaction at room temperature, after which the expected <sup>13</sup>C-labeled aryl nitrile product could be isolated in a 71% yield (Scheme S2).



**Scheme S2.** Reaction of oxidative addition complex **10** with <sup>13</sup>C-labeled potassium cyanide.

**NMR-experiments:** <sup>31</sup>P-NMR analysis within different reaction times was conducted to observe the catalyst resting state. After 1 hour of reaction with the optimized conditions, the only <sup>31</sup>P chemical shift that was observed was identical to the <sup>31</sup>P-shift of the oxidative addition complex **10** (36.2 ppm) (see Fig. S8). However, when conducting <sup>31</sup>P-NMR analysis of the reaction mixture after o/n stirring and complete conversion to the product nitrile (observed by GC-MS), only the chemical shift of non-coordinating XPhos is the result (-12.5

ppm), which is proposed to be due to deactivation of the catalyst after the reaction. Thus, from the above-mentioned observations we propose that complex **10** closely resembles the catalyst resting state.

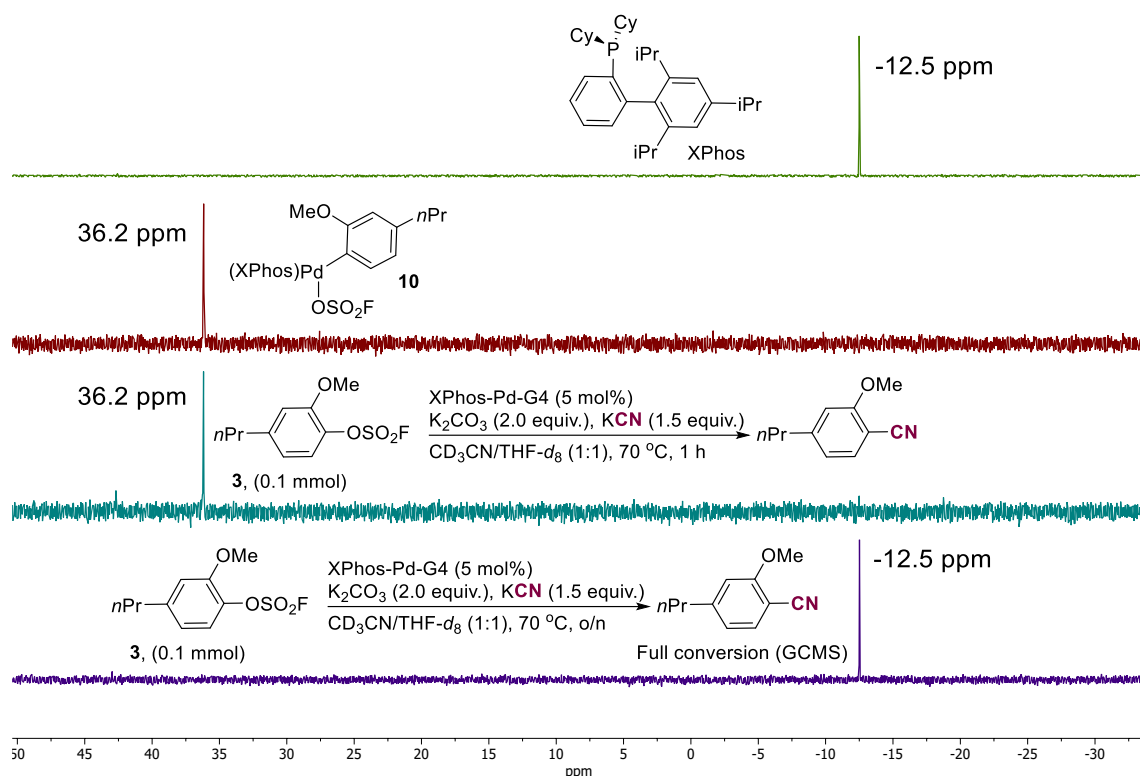


**Figure S8.** NMR-experiments to investigate the catalyst resting state and decomposition.

As reported by Grushin and co-workers, excess cyanide can deactivate the palladium catalyst, leading to inactive  $\text{Pd}^{\text{II}}(\text{CN})_x$  species alongside non-ligated phosphine ligand.<sup>7</sup> From our optimization, up to 6 equivalents of KCN were tolerated within the catalytic system (see Table S3), thus showing a remarkable stability. We propose that it is mainly an effect of KCN solubility in the solvent mixture (MeCN/2-MeTHF 1:1), since a more soluble cyanide source such as  $(\text{Bu})_4\text{NCN}$  was detrimental to the system leading to catalyst deactivation almost instantly (see Fig. S9). More specifically, when a mixture of XPhos-Pd-G4 (5 mol%),  $\text{Et}_3\text{N}$  (2 equiv.) and **3** (1 equiv.) was stirred at 70 °C for 20 min, the  $^{31}\text{P}$ -NMR chemical shift was rapidly converted to the signal corresponding to the oxidative addition complex (**10**, 36.2 ppm). The addition of  $(\text{Bu})_4\text{NCN}$  (1.5 equiv.) led instantaneously to a deep red solution, with which  $^{31}\text{P}$ -NMR-analysis only showed the signal corresponding to non-ligated XPhos (-12.5 ppm) that implies the formation of catalytically inactive  $\text{Pd}(\text{CN})_x$ -species (see Fig. S9).

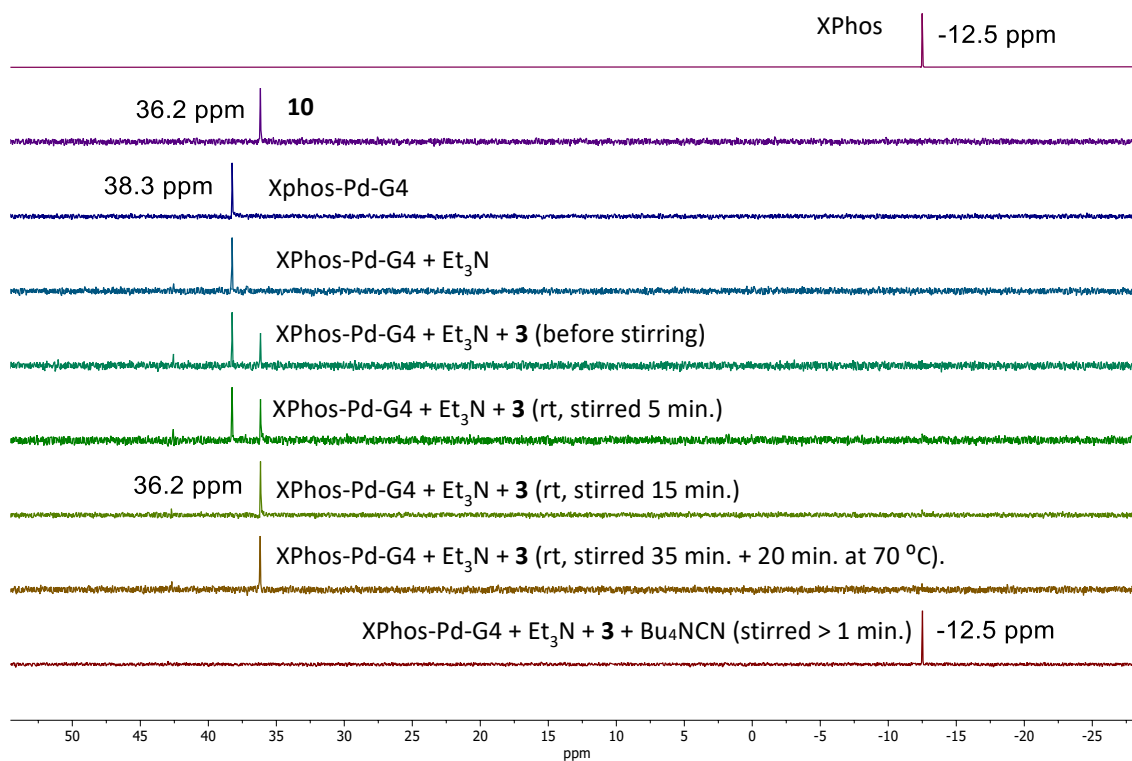
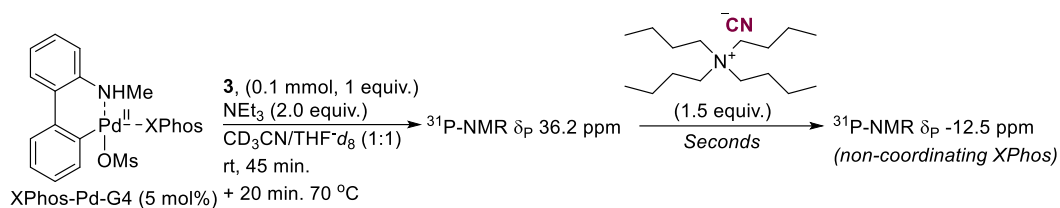


**Figure S9.** NMR-experiments at different times during the cyanation of **3**. The experiments show the formation of a 36.2 ppm phosphine signal, which corresponds to the oxidative addition complex. Adding Bu<sub>4</sub>NCN to the reaction mixture results in a full conversion to the -12.5 ppm signal for non-ligated XPhos, implying deactivation.

The solvent system used with the optimized conditions of MeCN and 2-MeTHF was found from screening (see Table S1-S3), and a similar solvent system of MeCN and THF has been reported for the cyanation of aryl bromides by Grushin and co-workers.<sup>8</sup> We observe that the reaction only renders trace or no product nitrile if the reaction is conducted in one of the individual solvents (see Table S3), although with HCN instead of KCN, the reaction in MeCN works to some degree (see Table S2). NMR-analysis of these crude reaction mixtures in the individual solvents with <sup>31</sup>P-NMR showed the signal for non-coordinating XPhos, which is a sign of deactivation (see Fig. S10). Thus besides an optimal solubility of KCN, the beneficial effect of the solvent mixture could be that it effectively dissolves all components of the reaction.

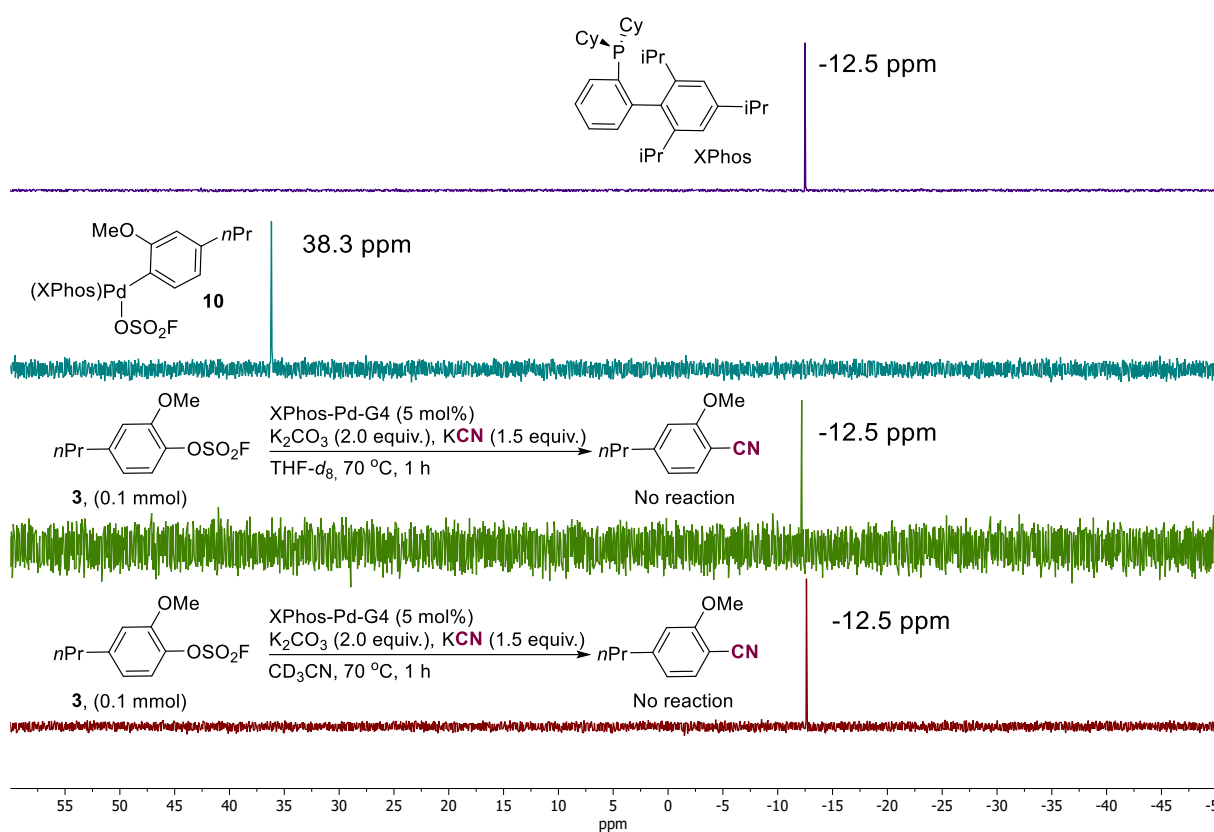


**Figure S10.** NMR experiments of the cyanation of **3** after 1 hour in either THF-*d*<sub>8</sub> or CD<sub>3</sub>CN.

**General procedure for the synthesis of oxidative addition complexes **10** and **11**:** In a glovebox, to a flame dried vial was added XPhos (0.5 equiv.), aryl fluorosulfate (1 equiv.), and pentane (2.5 mL) followed by the addition of (COD)Pd(CH<sub>2</sub>TMS)<sub>2</sub> (0.5 equiv.) in one portion. The vial was then closed, taken outside of the glovebox, and stirred overnight at room temperature. Thereafter, the precipitate was filtered and washed with pentane, after which drying under a reduced pressure yielded the desired product.

Following the general procedure with **3** (0.54 mmol), (COD)Pd(CH<sub>2</sub>TMS)<sub>2</sub> (0.27 mmol, 0.5 equiv.), and XPhos (0.27 mmol, 0.5 equiv.), **10** was obtained as a white powder (204 mg, 95%). Crystals could be obtained from slow vapor diffusion of pentane into CH<sub>2</sub>Cl<sub>2</sub>. <sup>1</sup>H-NMR (400 MHz, CDCl<sub>3</sub>) δ<sub>H</sub> (ppm) 7.72 – 7.63 (m, 1H), 7.54 – 7.45 (m, 2H), 7.30 (s, 2H), 7.04 – 6.97 (m, 1H), 6.62 (dd, *J*<sub>1</sub> = 7.8 Hz, *J*<sub>2</sub> = 3.2 Hz, 1H), 6.54 (d, *J* = 7.8 Hz, 1H), 6.33 (s, 1H), 3.77 (s, 3H), 3.14 (sep, *J* = 7.0 Hz, 1H), 2.48 (t, *J* = 7.5 Hz, 4H), 2.24 (q, *J* = 10.8 Hz, 5H), 1.80 (d, *J* = 11.9 Hz, 3H), 1.71 (d, *J* = 11.1 Hz, 7H), 1.64 (d, *J* = 6.7 Hz, 6H), 1.57 (sep, *J* = 7.3 Hz, 2H), 1.31 (d, *J* = 7.0 Hz, 6H), 1.28 – 1.08 (m, 6H), 0.94 (d, *J* = 6.7 Hz, 6H), 0.86 (t, *J* = 7.3 Hz, 3H), 0.83 – 0.70 (m, 1H). <sup>13</sup>C-NMR (101 MHz, CDCl<sub>3</sub>) δ<sub>C</sub> (ppm) 162.8, 154.8, 149.8, 146.0 (d, *J* = 16 Hz), 141.7, 136.0, 134.7 (d, *J* = 38 Hz), 132.7 (d, *J* = 11 Hz), 131.9, 131.3 (d, *J* = 2.6 Hz), 127.9 (d, *J* = 6.2 Hz), 123.6 (d, *J* = 3.7 Hz), 121.9, 121.8 (d, *J* = 2.9 Hz), 119.0, 110.6, 55.1, 37.8, 35.9, 35.6, 33.5, 31.7, 28.3, 27.6 (d, *J* = 2.9 Hz), 27.3, 27.2, 27.1, 27.1, 26.3, 26.0, 24.8, 23.5, 22.8, 13.6 ppm (observed complexity is due to <sup>13</sup>C-<sup>31</sup>P coupling). <sup>19</sup>F-NMR (376 MHz, CDCl<sub>3</sub>) δ<sub>F</sub> (ppm) 40.5. <sup>31</sup>P-NMR (162 MHz, CDCl<sub>3</sub>) δ<sub>P</sub> (ppm) 46.3.

Following the general procedure with **3b** (0.6 mmol), (COD)Pd(CH<sub>2</sub>TMS)<sub>2</sub> (0.3 mmol, 0.5 equiv.), and XPhos (0.3 mmol, 0.5 equiv.), **11** was obtained as a white powder (212 mg, 88%). Crystals could be obtained from slow diffusion of pentane into THF. <sup>1</sup>H-NMR (400 MHz, CDCl<sub>3</sub>) δ<sub>H</sub> (ppm) 7.74 – 7.66 (m, 1H), 7.58 – 7.51 (m, 2H), 7.27 (s, 2H), 7.19 – 7.11 (m, 1H), 6.65 (dd, *J*<sub>1</sub> = 7.8 Hz, *J*<sub>2</sub> = 3.6 Hz, 1H), 6.52 (d, *J* = 7.8 Hz, 1H), 6.30 (s, 1H),

3.74 (s, 3H), 3.10 (sep,  $J = 7.0$  Hz, 1H), 2.48 (quint  $J = 6.7$  Hz, 2H), 2.24 (s, 3H), 1.89 – 1.76 (m, 4H), 1.76 – 1.65 (m, 7H), 1.62 (d,  $J = 6.7$  Hz, 6H), 1.34 – 1.28 (m, 2H), 1.25 (d,  $J = 6.8$  Hz, 6H), 1.24 – 1.07 (m, 5H), 0.98 (d,  $J = 6.7$  Hz, 6H), 0.88 (t,  $J = 7.1$  Hz, 2H), 0.84 – 0.73 (m, 2H) ppm.  $^{13}\text{C}$ -NMR (101 MHz,  $\text{CDCl}_3$ )  $\delta_{\text{C}}$  (ppm) 162.6, 154.9, 150.1, 145.8 (d,  $J = 16$  Hz), 136.9, 135.7, 134.7 (d,  $J = 38$  Hz), 132.6 (d,  $J = 11$  Hz), 131.9, 131.4 (d,  $J = 2.6$  Hz), 128.0 (d,  $J = 6.2$  Hz), 123.6 (d,  $J = 3.7$  Hz), 122.4 (d,  $J = 3.3$  Hz), 121.9, 118.9, 111.1, 55.0, 36.0, 35.7, 34.2, 33.6, 31.7, 28.4, 27.6 (d,  $J = 2.9$  Hz), 27.2 (d,  $J = 4.8$  Hz), 27.1 (d,  $J = 2.9$  Hz), 26.2, 26.0, 23.5, 22.83, 22.5, 21.3, 14.2 ppm (observed complexity is due to  $^{13}\text{C}$ - $^{31}\text{P}$  coupling).  $^{19}\text{F}$ -NMR (376 MHz,  $\text{CDCl}_3$ )  $\delta_{\text{F}}$  (ppm) 40.0 ppm.  $^{31}\text{P}$ -NMR (162 MHz,  $\text{CDCl}_3$ )  $\delta_{\text{P}}$  (ppm) 46.8 ppm.

**General procedure for NMR-experiments (Fig. S8):** In a glovebox, to a flame dried vial (8 mL total volume) was added Pd-XPhos-G4 (5 mol%),  $\text{K}_2\text{CO}_3$  (2.0 equiv.), KCN (1.5 equiv.), **3** (0.1 mmol, 1 equiv.) and  $\text{CD}_3\text{CN}/\text{THF}-d_8$  (1:1, 1 mL). The vial was closed with a screwcap fitted with a Teflon<sup>®</sup>-coated silicone seal and stirred at 70 °C for 1-18 hours. At the desired time, the reaction was cooled to room temperature and taken inside the glovebox. The reaction content was transferred to a flame dried Young NMR-tube, which was then sealed with a screwcap and taken outside the glovebox for NMR analysis. GC-MS was also conducted of the reaction mixture at the specific time, however by firstly diluting the reaction with EtOAc and filtering through celite.

**General procedure for NMR-experiments (Fig. S9):** In a glovebox, to a flame dried Young NMR-tube was added Pd-XPhos-G4 (5 mol%) to a mixture of  $\text{CD}_3\text{CN}/\text{THF}-d_8$  (1:1, 1 mL). The tube was sealed with a screwcap and taken outside the glovebox for NMR-analysis. Subsequently, the tube was taken inside the glovebox and added  $\text{Et}_3\text{N}$  (2 equiv.), after which NMR-analysis was conducted again. In the glovebox, **3** (0.1 mmol, 1 equiv.) was added, and a new NMR spectrum was recorded. From  $^{31}\text{P}$ -NMR analysis, after 15 minutes there was still observable amounts of unreacted Pd-XPhos, thus the tube was heated to 70 °C for an additional 20 min. After this, only a single  $^{31}\text{P}$ -NMR shift of 36.2 ppm was the result. Then, to the reaction mixture was added  $\text{Bu}_4\text{NCN}$ , after which an instant color change from light yellow to dark red was observed, and NMR was recorded.

## Density Functional Theory (DFT) study

**Computational details:** All DFT calculations presented in this paper were performed with the Gaussian 16 package, at 1 atm and with temperature correction at the frequency calculation for 343.15 K (with the addition of the temperature=343.15 keyword).<sup>9</sup> The geometry optimization of all molecules was executed at the PBE-D3/Def2SVP level of theory with the Solvation Model based on Density (SMD) for acetonitrile.<sup>10-14</sup> To confirm all minima and saddle points vibrational analysis was done at the same level as the geometry optimization, this also provides the Gibbs free energy corrections. Besides the vibrational analysis, the transition states were further confirmed through IRC calculations. Single point calculations of all structures were done at the PBE-D3/Def2TZVPP level of theory with SMD for MeCN.<sup>15</sup>

All structures were treated as full models with no symmetry constrains. For the species involved in the reaction cycle and deactivation pathway, different conformations were searched manually. During the whole catalytic cycle and deactivation pathway, all computed species were computed as singlet neutral species. For structures involving counterions, explicit counterions were included in the chemical model based on the X-ray structure of **11**. This avoids artefacts that may arise from comparing structures with different charges. The relative energies of the optimized intermediates may be affected by the exact placement of the explicit anion in the model, however, we note that none of the species with included counterion is involved in the rate determining step. The salts (KCN,  $\text{KOSO}_2\text{F}$ ) were computed as monomeric units in an implicit solvation model. Higher order aggregates were not considered, as the state of aggregation of the solvated salts under the reaction conditions is not known. Although the choice of reference state of the salts may affect the computed energies, we do not expect the state of aggregation to affect the mechanistic conclusions.<sup>16</sup> It is



important to highlight that the salt exchange (**S** --> **MC1**) does not involve any species that affects the transition state barriers.

Additionally, the ultrafine grid was used for the computed species. For the deactivation pathway using the  $P(tBu)_3$  ligand system the geometry optimization of the transition state was showing convergence problems due to instabilities in the solvent cavity. Thus, for these results the geometry optimization was run without implicit solvent at the PBE-D3/Def2SVP level of theory with single point calculations at the same level as previously described (PBE-D3/Def2TZVPP level of theory with SMD for MeCN).

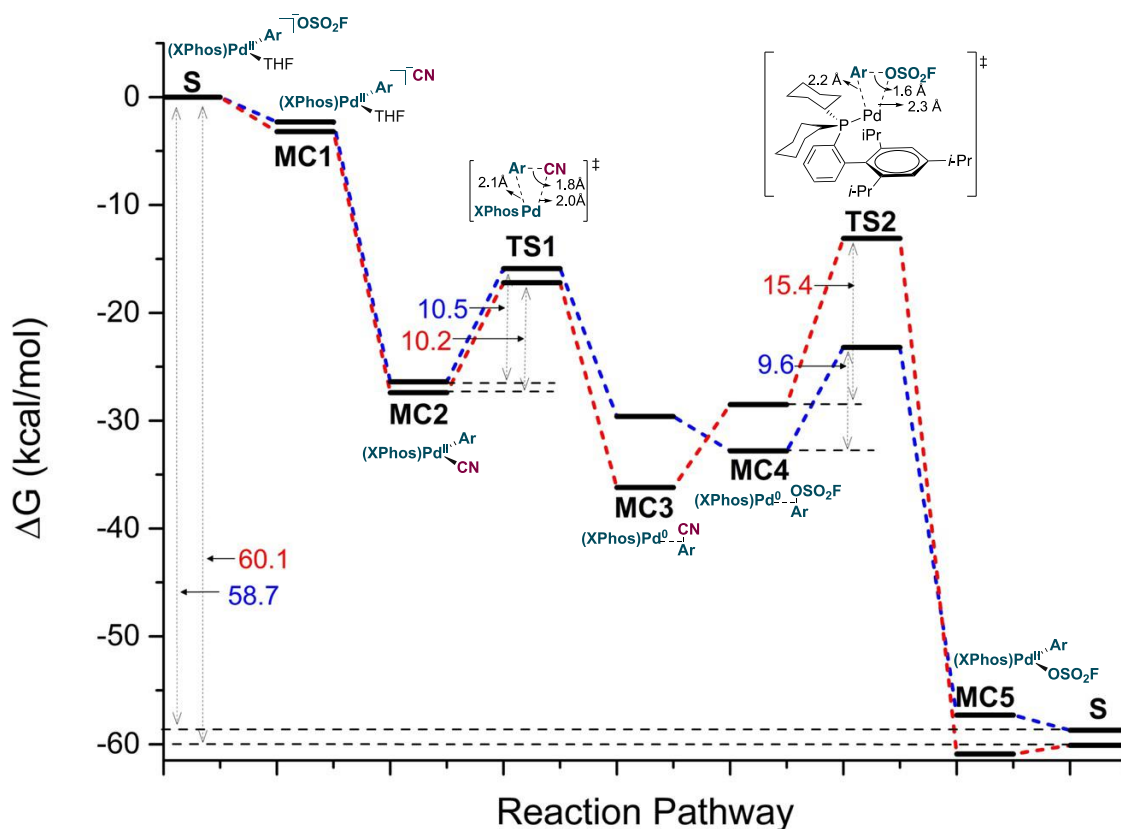


**Figure S11.**  $\Delta G$  change during the reaction pathway for cyanation of aryl fluorosulfate **3** or **4**. All the presented results were calculated at the PBE-D3/Def2TZVPP//PBE-D3/Def2SVP level of theory with Solvent Model based on Density (SMD) (acetonitrile) and temperature correction to 343.15 K at the frequency calculation. Notice that after significant amounts of **MC3** are formed, the barrier to **TS2** may increase.

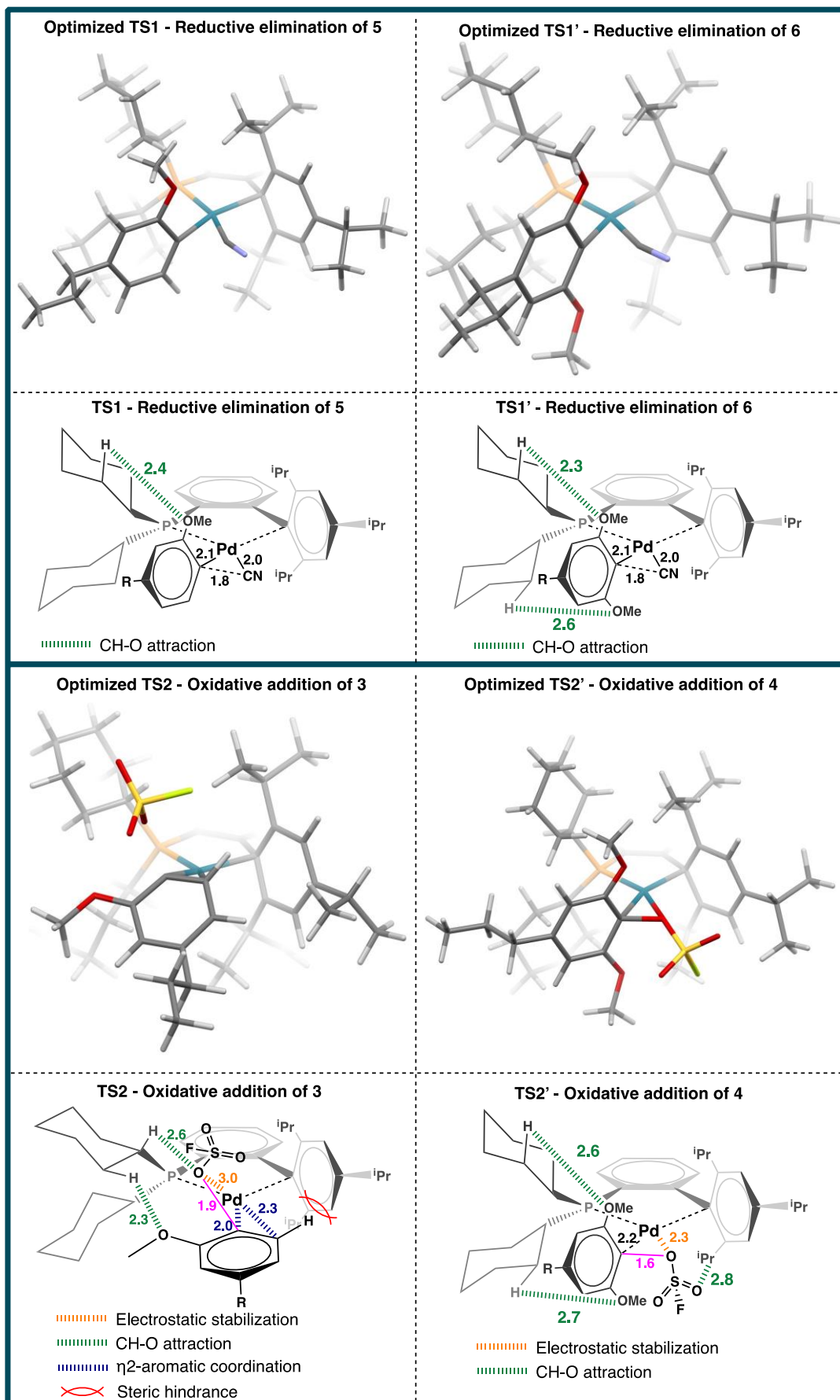


**Figure S12.** Optimized structures of TS1, TS1', TS2 and TS2'. All the presented results were calculated at the PBE-D3/Def2TZVPP//PBE-D3/Def2SVP level of theory with Solvent Model based on Density (SMD) (acetonitrile) and temperature correction to 343.15 K.

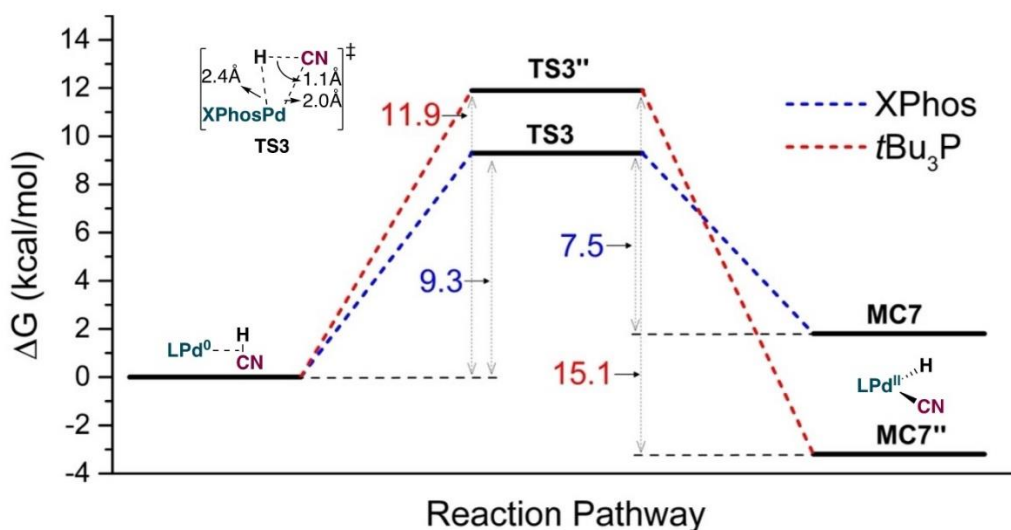
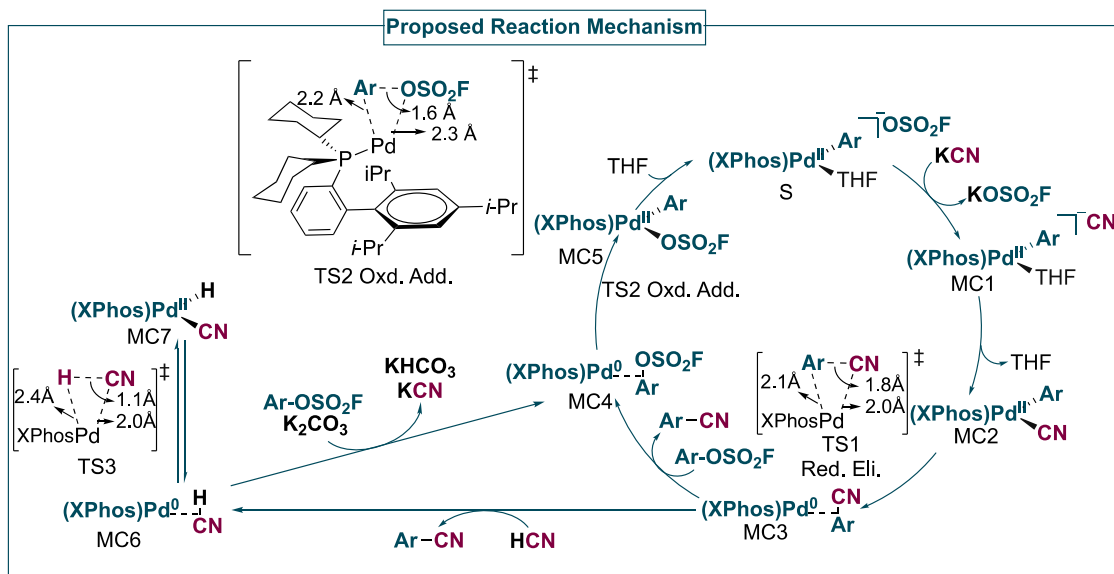


**Figure S13.**  $\Delta G$  change for the HCN oxidative addition pathway. L = XPhos (blue dashed line), L =  $P(tBu)_3$  (red dashed line). The results for the XPhos ligand system were calculated at the PBE-D3Def2TZVPP// PBE-D3/Def2SVP level of theory with Solvent Model based on Density (SMD) (acetonitrile) for both optimization and single point energy and temperature correction to 343.15 K at the frequency calculation. The results for the  $P(tBu)_3$  ligand system were calculated at the PBE-D3Def2TZVPP// PBE-D3/Def2SVP level of theory. The Solvent Model based on Density (SMD) (acetonitrile) was only used in the single point energy as described in the computational details session above, and temperature correction to 343.15 K.



**Scheme S3.** Proposed cyanation mechanism including the HCN deactivation. The provided distances given are for intermediates deriving from the reaction with aryl fluorosulfate **3**.

### Imaginary frequencies for all transition states (TSs):

Sample	Frequencies
TS1	324.0i
TS2	215.1i
TS1'	314.2i
TS2'	299.5i
TS3	108.4i
TS3''	281.5i

Table S5. Imaginary frequencies of the transition states.

### Reported energies:

	E kcal mol <sup>-1</sup>	G <sub>343.15 K</sub> kcal mol <sup>-1</sup>	H <sub>343.15 K</sub> kcal mol <sup>-1</sup>
3	-744899.5	-744798.4	-744749.1
KCN	-434558.2	-434573.9	-434550.7
THF	-145733.7	-145682.9	-145659.5
MC1	-1596226.9	-1595645.9	-1595518.4
MC2	-1450504.2	-1449987.1	-1449872.8
MC3	-1450505.8	-1449990.3	-1449875.0
MC4	-1846214.8	-1845697.6	-1845577.0
MC5	-1846240.9	-1845722.1	-1845601.9
TS1	-1450492.2	-1449976.7	-1449861.3
TS2	-1846204.7	-1845688.0	-1845567.5
S	-1991989.2	-1991406.4	-1991272.6
5	-349195.5	-349094.3	-349052.2

Table S6. Energies for molecules involved in the catalytic cycle with aryl fluorosulfate **3**.

	E kcal mol <sup>-1</sup>	G <sub>343.15 K</sub> kcal mol <sup>-1</sup>	H <sub>343.15 K</sub> kcal mol <sup>-1</sup>
4	-816713.2	-816595.4	-816540.9
KCN	-434558.2	-434573.9	-434550.7
THF	-145733.7	-145682.9	-145659.5
MC1'	-1668043.4	-1667444.0	-1667312.9
MC2'	-1522320.1	-1521785.3	-1521667.1
MC3'	-1522327.7	-1521794.1	-1521674.8
MC4'	-1918023.9	-1917489.0	-1917364.1
MC5'	-1918056.2	-1917521.4	-1917396.4
TS1'	-1522308.8	-1521775.1	-1521657.1
TS2'	-1918007.4	-1917473.6	-1917354.5
S'	-2063806.0	-2063203.6	-2063067.4
6	-421011.1	-420892.8	-420845.9

Table S7. Energies for molecules involved in the catalytic cycle with aryl fluorosulfate **4**.

	E kcal mol <sup>-1</sup>	G <sub>343.15 K</sub> kcal mol <sup>-1</sup>	H <sub>343.15 K</sub> kcal mol <sup>-1</sup>
MC6	-1159896.0	-1159488.3	-1159395.7
TS3	-1159884.1	-1159479.0	-1159385.5
MC7	-1159891.6	-1159486.4	-1159392.6

**Table S8.** Energies for molecules involved in the HCN deactivation pathway with L = XPhos.

	E kcal mol <sup>-1</sup>	G <sub>343.15 K</sub> kcal mol <sup>-1</sup>	H <sub>343.15 K</sub> kcal mol <sup>-1</sup>
MC6''	-649857.0	-649662.8	-649603.0
TS3''	-649844.9	-649650.9	-649591.3
MC7''	-649850.9	-649654.1	-649595.6

**Table S9.** Energies for molecules involved in the HCN deactivation pathway with L = tBu<sub>3</sub>P.

	$\Delta G_{343.15 K}$ kcal/mol	$\Delta H_{343.15 K}$ kcal/mol
S + KCN + 3	0	0
MC1 + KOSO <sub>2</sub> F + 3	-2.3	-1.7
MC2 + KOSO <sub>2</sub> F + 3 + THF	-26.4	-15.5
TS1 + KOSO <sub>2</sub> F + THF + 3	-15.9	-4.1
MC3 + KOSO <sub>2</sub> F + THF + 3	-29.6	-17.8
MC4 + KOSO <sub>2</sub> F + THF + 5	-32.8	-22.3
TS2 + KOSO <sub>2</sub> F + THF + 5	-23.2	-13.4
MC5 + KOSO <sub>2</sub> F + THF + 5	-57.3	-47.9
S + KOSO <sub>2</sub> F + 5	-58.7	-59.1

**Table S10.** Energy (H and G) change along the reaction pathway for aryl fluorosulfate **3**.

	$\Delta G_{343.15 K}$ kcal/mol	$\Delta H_{343.15 K}$ kcal/mol
S' + KCN + 4	0	0
MC1' + KOSO <sub>2</sub> F + 4	-3.2	-1.4
MC2' + KOSO <sub>2</sub> F + THF + 4	-27.4	-15.1
TS1' + KOSO <sub>2</sub> F + THF + 4	-17.2	-5.1
MC3' + KOSO <sub>2</sub> F + THF + 4	-36.2	-22.8
MC4' + KOSO <sub>2</sub> F + THF + 6	-28.5	-17.1
TS2' + KOSO <sub>2</sub> F + THF + 6	-13.1	-7.5
MC5' + KOSO <sub>2</sub> F + THF + 6	-60.9	-49.5
S' + KOSO <sub>2</sub> F + 6	-60.1	-60.9

**Table S11.** Energy (H and G) change along the reaction pathway for aryl fluorosulfate **4**.

	$\Delta G_{343.15\text{ K}}$ kcal/mol	$\Delta H_{343.15\text{ K}}$ kcal/mol
MC6	0	0
TS3	9.3	10.2
MC7	1.9	3.0

**Table S12.** Energy (H and G) change along the deactivation pathway with HCN with L = XPhos.

	$\Delta G_{343.15\text{ K}}$ kcal/mol	$\Delta H_{343.15\text{ K}}$ kcal/mol
MC6''	0	0
TS3''	11.9	11.7
MC7''	-3.2	-4.3

**Table S13.** Energy (H and G) change along the deactivation pathway with HCN with L = *t*Bu<sub>3</sub>P.

**Intrinsic reaction coordinate (IRC):**

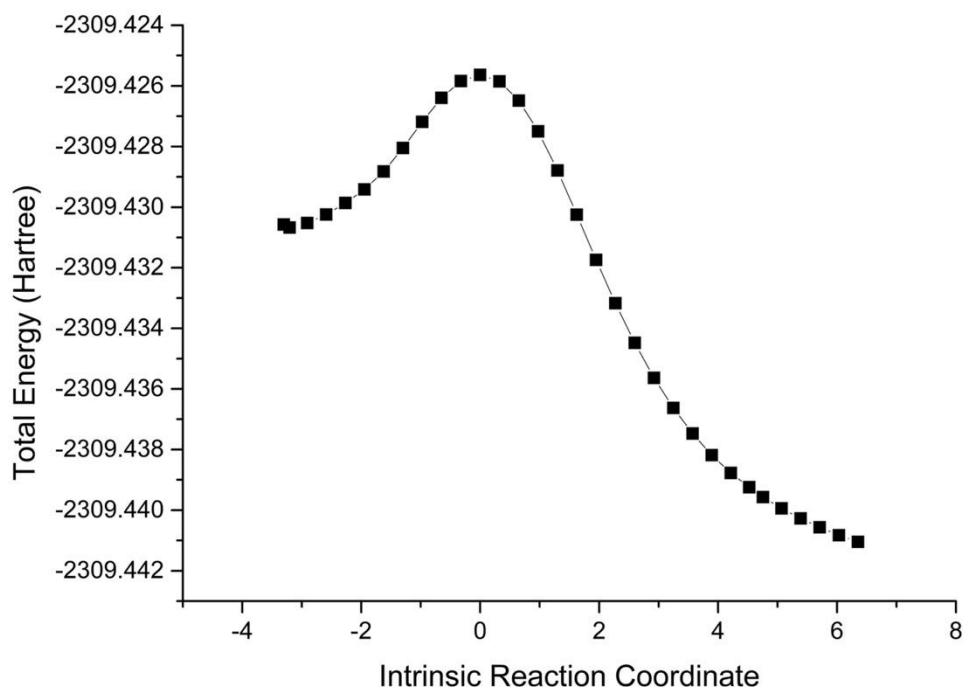


**Figure S14.** IRC calculation for TS1.

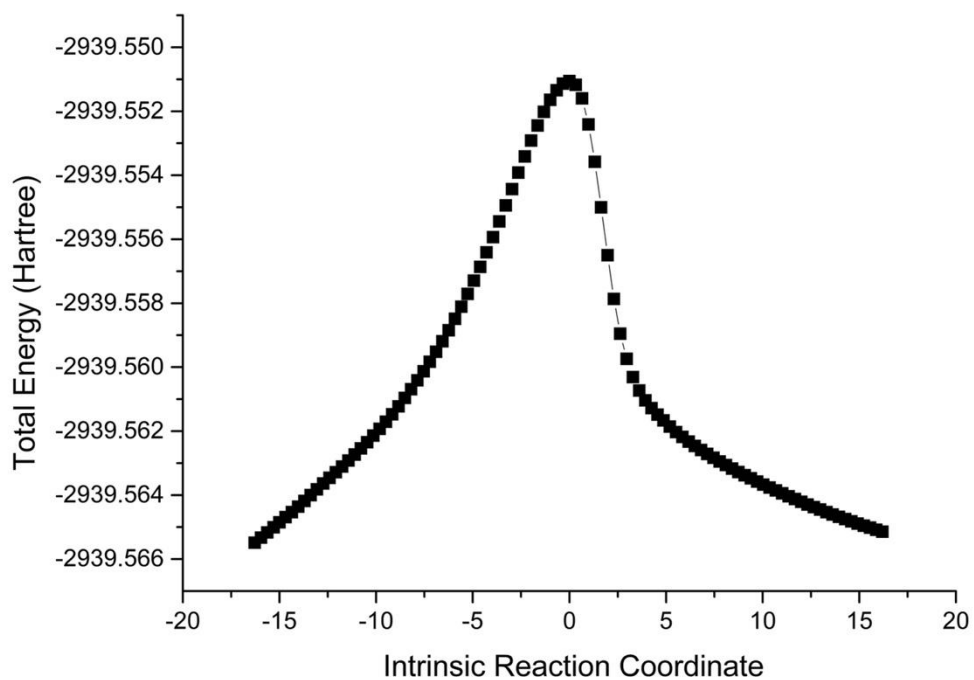


Figure S15. IRC calculation for TS2.

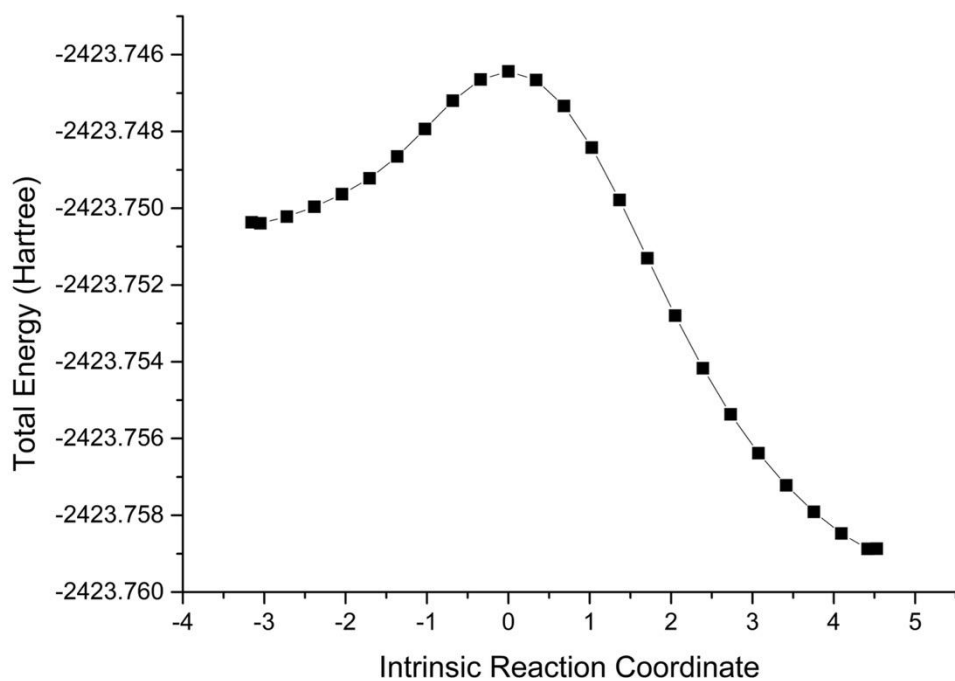


Figure S16. IRC calculation for TS1'.

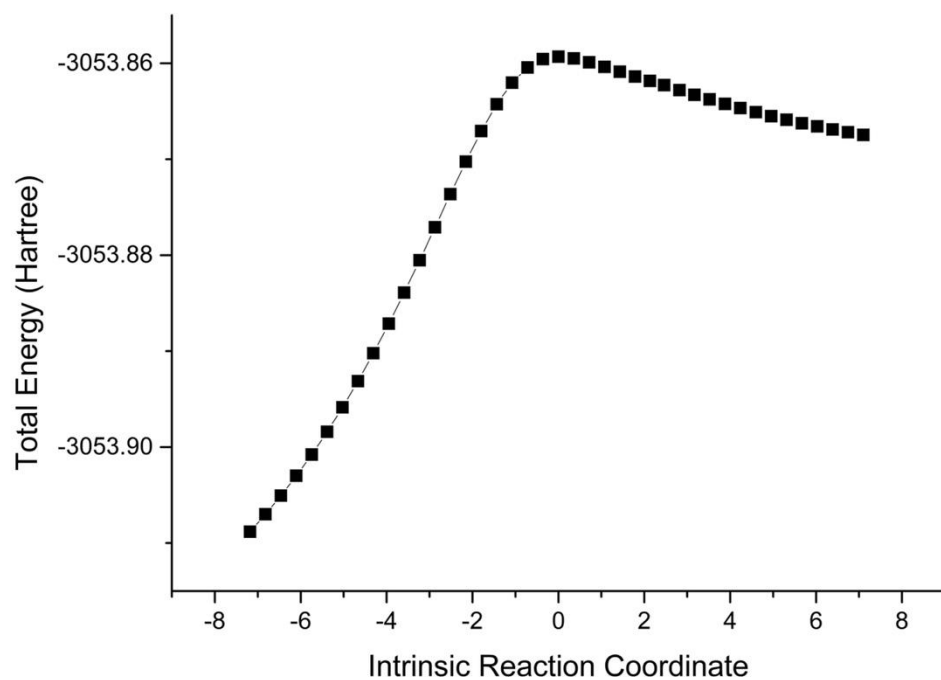


Figure S17. IRC calculation for TS2'.

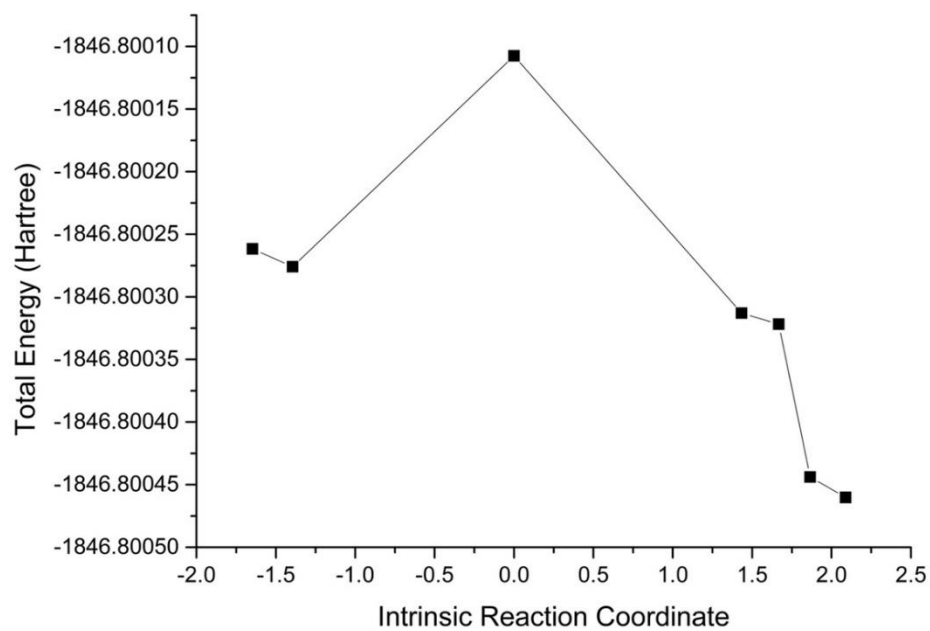
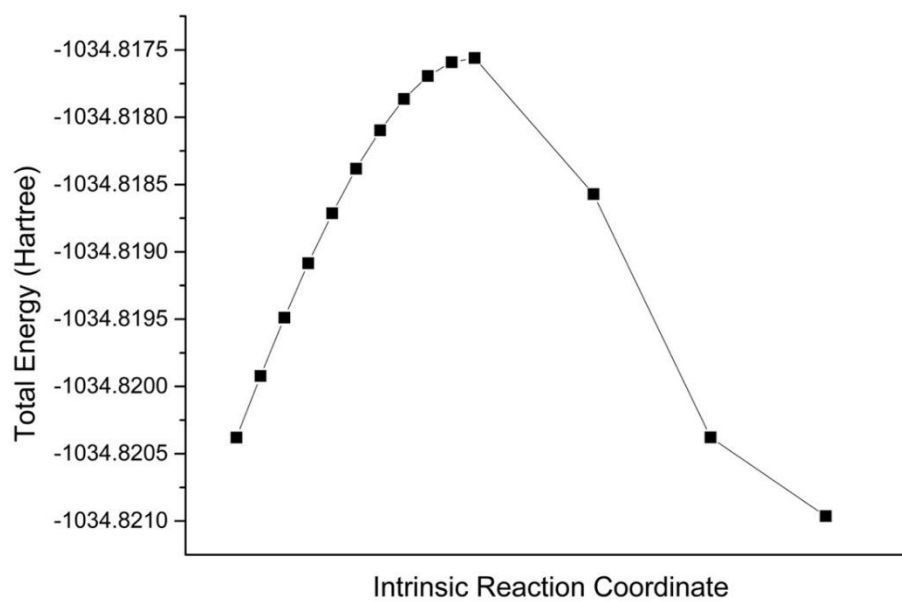


Figure S18. IRC calculation for TS3.





**Figure S19.** IRC calculation for **TS3''**.

## X-ray crystallography

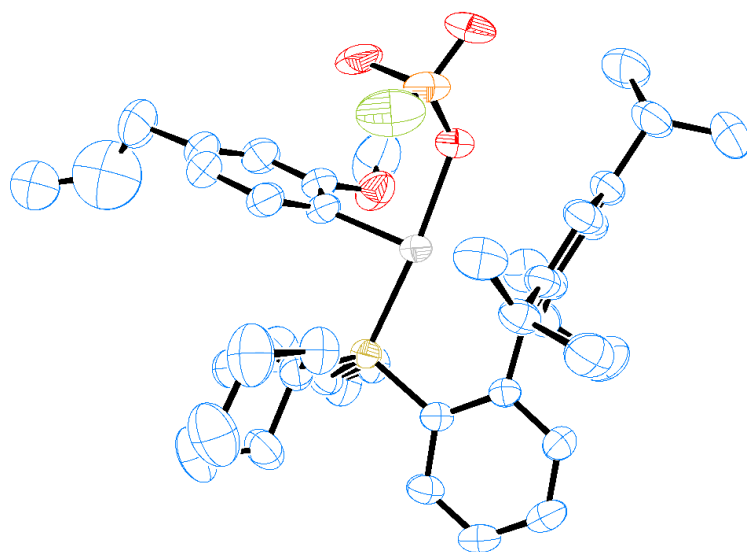


**Figure S20.** X-ray crystal structure of complex 10 (carbon atoms in blue). Hydrogen atoms are omitted for clarity. Ellipsoids are at 50% probability.

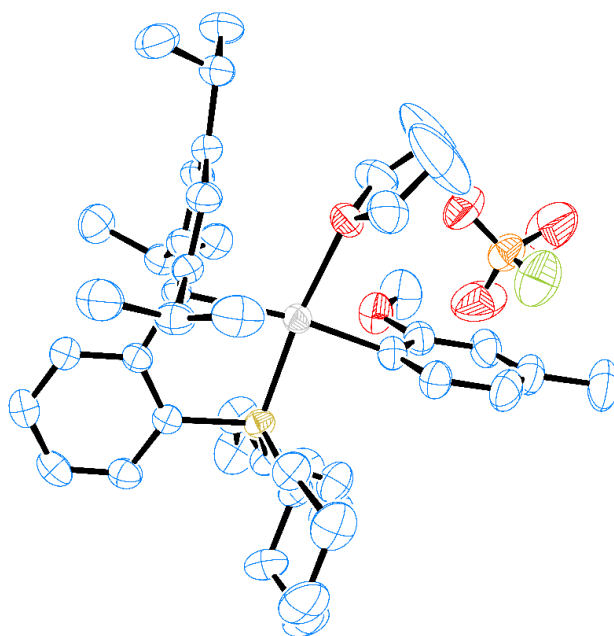


**Figure S21.** X-ray crystal structure of complex 11 (carbon atoms in blue). Hydrogen atoms are omitted for clarity. Ellipsoids are at 50% probability.

The intensities were empirically corrected for absorption using SCALE3 ABSPACK implemented in CrysAlisPRO.<sup>17</sup> The unit cell parameters were determined, and the Bragg intensities were integrated using CrysAlisPRO. The structure was solved and refined with SHELXS and SHELXL, respectively, in Olex2.<sup>18-20</sup>

CCDC no. of **10** is **2158941**. One level B alert is originating from an uncertainty in the element type of one of the second carbon in the propyl group (C8). However, no chemical justification exists for a different assignment of element. Another level B alert is originating from the use of isotropic displacement for two carbons in this propyl chain (C8 and C9). Refinement with these carbons with anisotropic displacement yielded a model with displacement of said carbons, that did not make chemical sense.

Item	value
Molecular formula	C <sub>43</sub> H <sub>60</sub> FO <sub>4</sub> PPdS
Formula weight	829.34
Crystal system	Monoclinic
Space group	<i>P</i> 2 <sub>1</sub> / <i>c</i>
a (Å)	14.3384
b (Å)	20.2920
c (Å)	14.8396
α (°)	90
β (°)	98.278
γ (°)	90
Volume (Å <sup>3</sup> )	4272.67
Z	4
T (K)	100
ρ (g cm <sup>-3</sup> )	1.289
λ (Å)	0.71073
μ (mm <sup>-1</sup> )	0.56
# measured refl	191370
# unique refl	10667
R <sub>int</sub>	0.0318
# parameters	492
R(F <sup>2</sup> ), all refl	0.0344
R <sub>w</sub> (F <sup>2</sup> ), all refl	0.0980
Goodness of fit	1.097

CCDC no. of **11** is **2158948**. The level B alert is originating from vibration of aliphatic carbon in coordinating THF group (C01I).

Item	value
Molecular formula	C <sub>45</sub> H <sub>66</sub> FO <sub>5</sub> PPdS
Formula weight	875.40
Crystal system	Monoclinic
Space group	Cc
a (Å)	17.9004
b (Å)	14.4683
c (Å)	17.1498
α (°)	90
β (°)	95.038
γ (°)	90
Volume (Å <sup>3</sup> )	4424.44
Z	4
T (K)	300
ρ (g cm <sup>-3</sup> )	1.314
λ (Å)	0.71073
μ (mm <sup>-1</sup> )	0.549
# measured refl	50521
# unique refl	10574
R <sub>int</sub>	0.0344
# parameters	495
R(F <sup>2</sup> ), all refl	0.0277
R <sub>w</sub> (F <sup>2</sup> ), all refl	0.0699
Goodness of fit	1.04

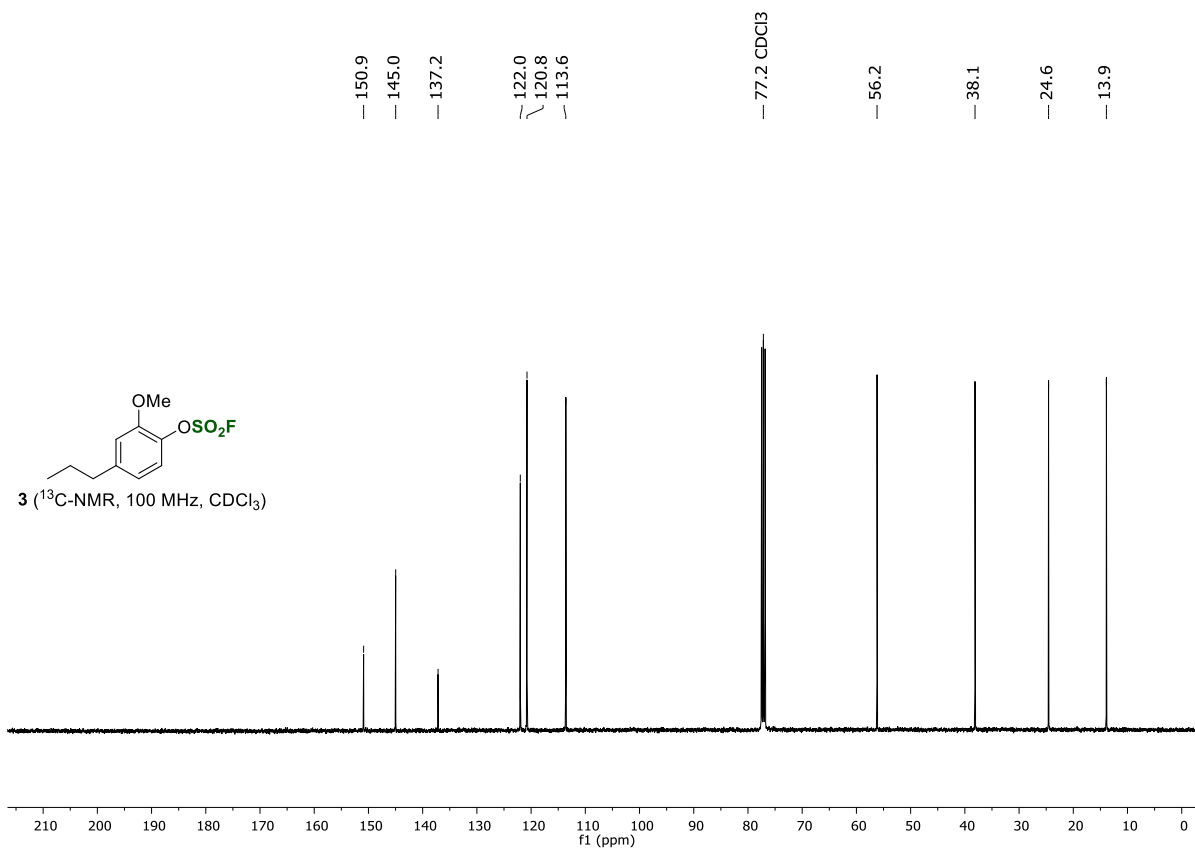
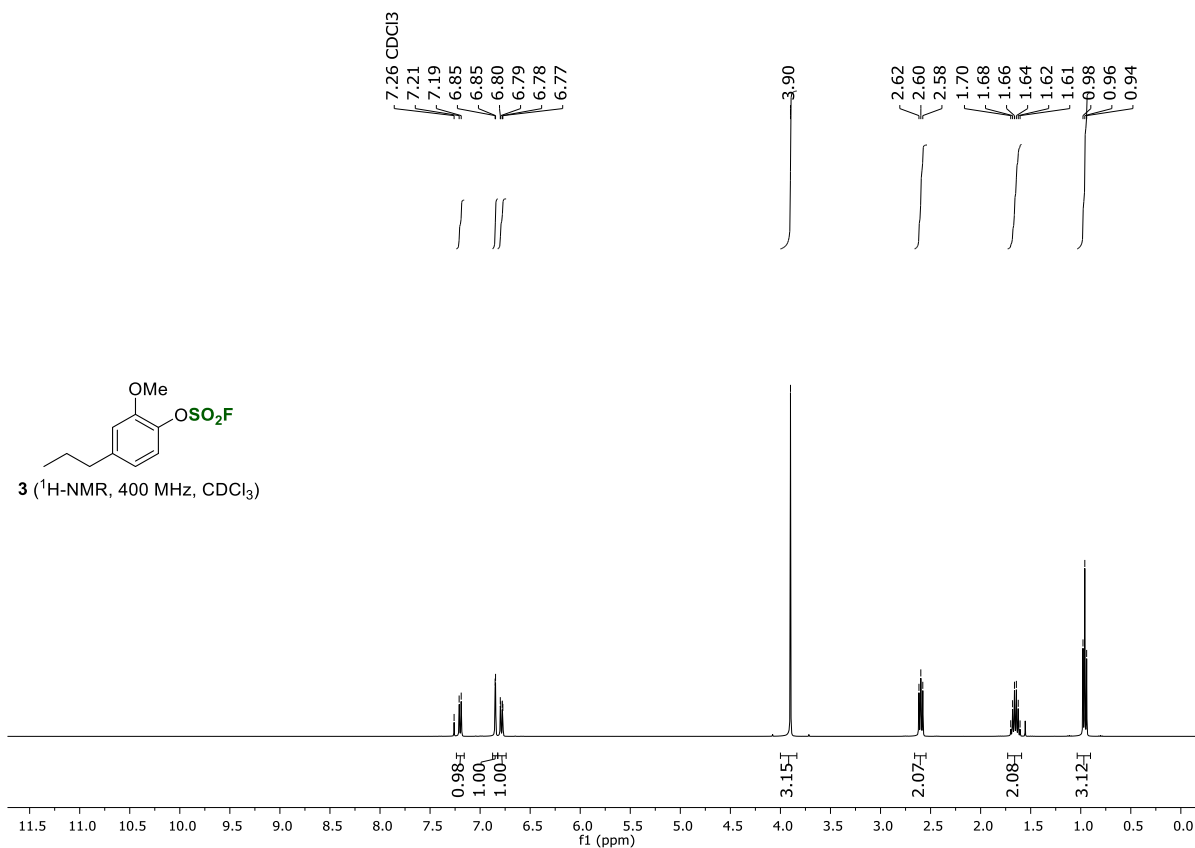
## References

- (1) Kristensen, S. K.; Eikeland, E. Z.; Taarning, E.; Lindhardt, A. T.; Skrydstrup, T. *Ex situ* generation of stoichiometric HCN and its application in the Pd-catalysed cyanation of aryl bromides: evidence for a transmetallation step between two oxidative addition Pd-complexes. *Chem. Sci.* **2017**, *8*, 8094–8105.
- (2) Veryser, C.; Demaerel, J.; Bieliunas V.; Gilles, P.; De Borggraeve, W. M. Ex Situ Generation of Sulfuryl Fluoride for the Synthesis of Aryl Fluorosulfates. *Org. Lett.* **2017**, *19*, 5244–5247.
- (3) Van den Bosch, S.; Schutyser, W.; Vanholme, R.; Driessen, T.; Koelewijn, S.-F.; Renders, T.; De Meester, B.; Huijgen, W. J. J.; Dehaen, W.; Courtin, C. M.; Lagrain, B.; Boerjan, W.; Sels, B. F. Reductive lignocellulose fractionation into soluble lignin-derived phenolic monomers and dimers and processable carbohydrate pulps. *Energy Environ. Sci.* **2015**, *8*, 1748–1763.
- (4) Large-scale synthesis of methoxyterephthalic acid for the study of MPET polymer was achieved by KMnO<sub>4</sub> oxidation of 2,5-dimethylanisole: Vermoortele, F.; Vandichel, M.; Van de Voorde, B.; Ameloot, R.; Waroquier, M. Electronic Effects of Linker Substitution on Lewis Acid Catalysis with Metal-Organic Frameworks. *Angew. Chem. Int. Ed.* **2012**, *51*, 4887–4890.
- (5) Andersen, T. L.; Friis, S. D.; Audrain, H.; Nordeman, P.; Antoni, G.; Skrydstrup, T. Efficient 11 C-Carbonylation of Isolated Aryl Palladium Complexes for PET: Application to Challenging Radiopharmaceutical Synthesis. *J. Am. Chem. Soc.* **2015**, *137*, 1548–1555.
- (6) Klinkenberg, J. L.; Hartwig, J. F. Reductive elimination from arylpalladium cyanide complexes. *J. Am. Chem. Soc.* **2012**, *134*, 5758–5761.
- (7) Erhardt, S.; Grushin, V. V.; Kilpatrick, A. H.; Macgregor, S. A.; Marshall, W. J.; Roe, D. C. Mechanisms of Catalyst Poisoning in Palladium-Catalyzed Cyanation of Haloarenes. Remarkably Facile C-N Bond Activation in the [(Ph<sub>3</sub>P)<sub>4</sub>Pd]/[Bu<sub>4</sub>N]<sup>+</sup> CN<sup>-</sup> System. *J. Am. Chem. Soc.* **2008**, *130*, 4828–4845.
- (8) Ushkov, A. V.; Grushin, V. V. Rational Catalysis Design on the Basis of Mechanistic Understanding: Highly Efficient Pd-Catalyzed Cyanation of Aryl Bromides with NaCN in Recyclable Solvents. *J. Am. Chem. Soc.* **2011**, *133*, 10999–11005.
- (9) Frisch, M. J.; Trucks, G. W.; Schlegel, H. B.; Scuseria, G. E.; Robb, M. A.; Cheeseman, J. R.; Scalmani, G.; Barone, V.; Petersson, G. A.; Nakatsuji, H.; Li, X.; Caricato, M.; Marenich, A. V.; Bloino, J.; Janesko, B. G.; Gomperts, R.; Mennucci, B.; Hratch, D. J. Gaussian 16, Revision B.01., **2016**.
- (10) Weigend, F.; Ahlrichs, R. Balanced basis sets of split valence, triple zeta valence and quadruple zeta valence quality for H to Rn: Design and assessment of accuracy. *Phys. Chem. Chem. Phys.* **2005**, *7*, 3297.
- (11) Weigend, F. Accurate Coulomb-fitting basis sets for H to Rn. *Phys. Chem. Chem. Phys.* **2006**, *8*, 1057.
- (12) Grimme, S.; Antony, J.; Ehrlich, S.; Krieg, H. A consistent and accurate ab initio parametrization of density functional dispersion correction (DFT-D) for the 94 elements H-Pu. *J. Chem. Phys.* **2010**, *132*, 154104.
- (13) Perdew, J. P.; Burke, K.; Ernzerhof, M. Generalized Gradient Approximation Made Simple. *Phys. Rev. Lett.* **1996**, *77*, 3865–3868.
- (14) Perdew, J. P.; Burke, K.; Ernzerhof, M. Generalized Gradient Approximation Made Simple. *Phys. Rev. Lett.* **1997**, *78*, 1396–1396.
- (15) Marenich, A. V.; Cramer, C. J.; Truhlar, D. G. Universal Solvation Model Based on Solute Electron Density and on a Continuum Model of the Solvent Defined by the Bulk Dielectric Constant and Atomic Surface Tensions. *J. Phys. Chem. B*, **2009**, *113*, 6378–6396.
- (16) Obst, M. F.; Gevorgyan, A.; Bayer, A.; Hopmann, K. H. Mechanistic Insights into Copper-Catalyzed Carboxylations. *Organometallics*, **2020**, *39*, 1545–1552.
- (17) CrysAlisPRO, Oxford Diffraction /Agilent Technologies UK Ltd, Yarnton, England.

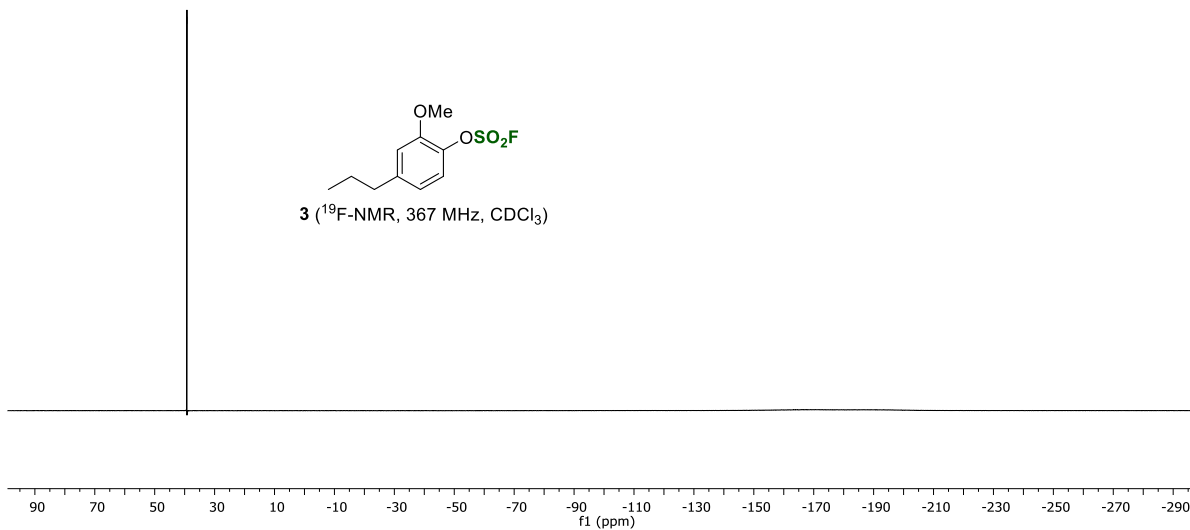
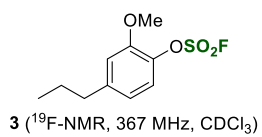
- (18) Dolomanov, O.V.; Bourhis, L. J.; Gildea, R. J.; Howard, J. A. K.; Puschmann, H. OLEX2: a complete structure solution, refinement and analysis program. *J. Appl. Cryst.* **2009**, *42*, 339–341.
- (19) Sheldrick, G. M. A short history of SHELX. *Acta Cryst.* A64, **2008**, 112–122.
- (20) Sheldrick, G. M. Crystal structure refinement with SHELXL *Acta Cryst.* C71, **2015**, 3–8.

# NMR Spectra

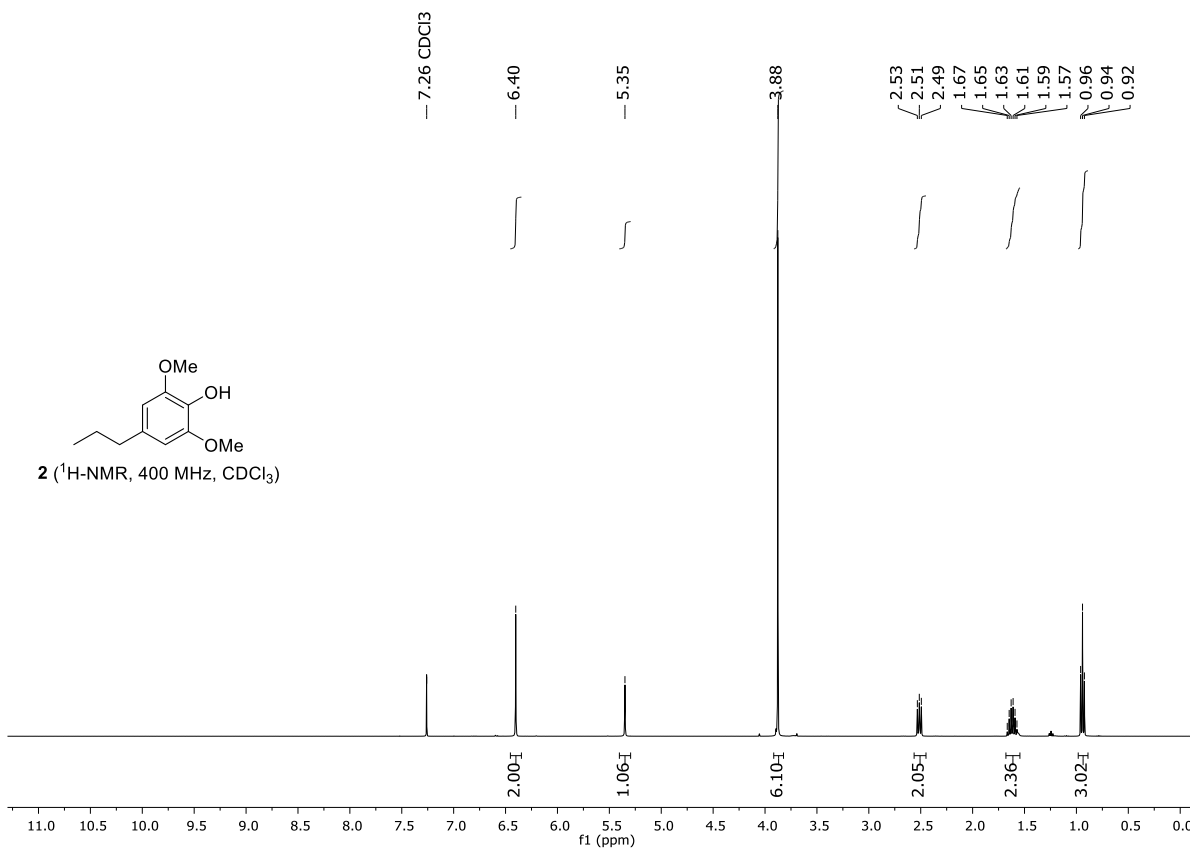
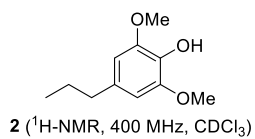
2-methoxy-4-propylphenyl sulfurofluoridate (<sup>1</sup>H-NMR, <sup>13</sup>C-NMR, and <sup>19</sup>F-NMR)

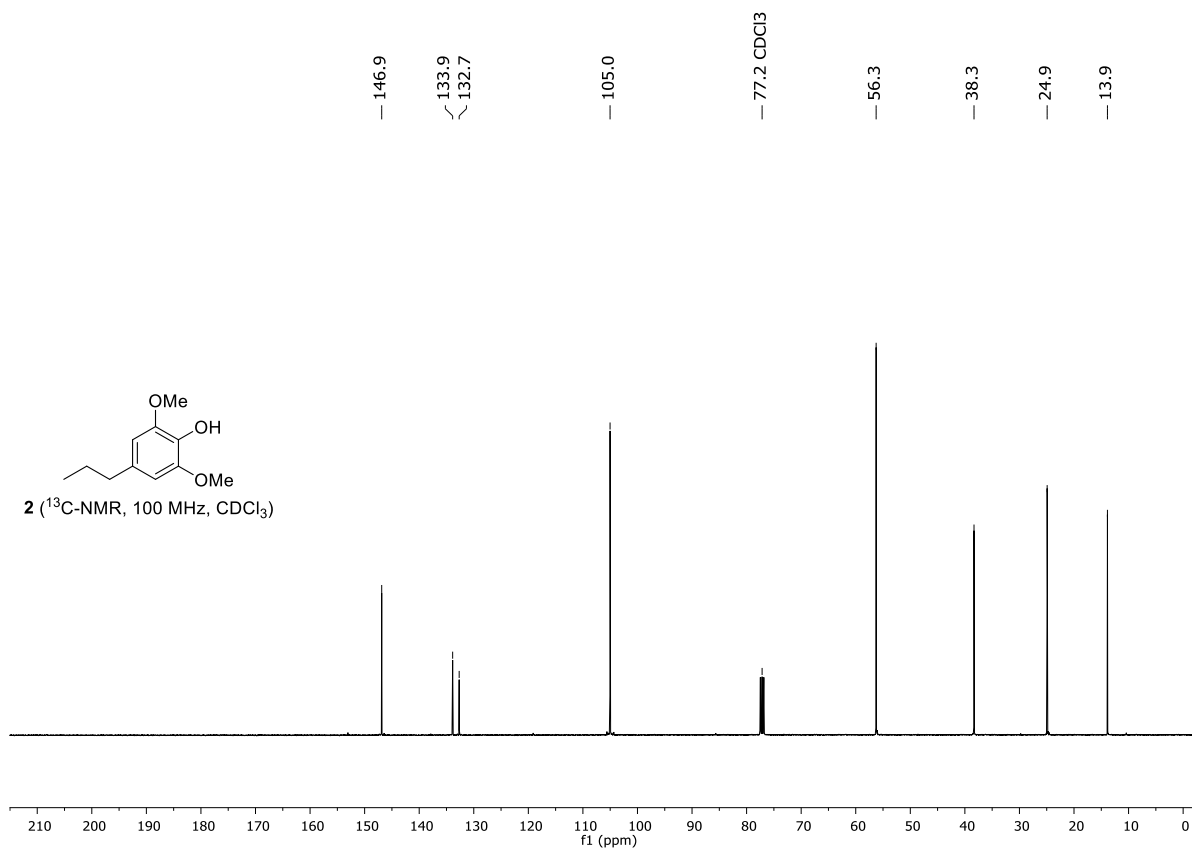




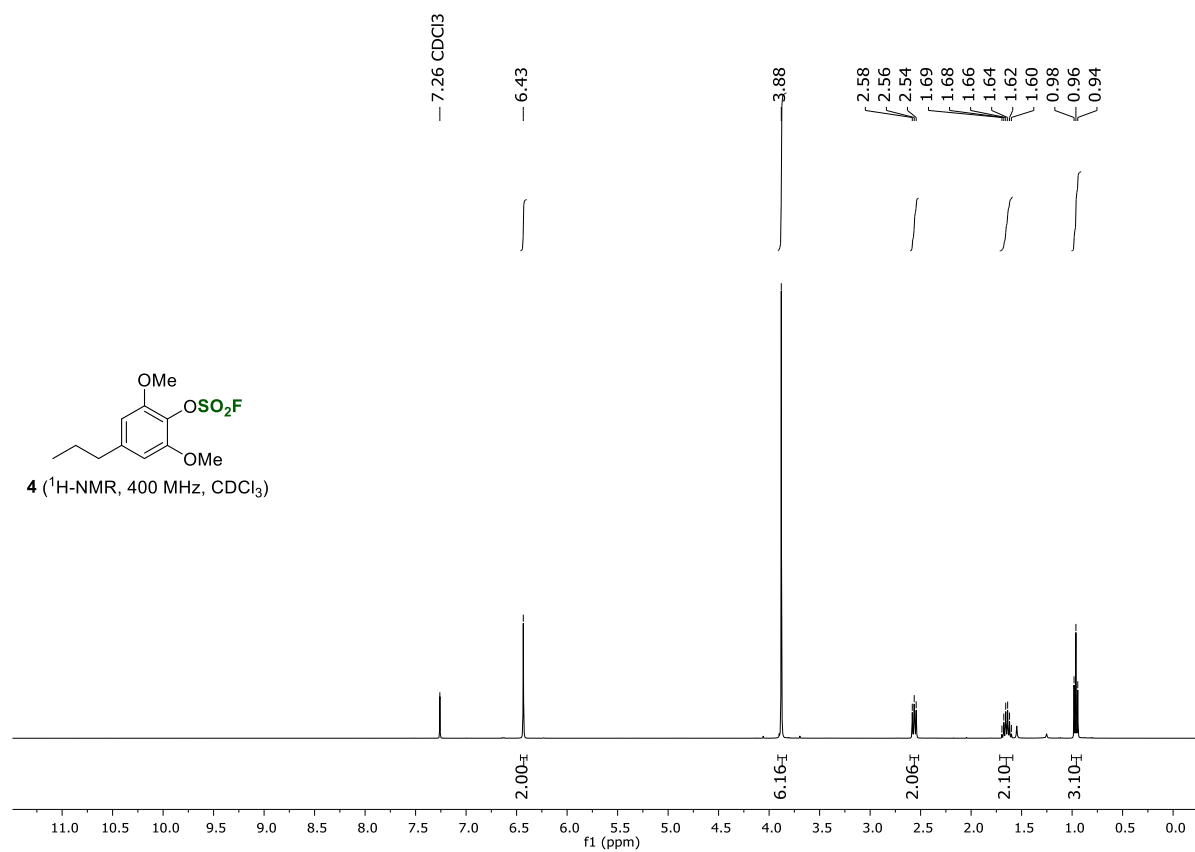


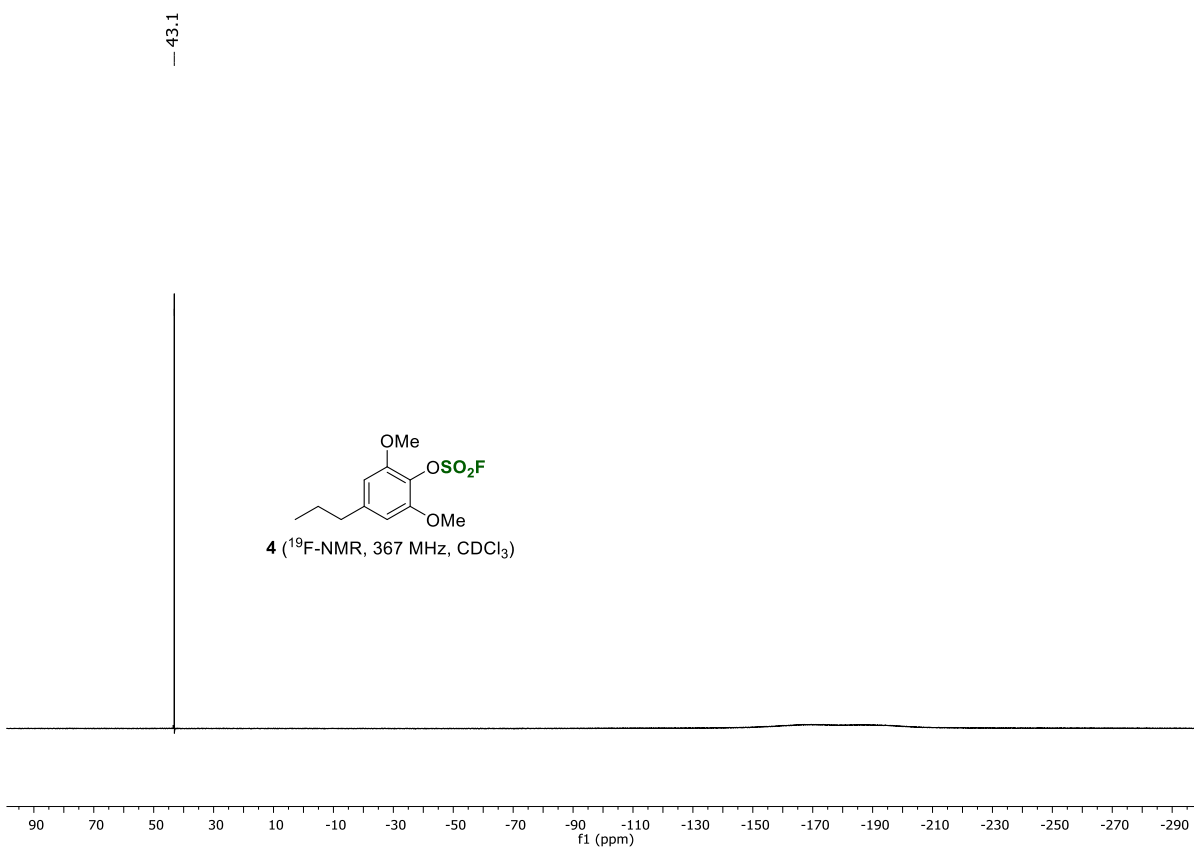
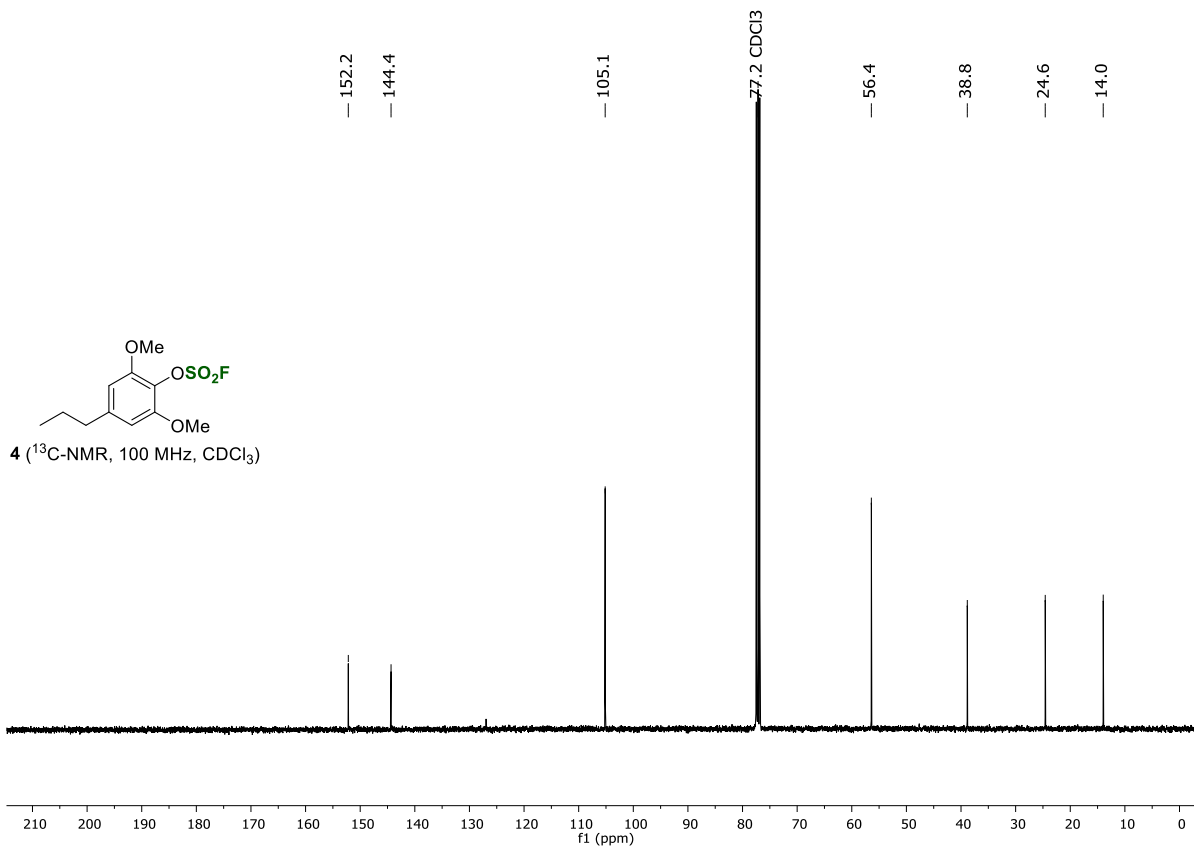
### 2,6-dimethoxy-4-propylphenol ( $^1\text{H}$ -NMR and $^{13}\text{C}$ -NMR)



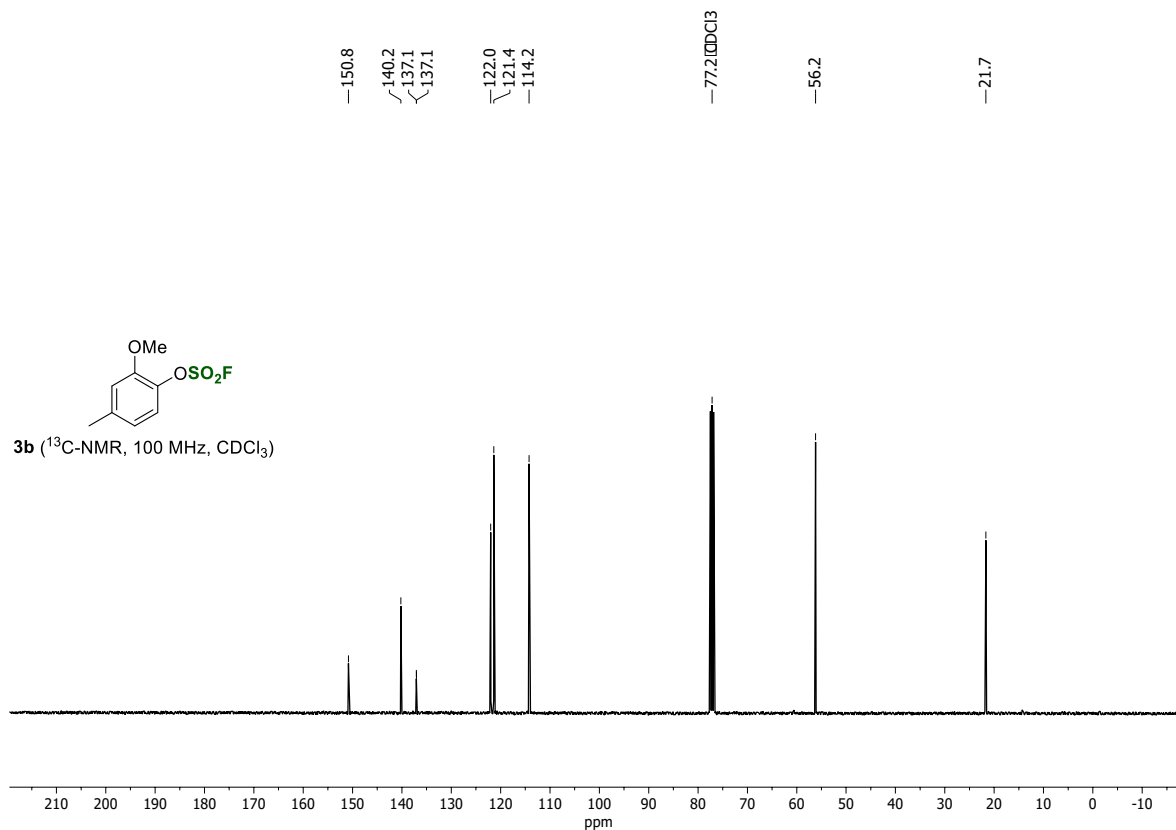
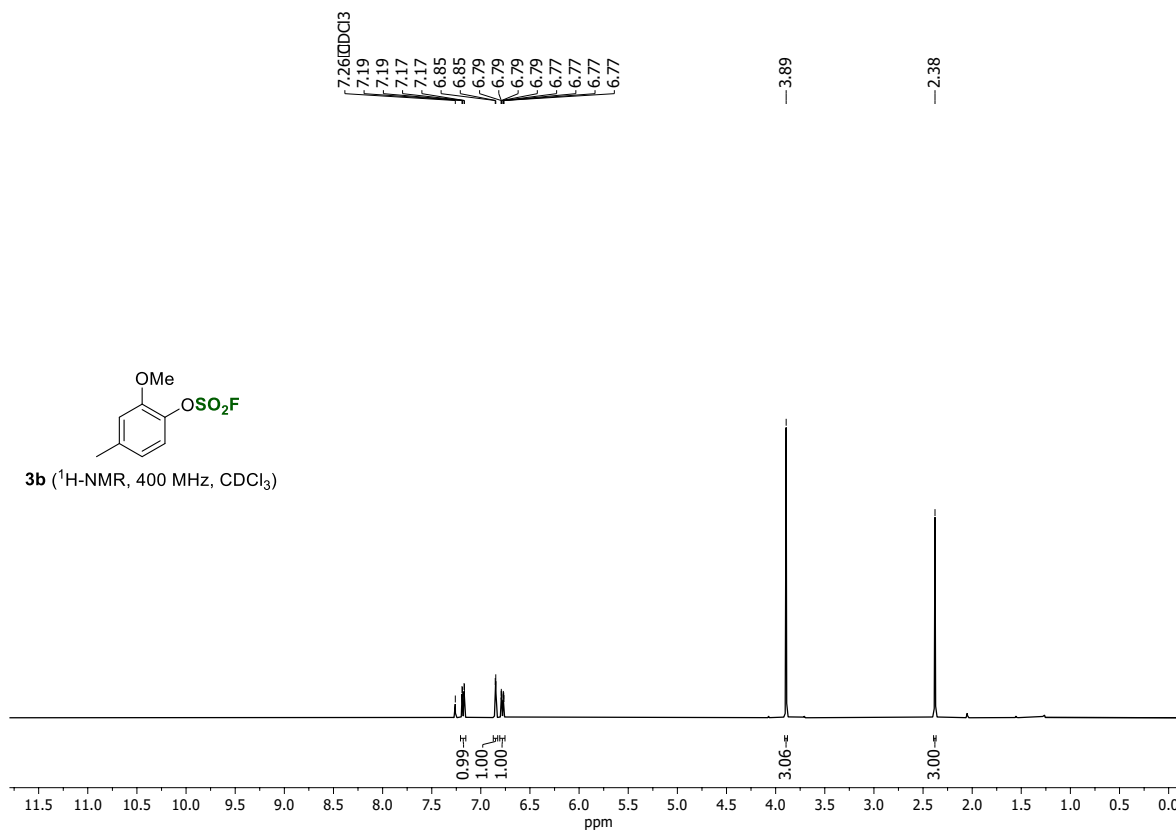


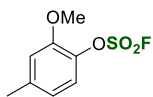
**2,6-dimethoxy-4-propylphenyl sulfurofluoridate** (<sup>1</sup>H-NMR, <sup>13</sup>C-NMR, and <sup>19</sup>F-NMR)



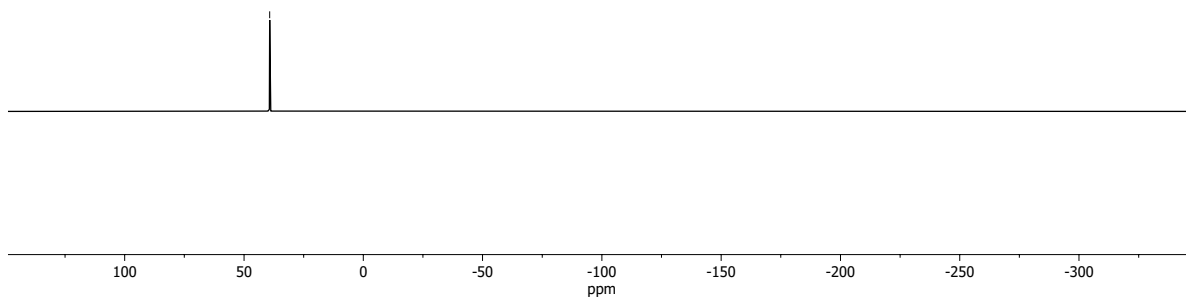


2-methoxy-4-methylphenyl sulfurofluoridate (<sup>1</sup>H-NMR, <sup>13</sup>C-NMR, and <sup>19</sup>F-NMR)

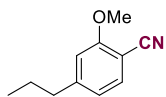




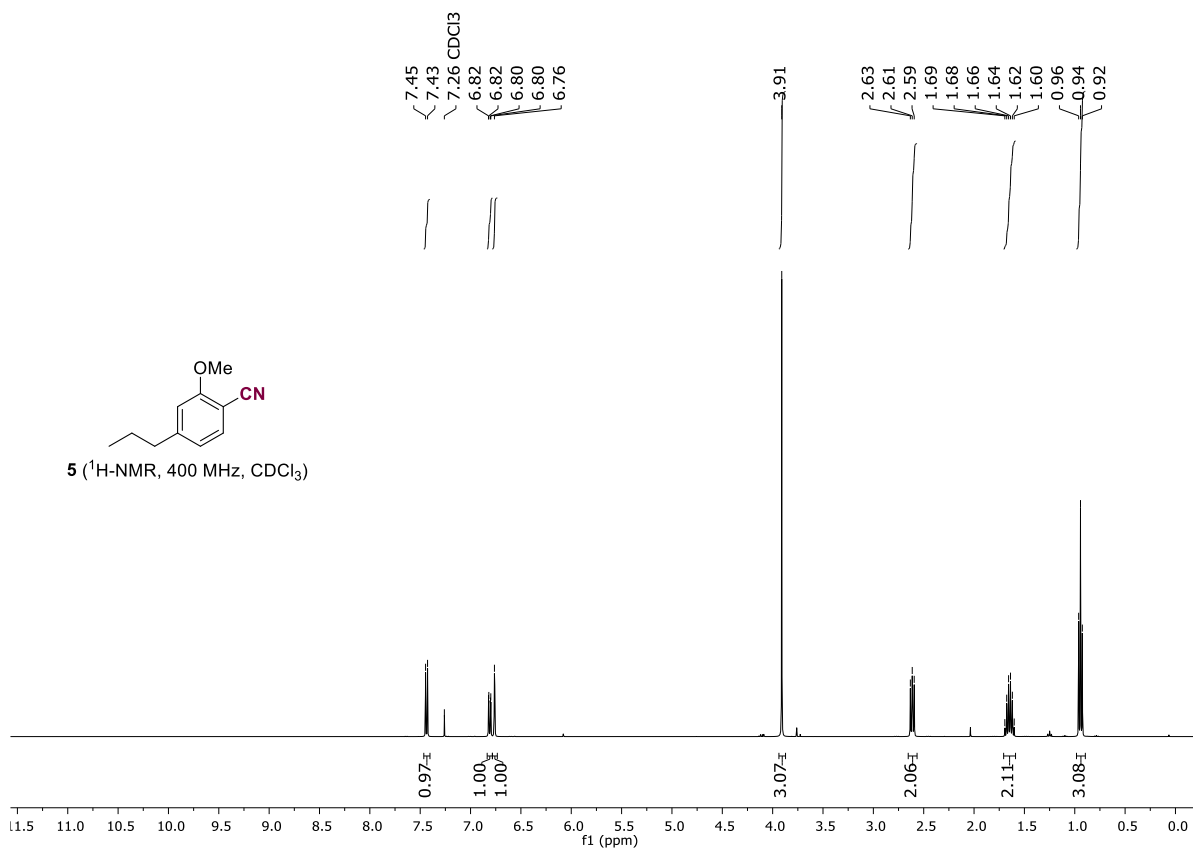
**3b** ( $^{19}\text{F}$ -NMR, 367 MHz,  $\text{CDCl}_3$ )

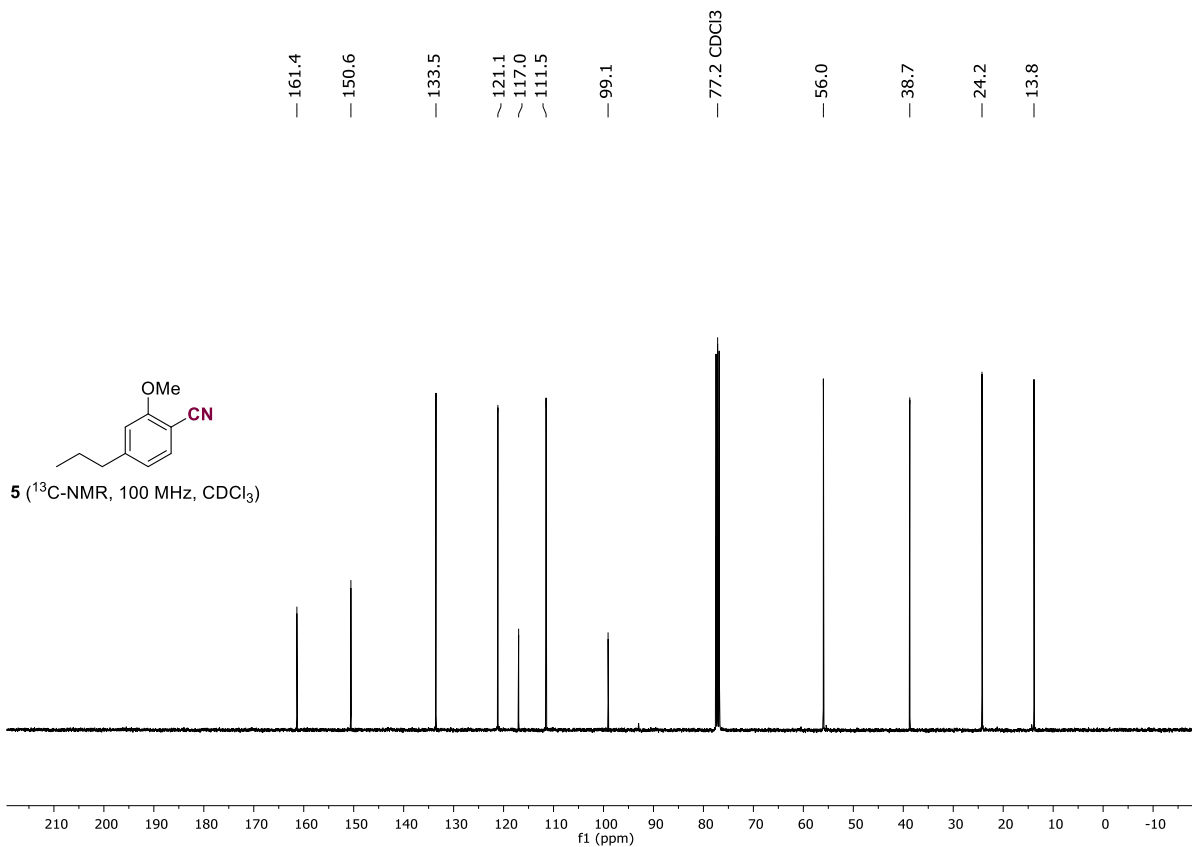


**2-methoxy-4-propylbenzonitrile from isolated aryl fluorosulfate ( $^1\text{H}$ -NMR and  $^{13}\text{C}$ -NMR)**

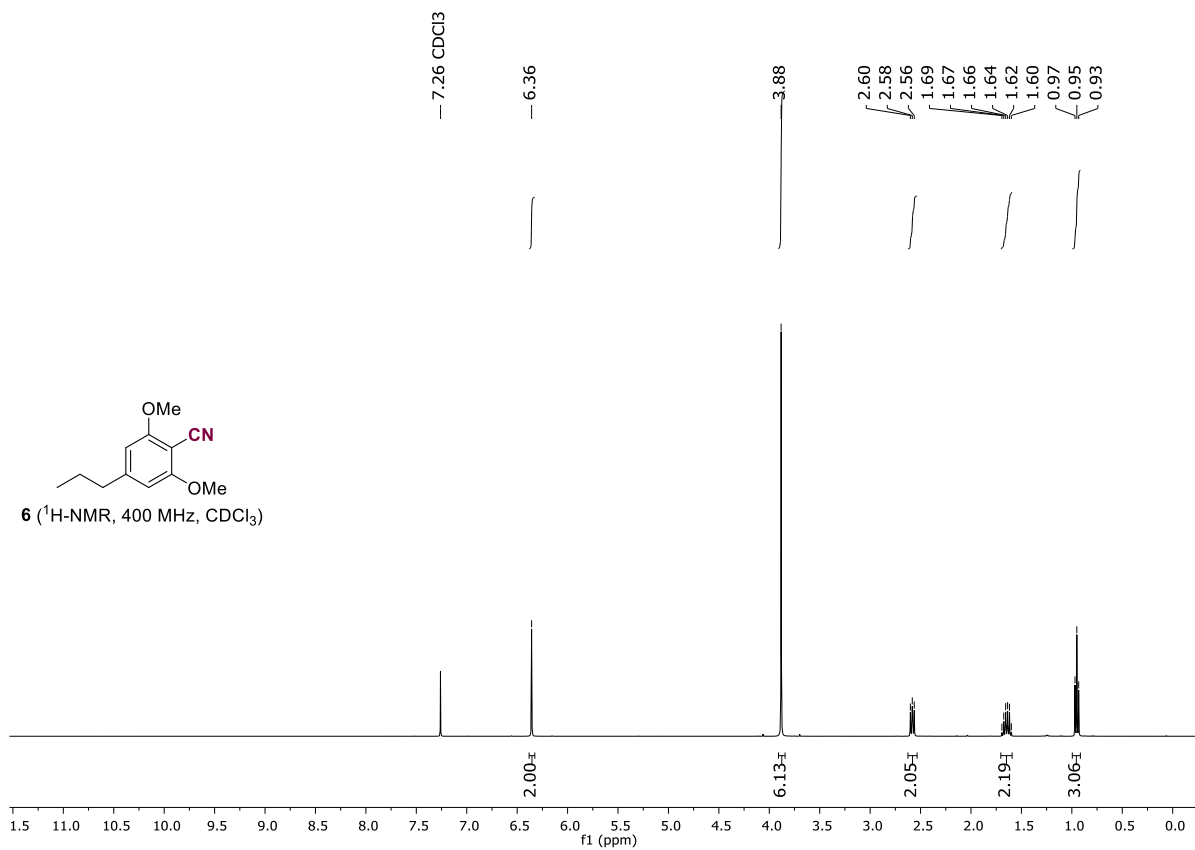


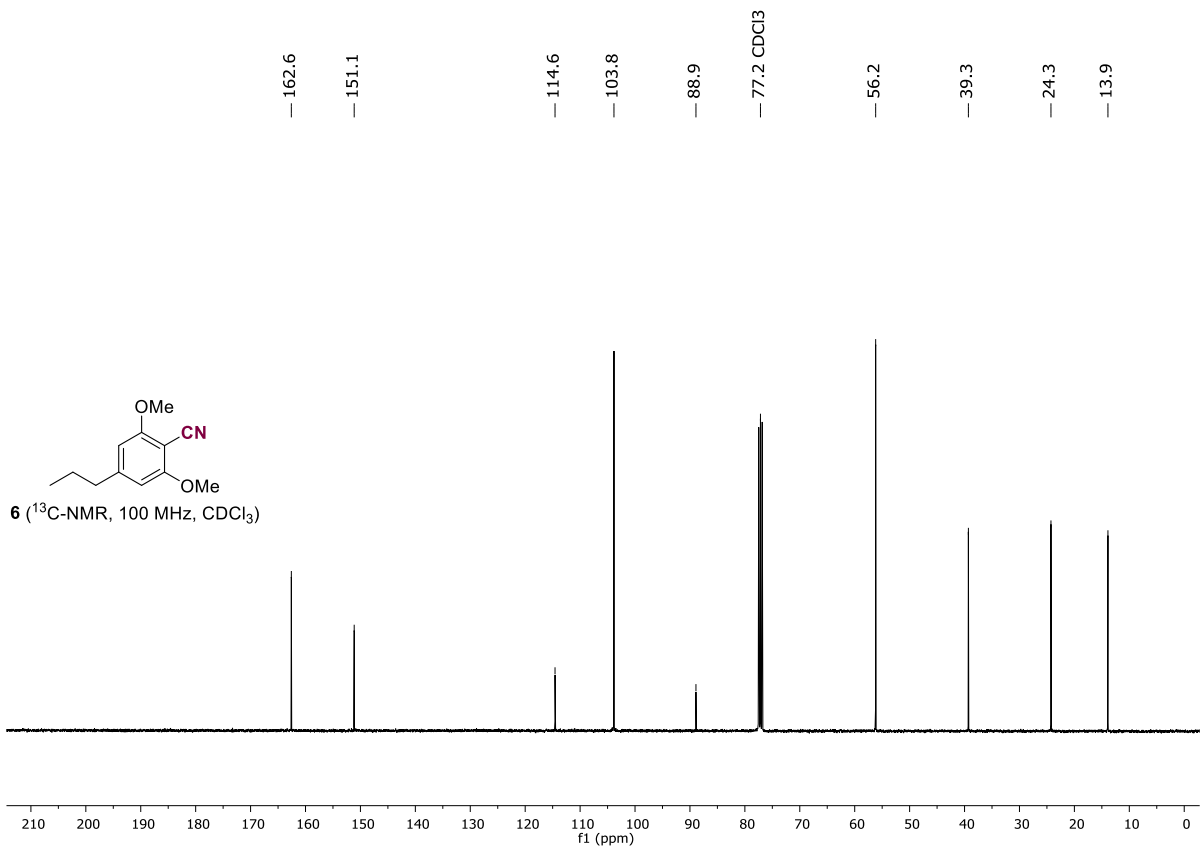
**5** ( $^1\text{H}$ -NMR, 400 MHz,  $\text{CDCl}_3$ )



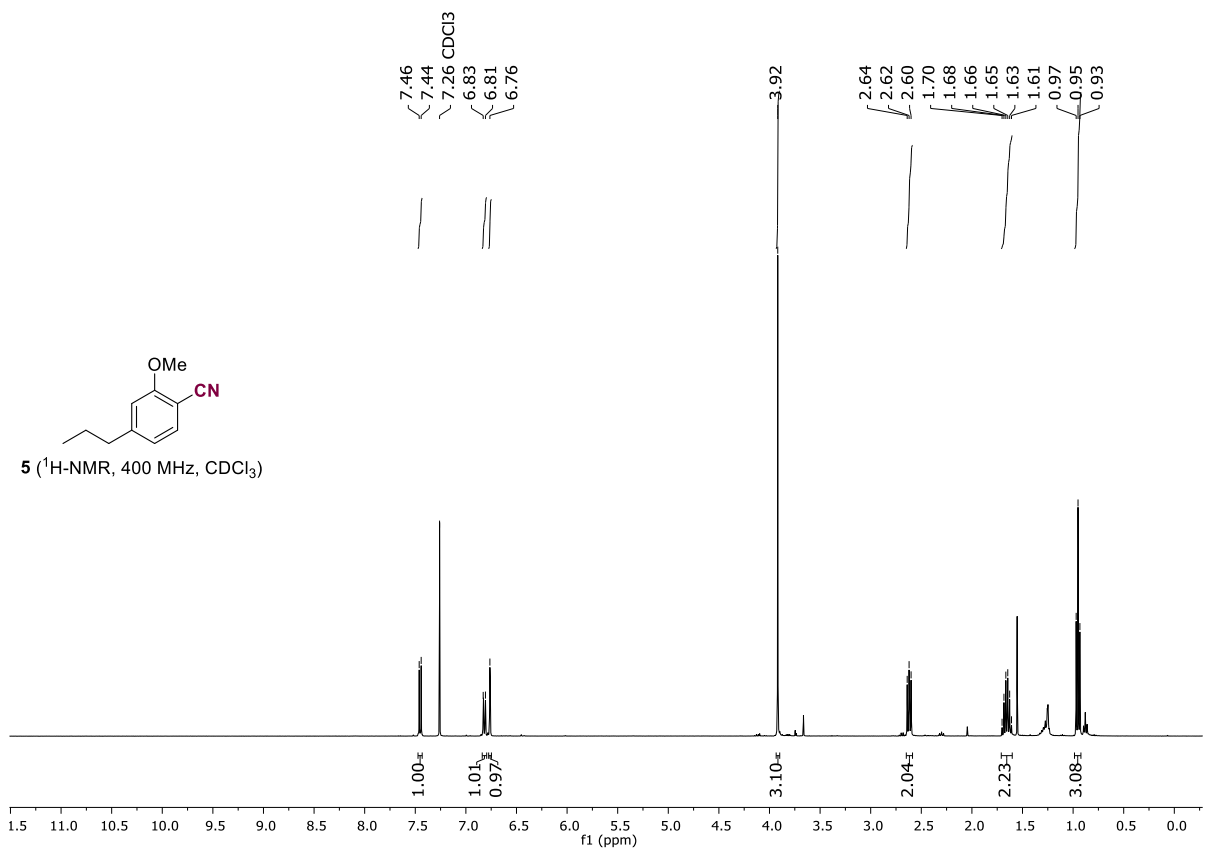


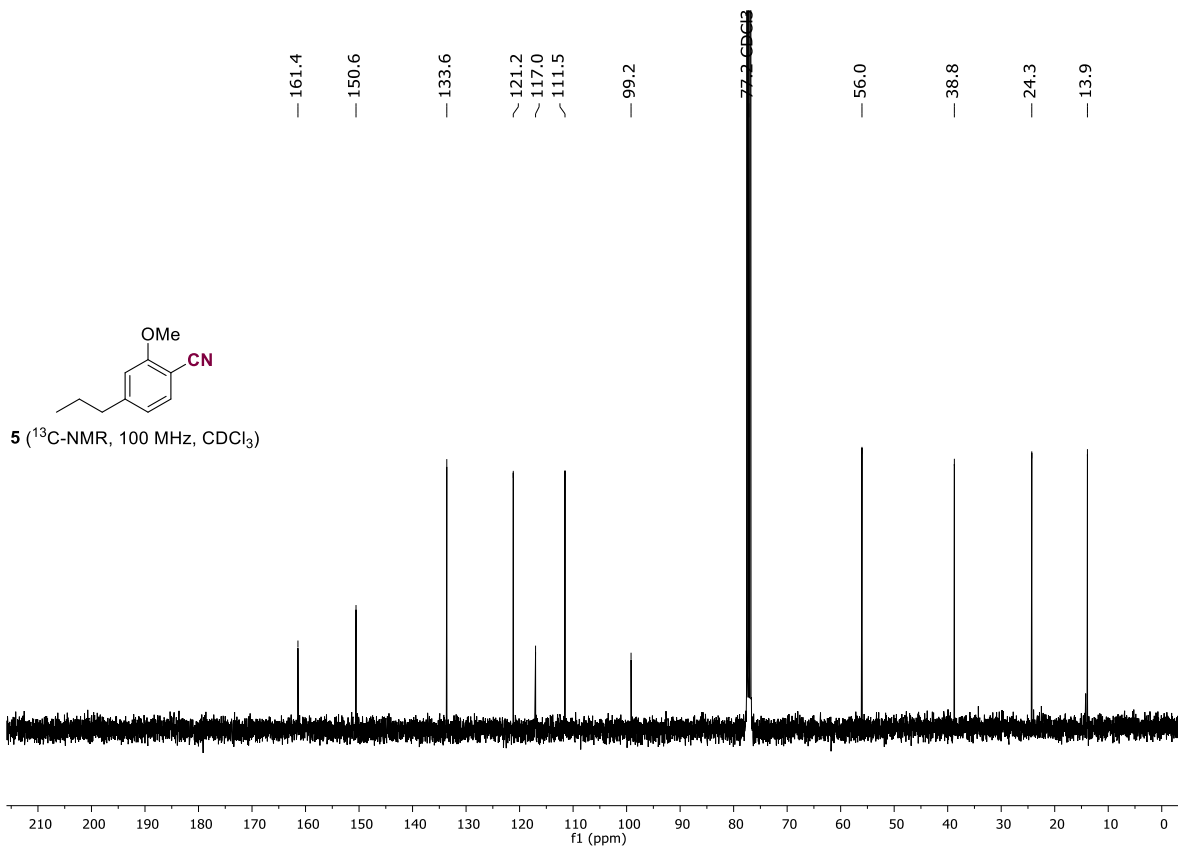
**2,6-Dimethoxy-4-propylbenzonitrile from isolated aryl fluorosulfate (<sup>1</sup>H-NMR and <sup>13</sup>C-NMR)**



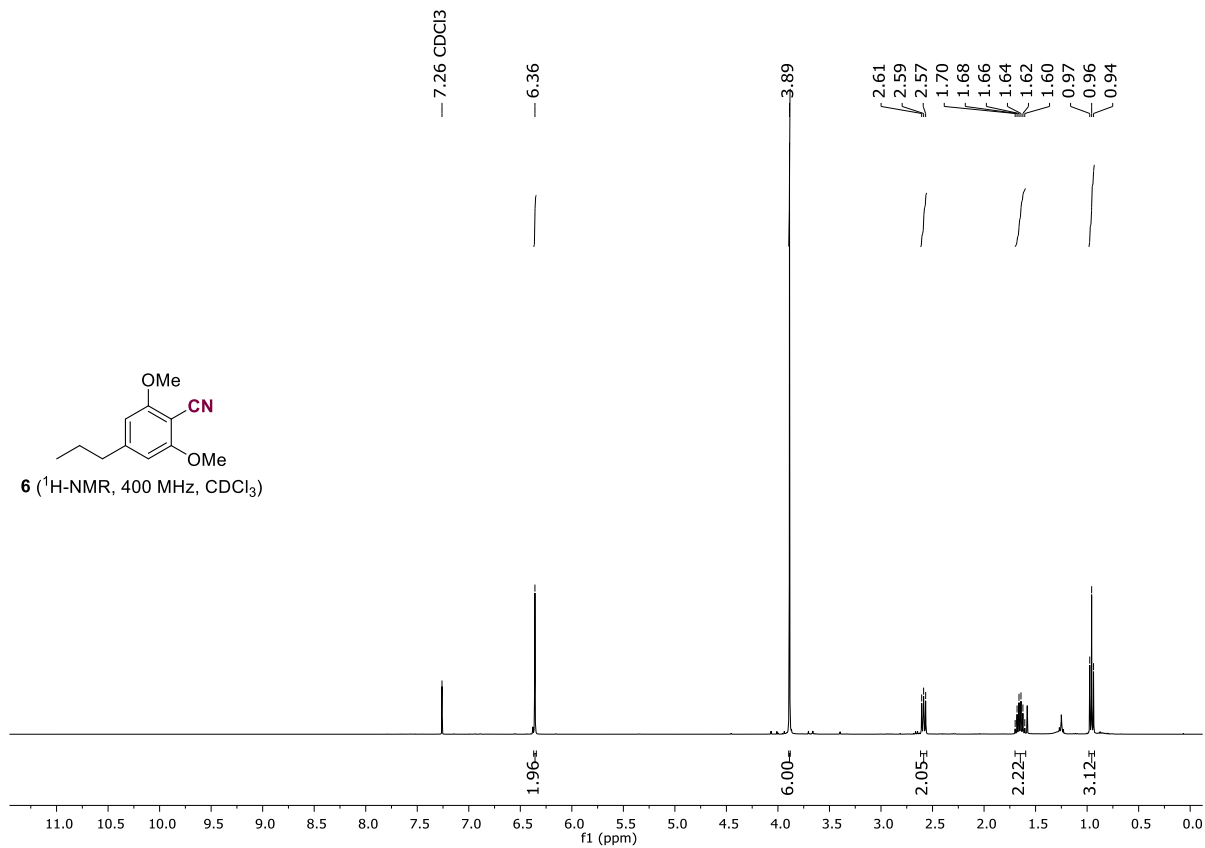


**2-methoxy-4-propylbenzotrile from Birch sawdust (1<sup>1</sup>H-NMR and 1<sup>3</sup>C-NMR)**

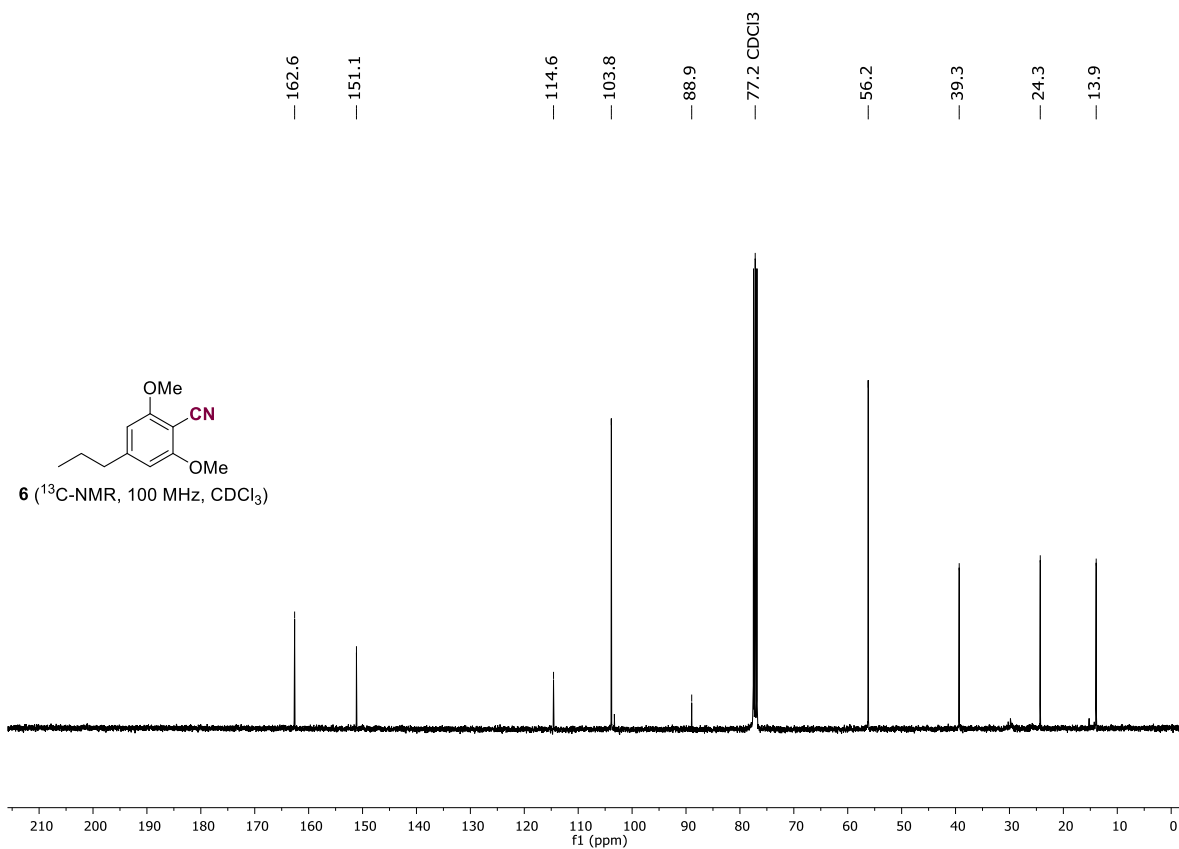




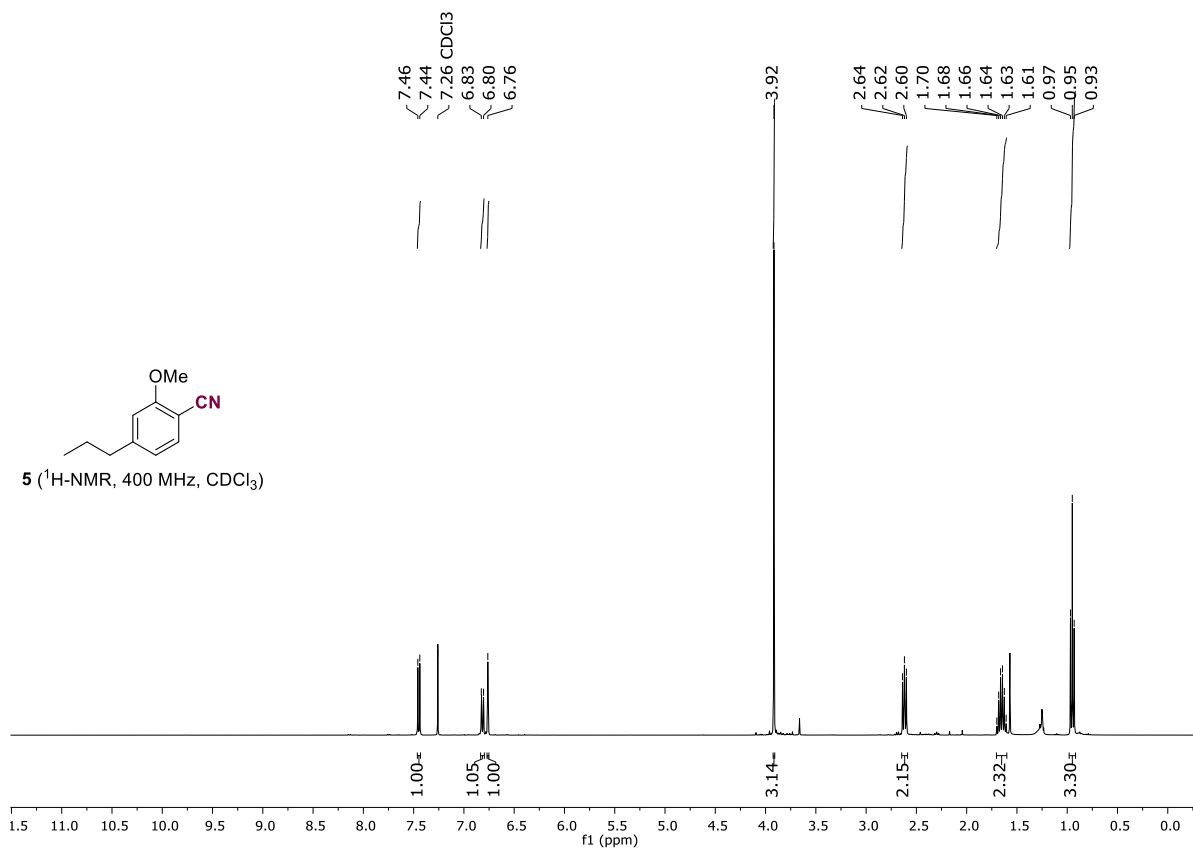
**2,6-dimethoxy-4-propylbenzonitrile from Birch sawdust ( $^1\text{H-NMR}$  and  $^{13}\text{C-NMR}$ )**

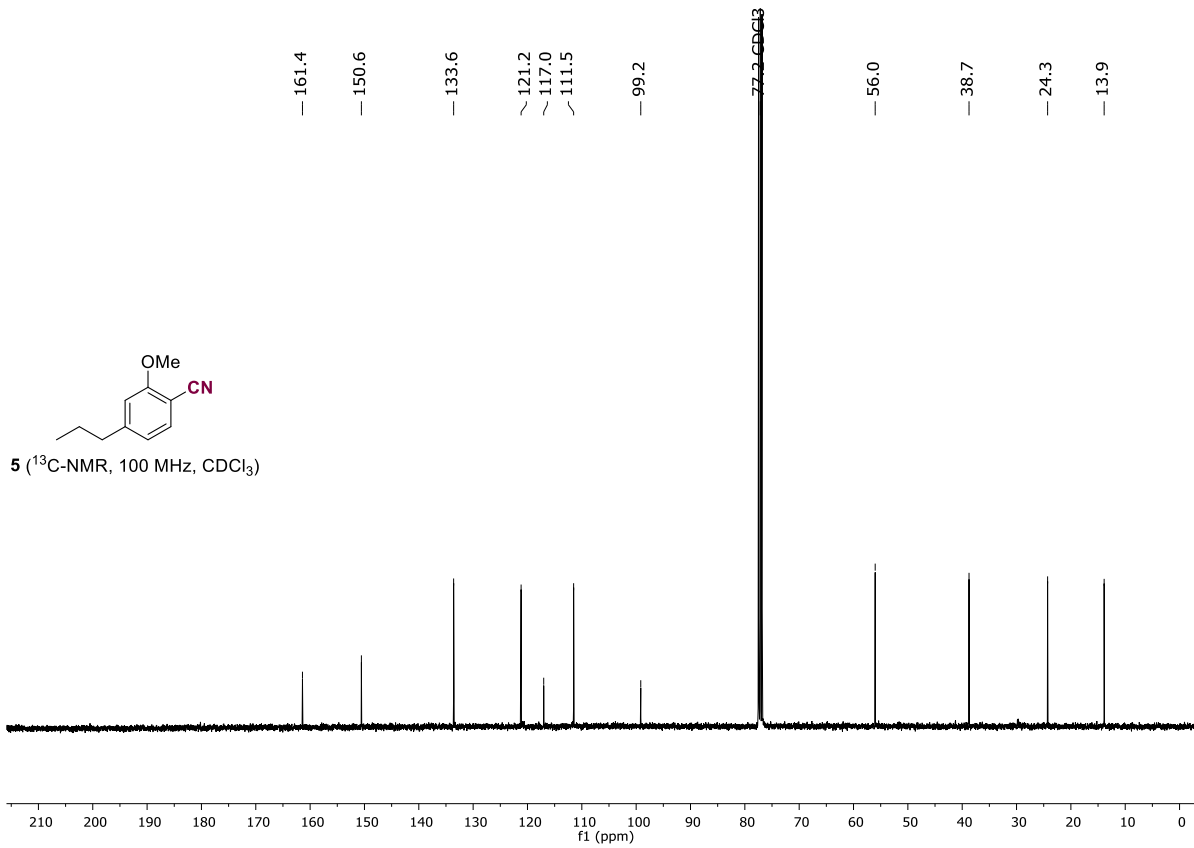




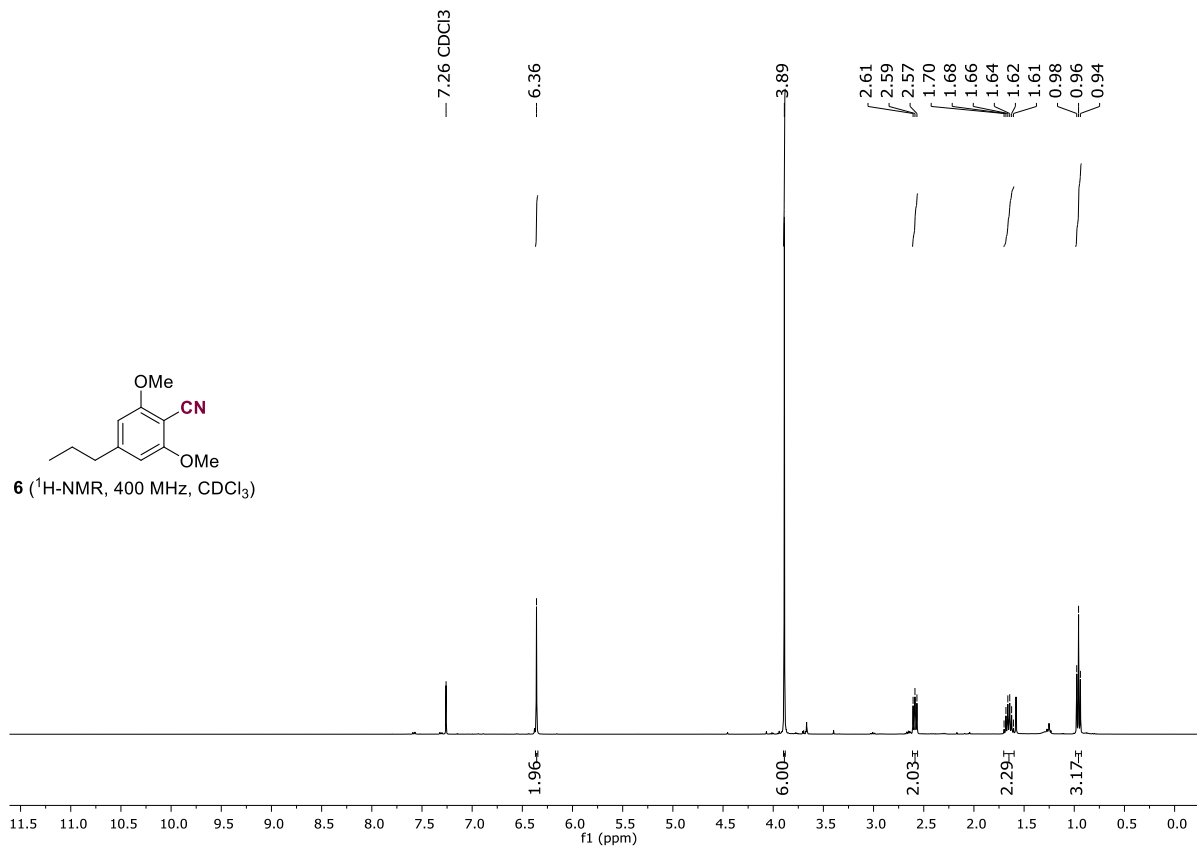


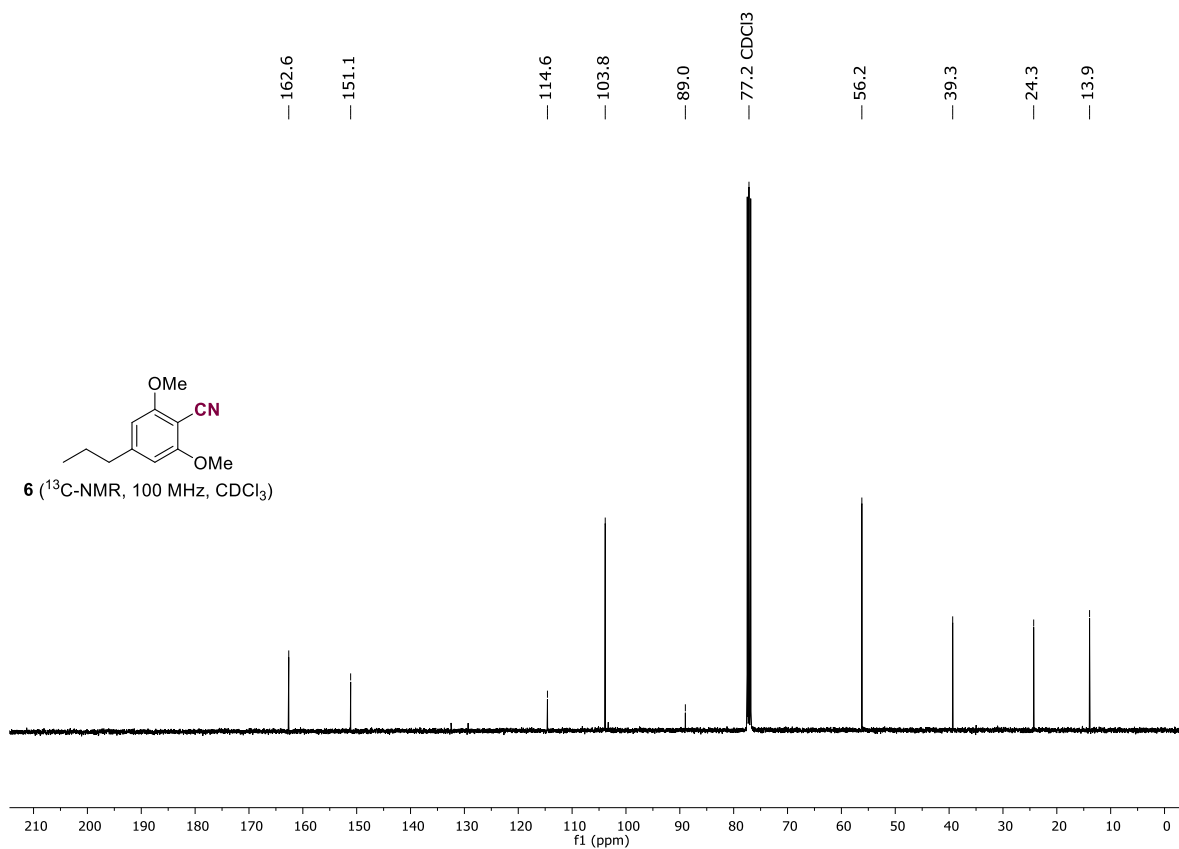
**2-methoxy-4-propylbenzonitrile from Willow sawdust (<sup>1</sup>H-NMR and <sup>13</sup>C-NMR)**



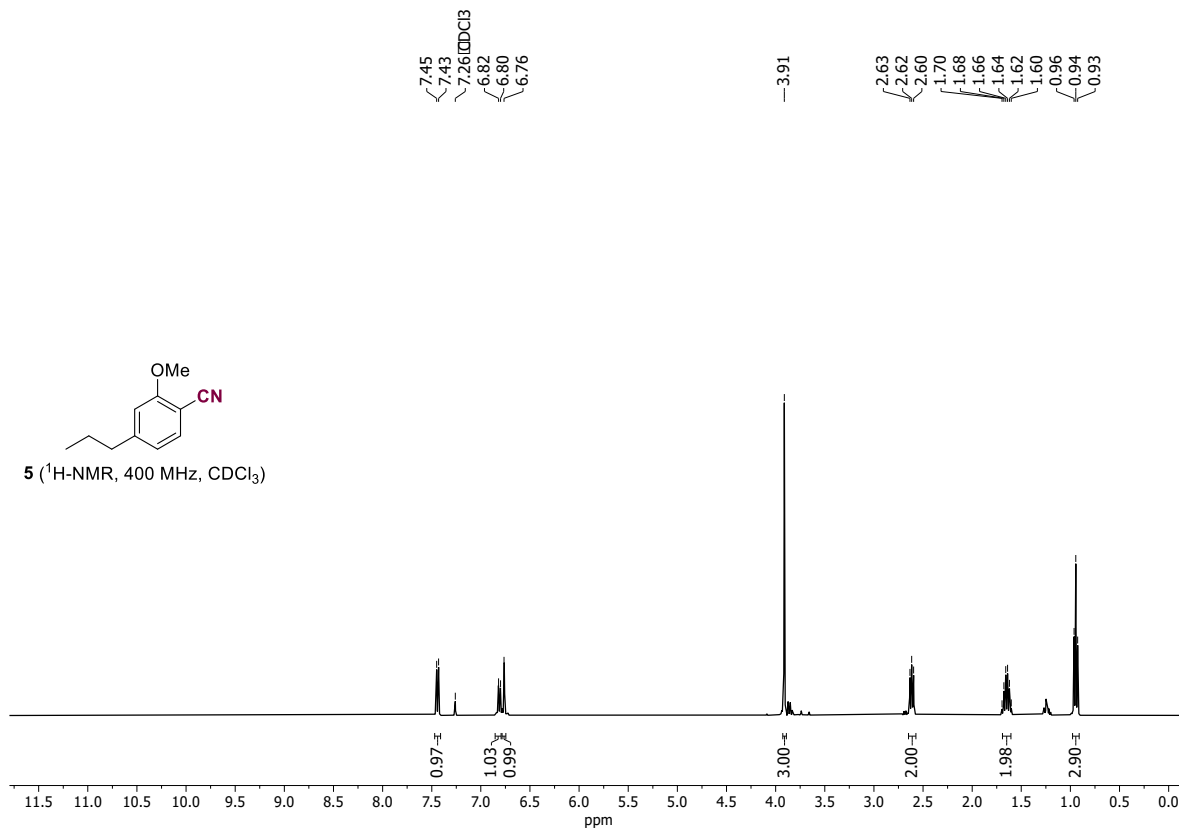


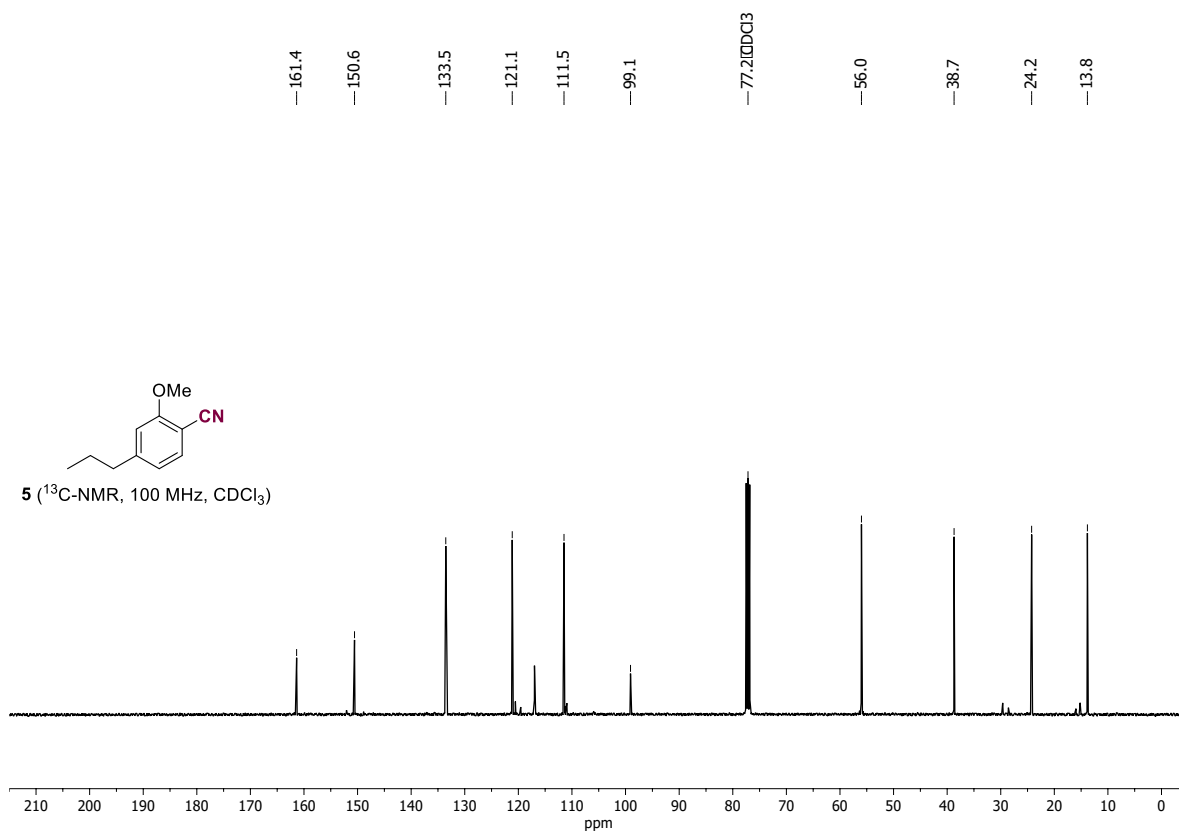
**2,6-dimethoxy-4-propylbenzonitrile from Willow sawdust (<sup>1</sup>H-NMR and <sup>13</sup>C-NMR)**



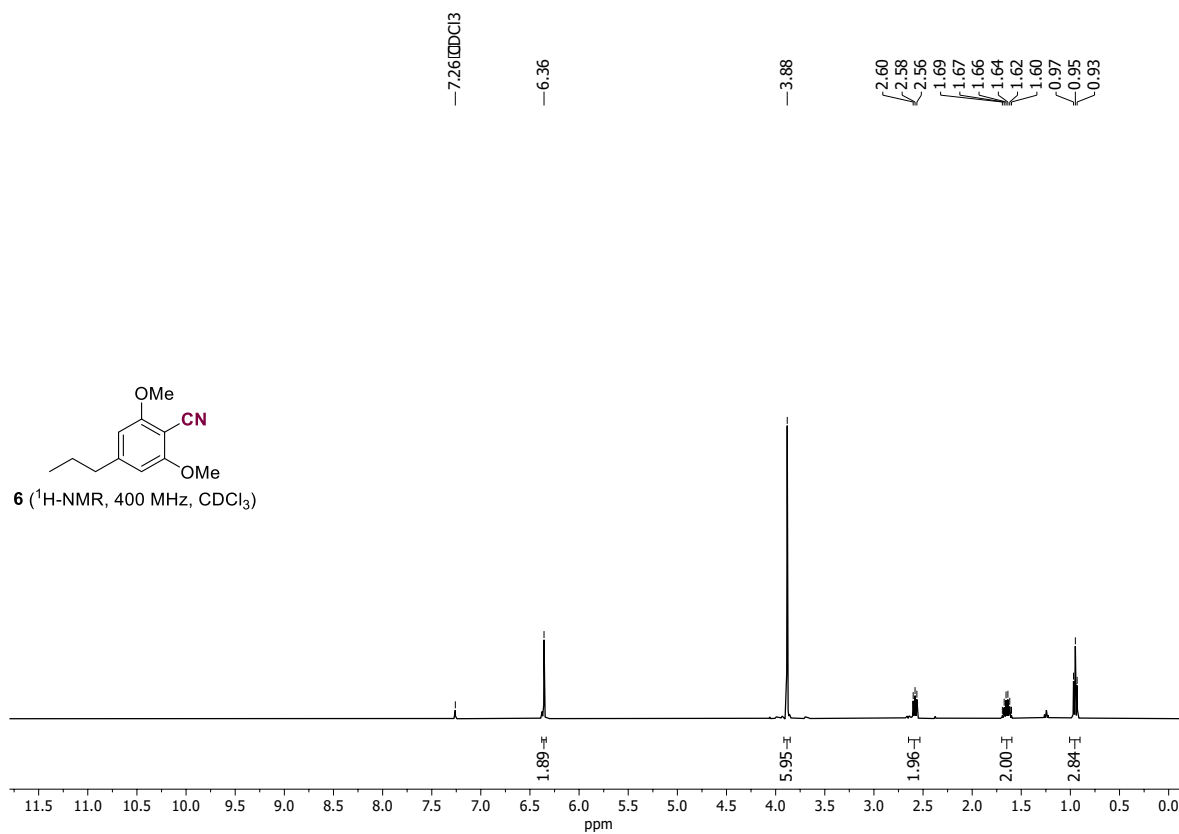


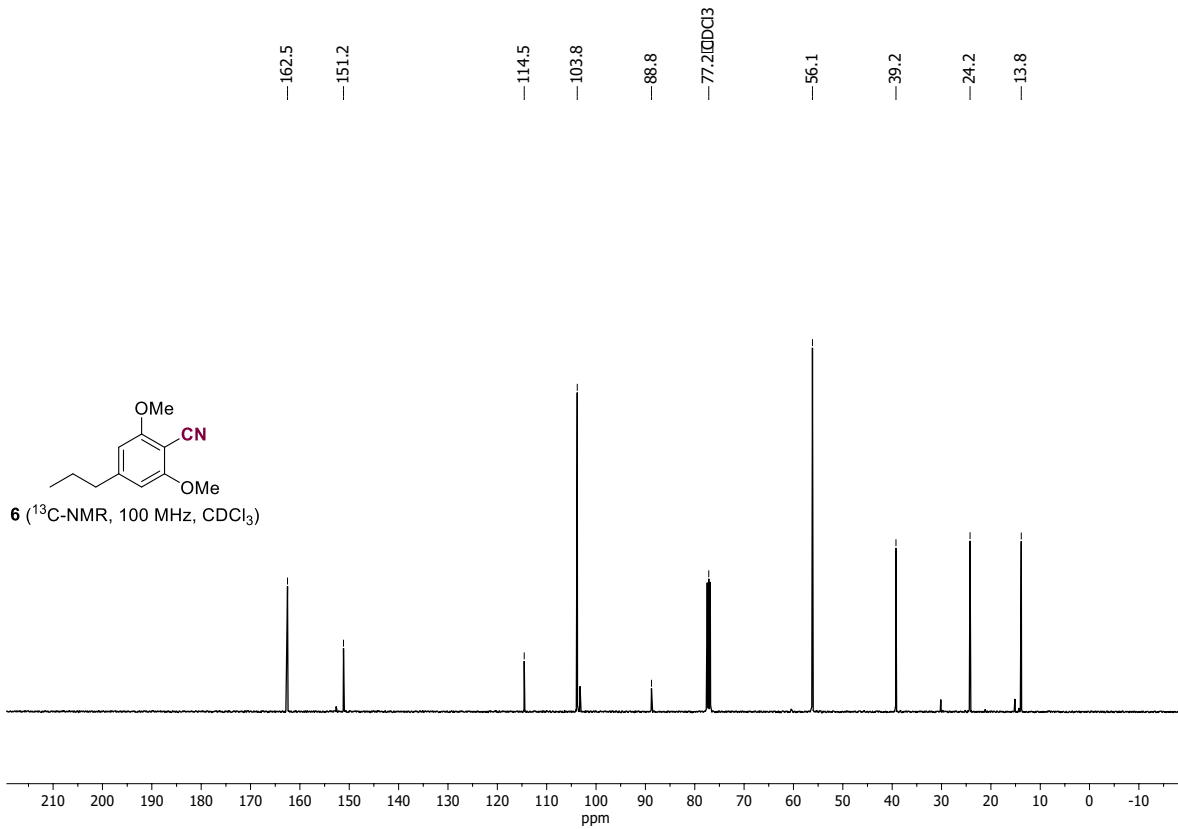
**2-methoxy-4-propylbenzonitrile from Oak sawdust (<sup>1</sup>H-NMR and <sup>13</sup>C-NMR)**



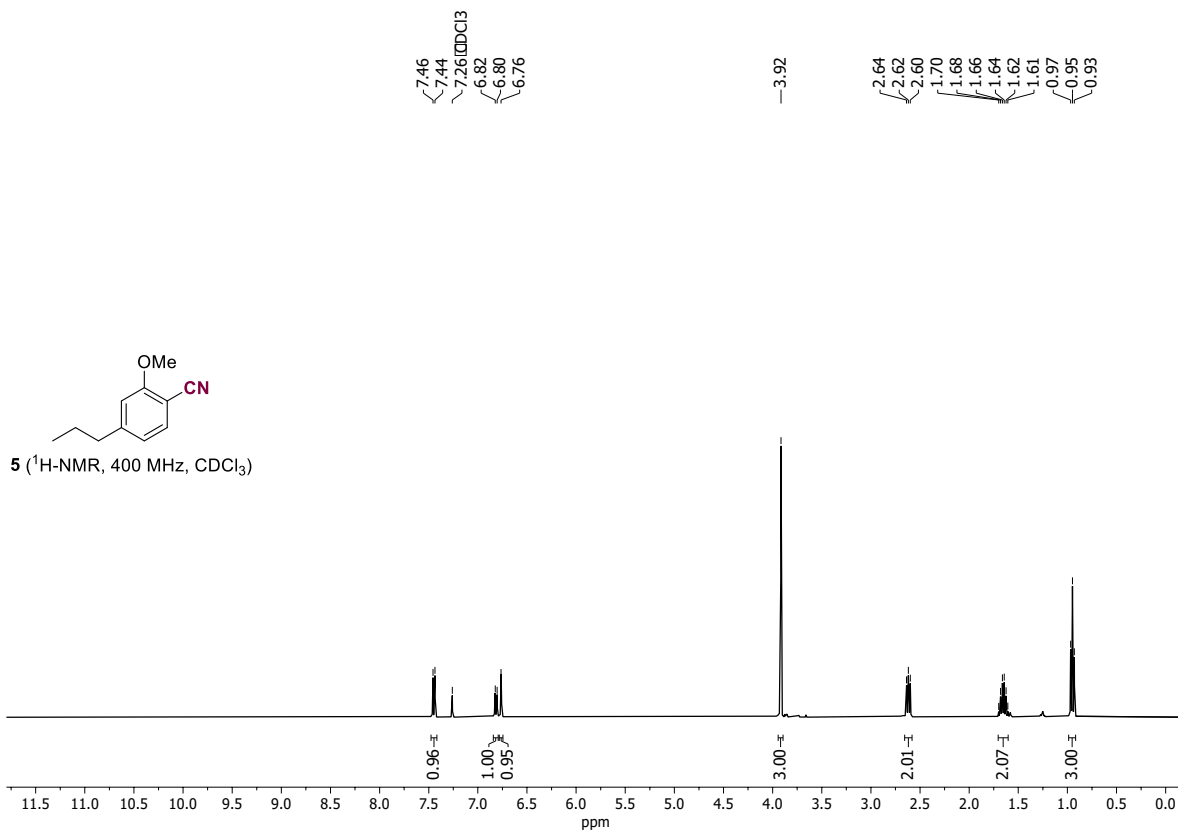


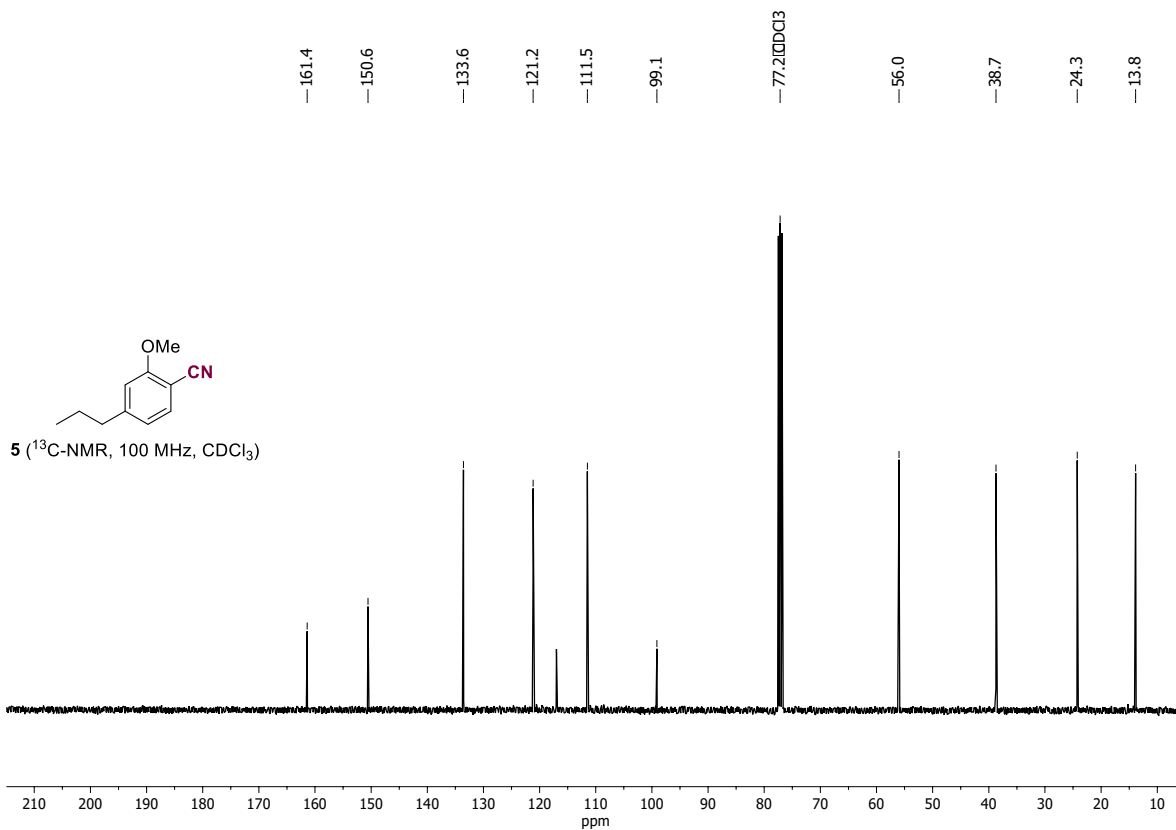
**2,6-dimethoxy-4-propylbenzonitrile from Oak sawdust ( $^1\text{H-NMR}$  and  $^{13}\text{C-NMR}$ )**



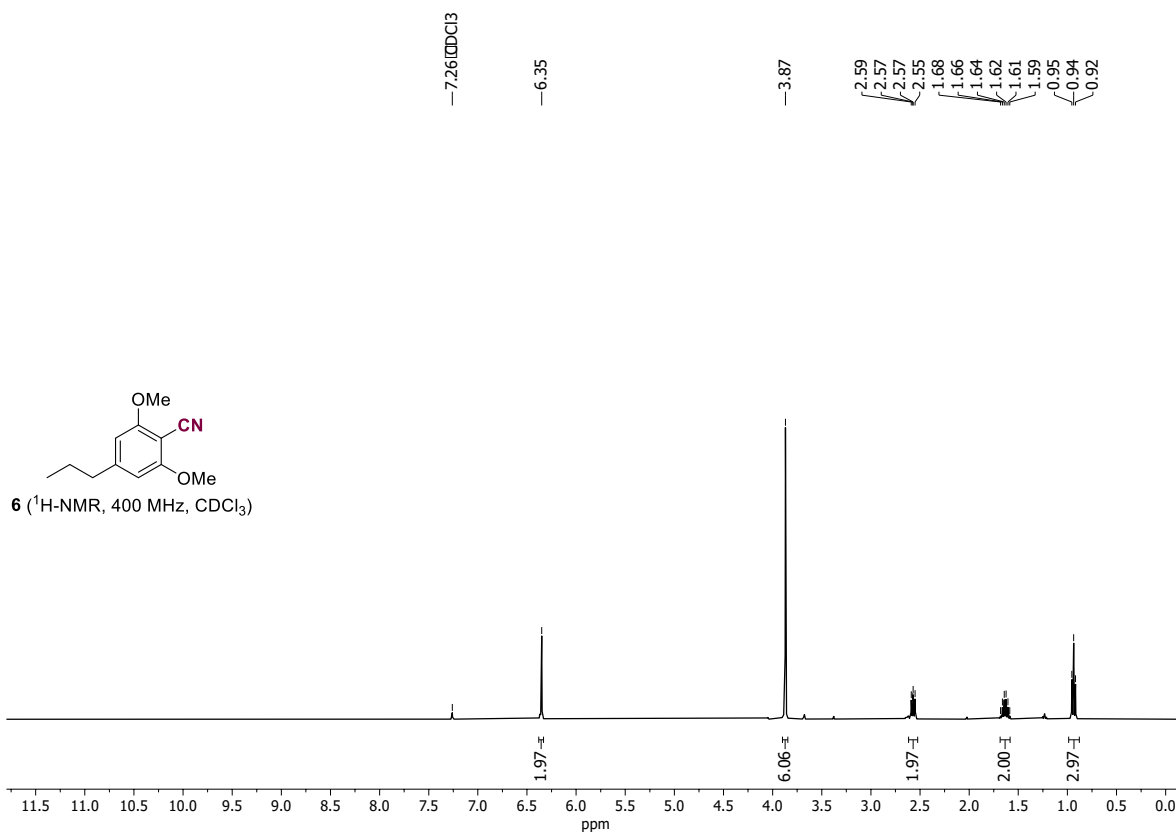


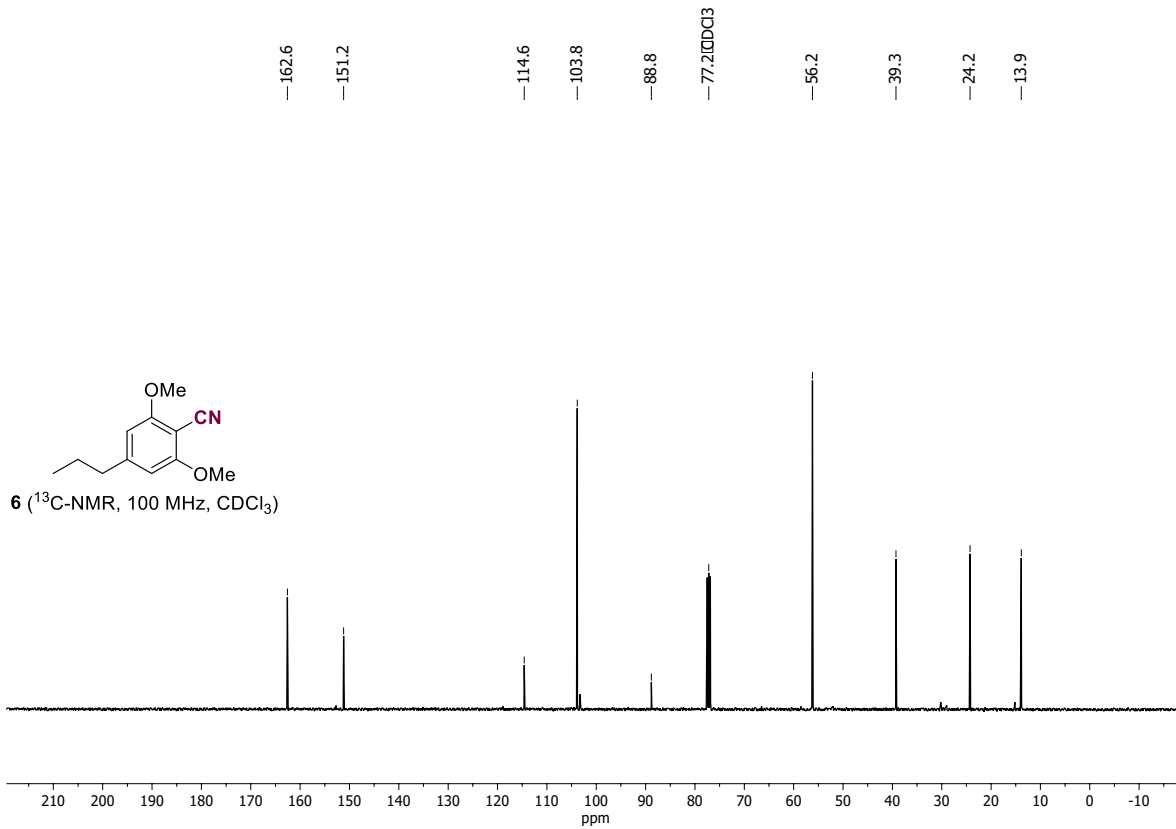
**2-methoxy-4-propylbenzonitrile from Hazel sawdust ( $^1\text{H-NMR}$  and  $^{13}\text{C-NMR}$ )**



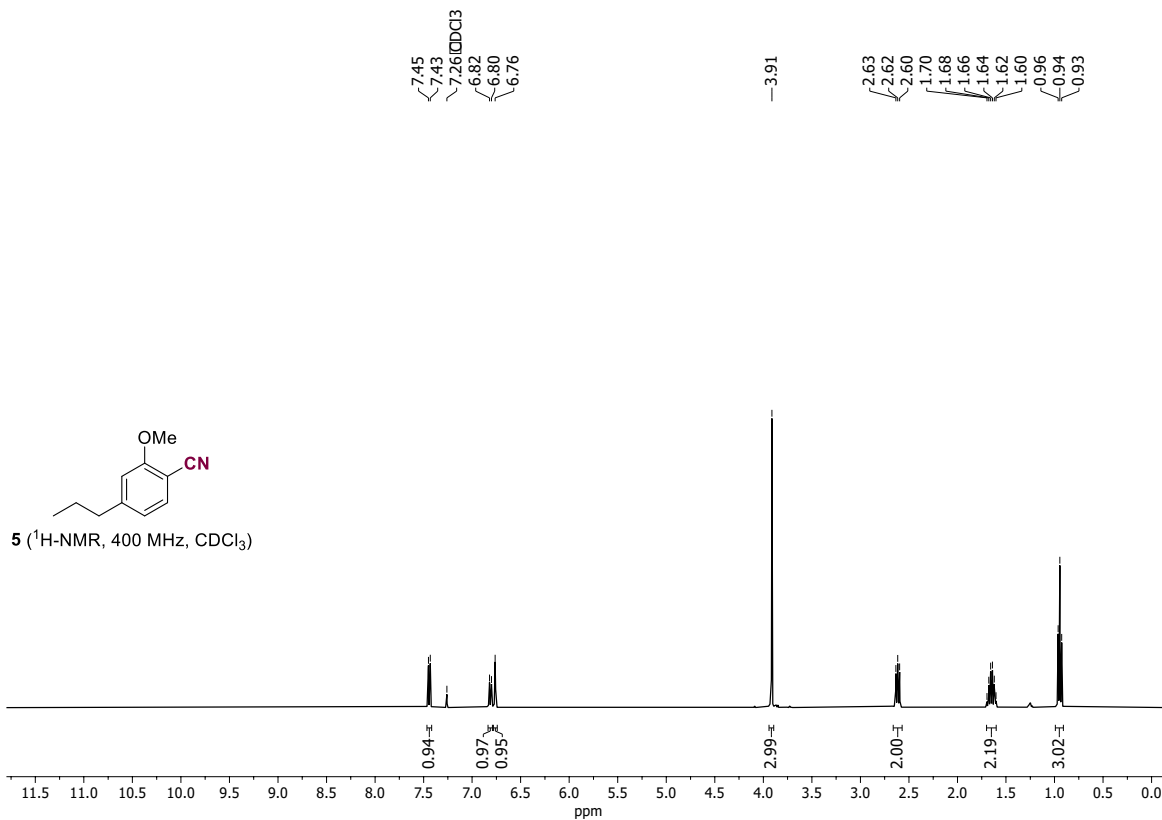


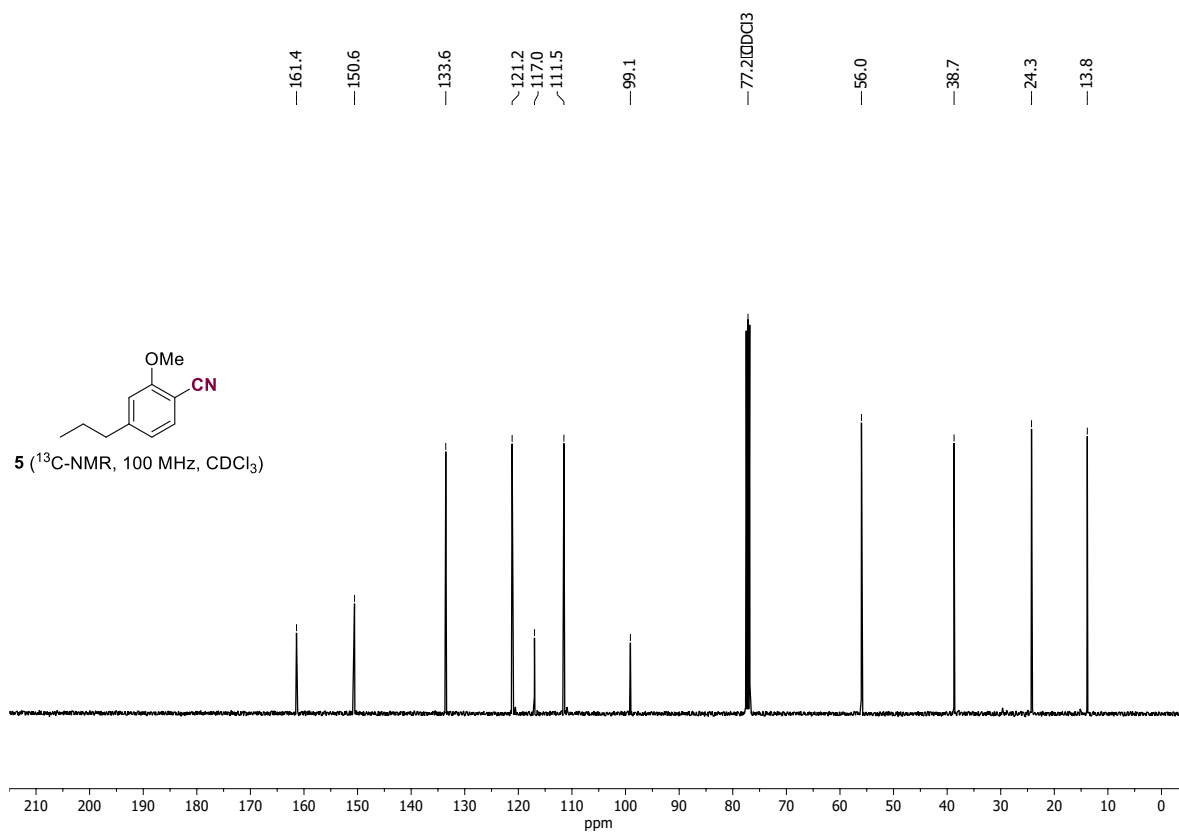
**2,6-dimethoxy-4-propylbenzonitrile from Hazel sawdust ( $^1\text{H-NMR}$  and  $^{13}\text{C-NMR}$ )**



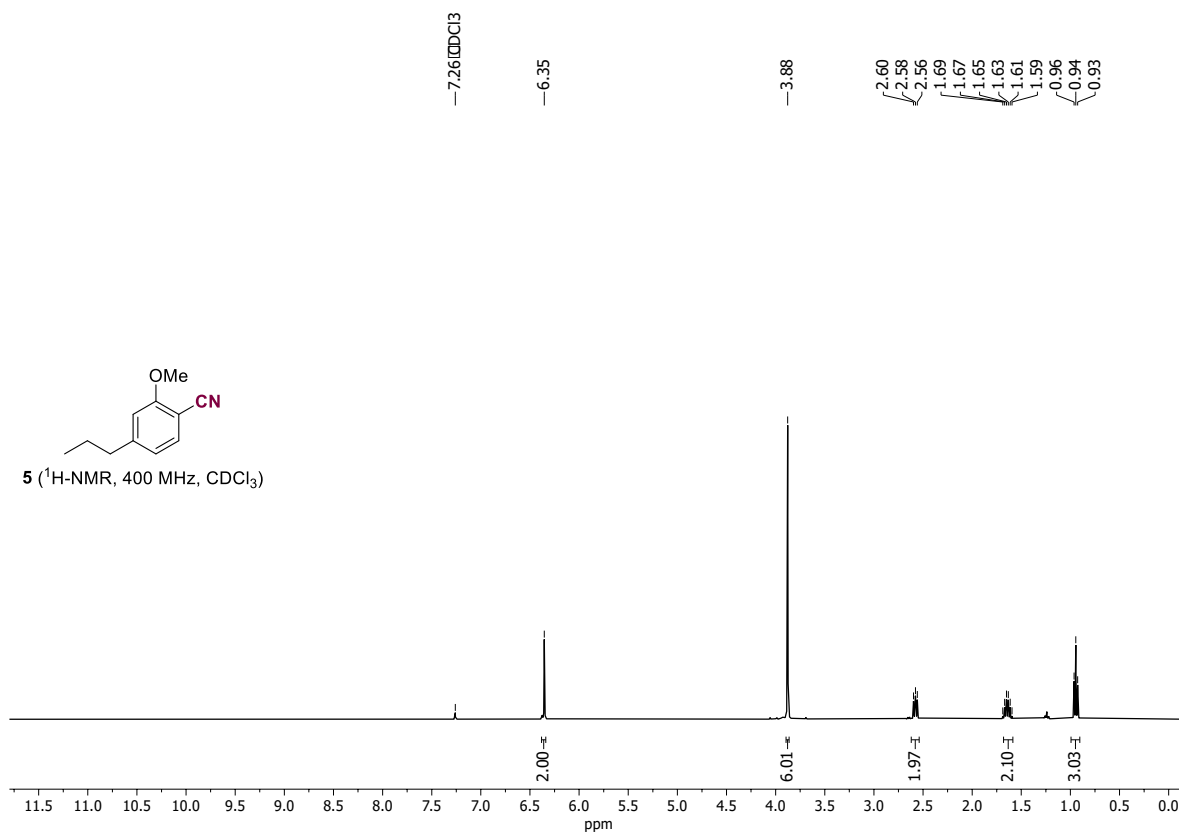


**2-methoxy-4-propylbenzonitrile from Sycamore Maple sawdust (<sup>1</sup>H-NMR and <sup>13</sup>C-NMR)**

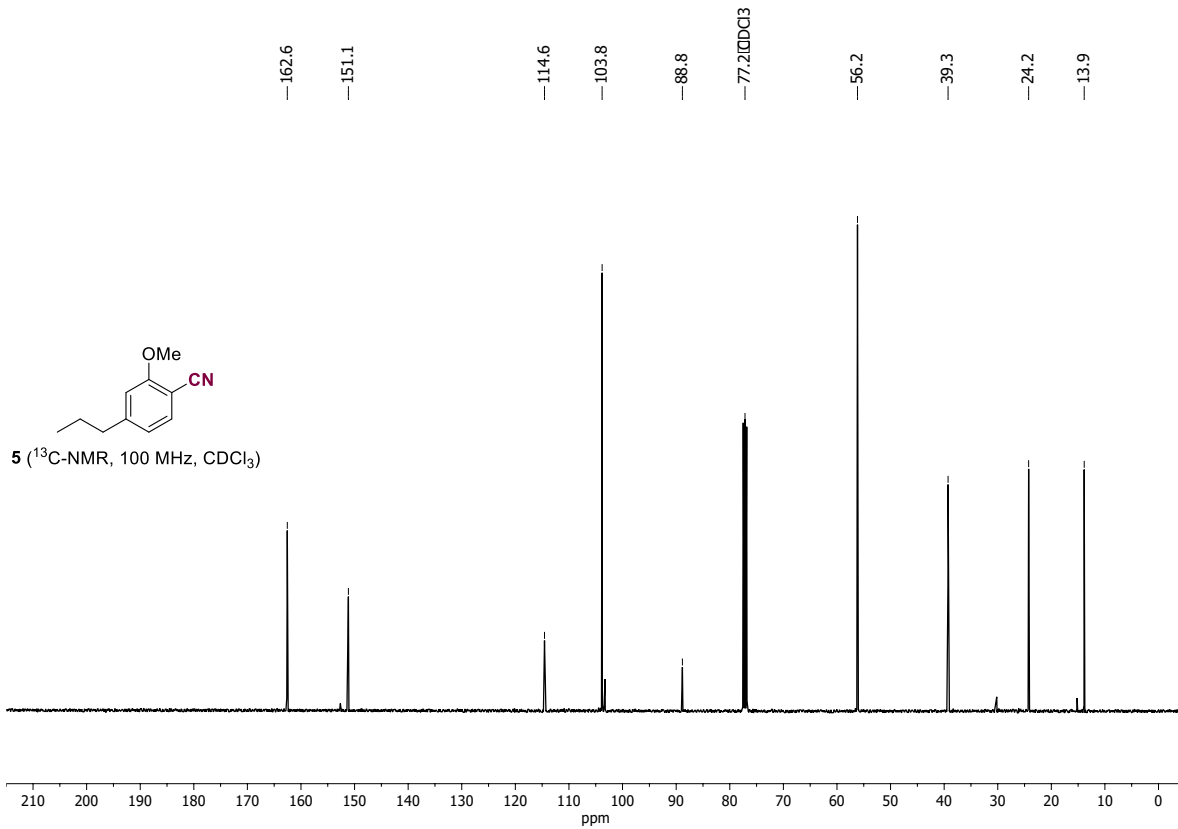




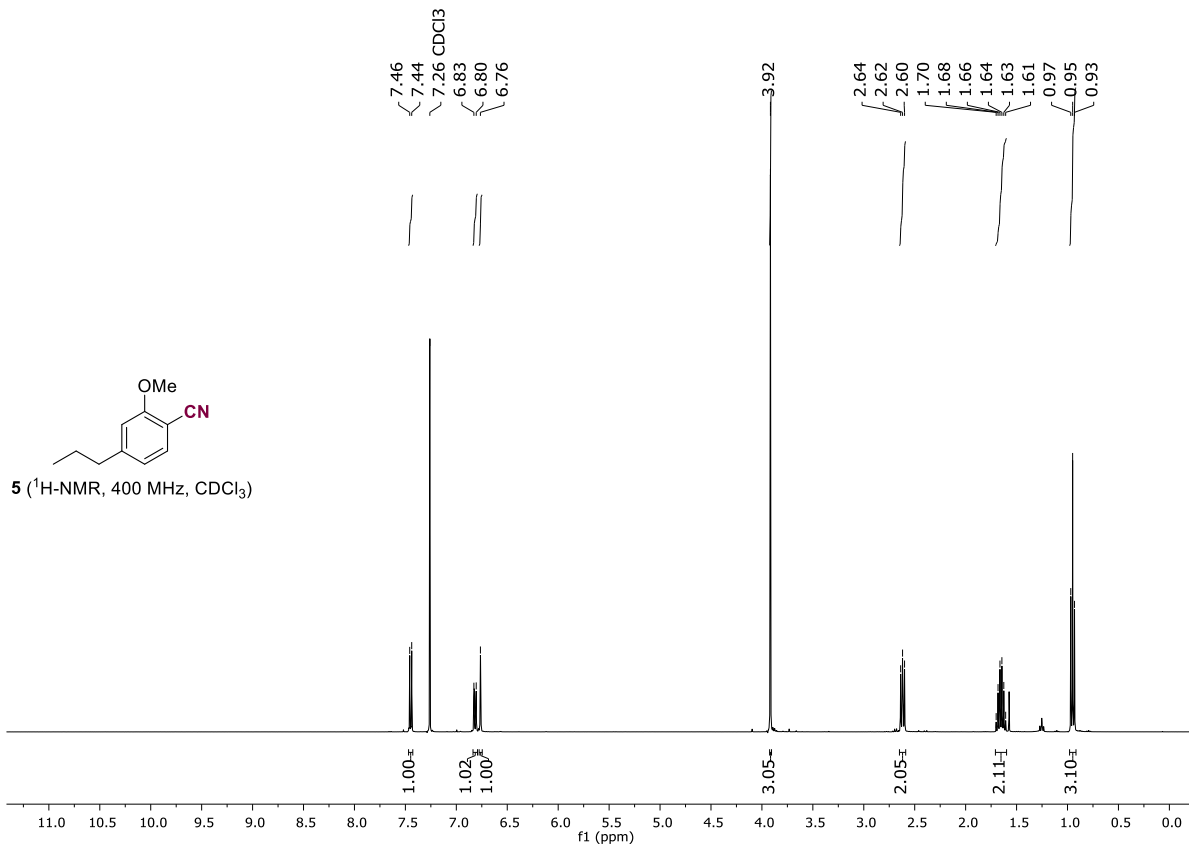
**2,6-dimethoxy-4-propylbenzonitrile from Sycamore Maple sawdust ( $^1\text{H-NMR}$  and  $^{13}\text{C-NMR}$ )**

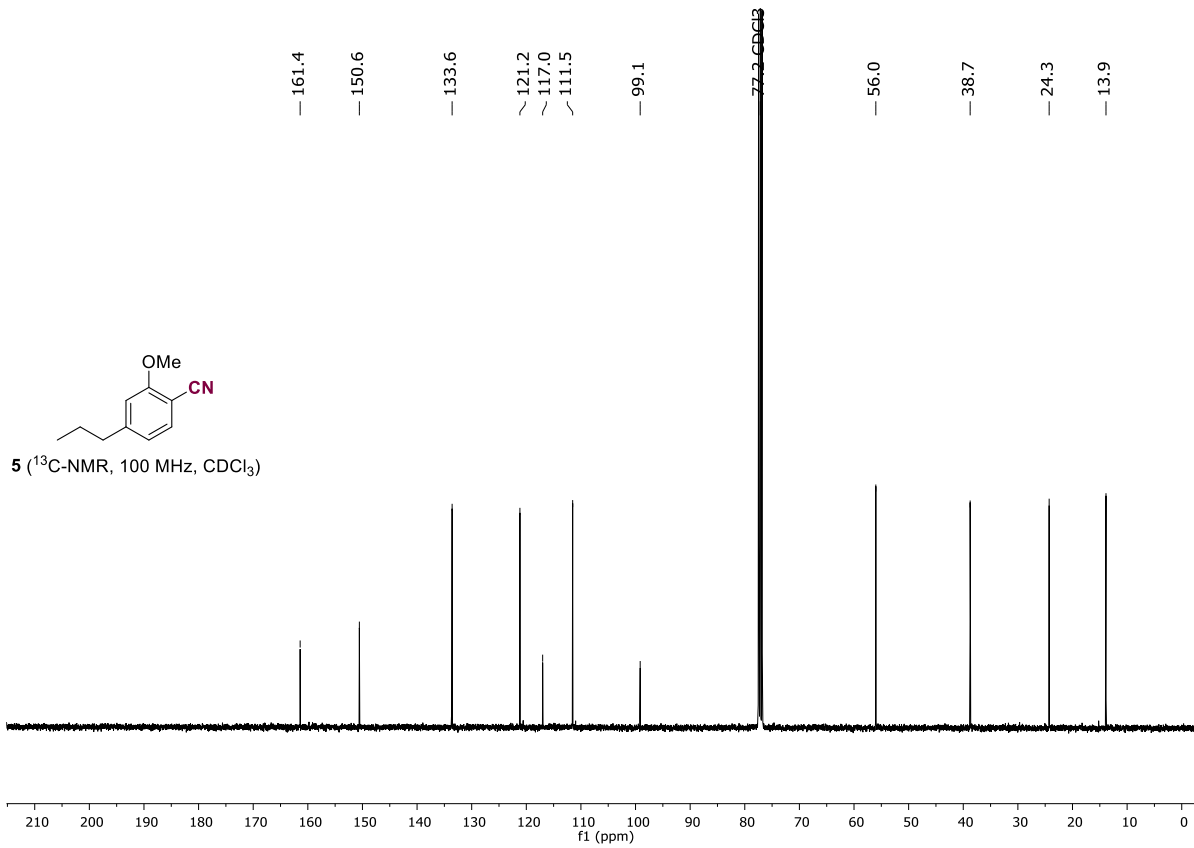




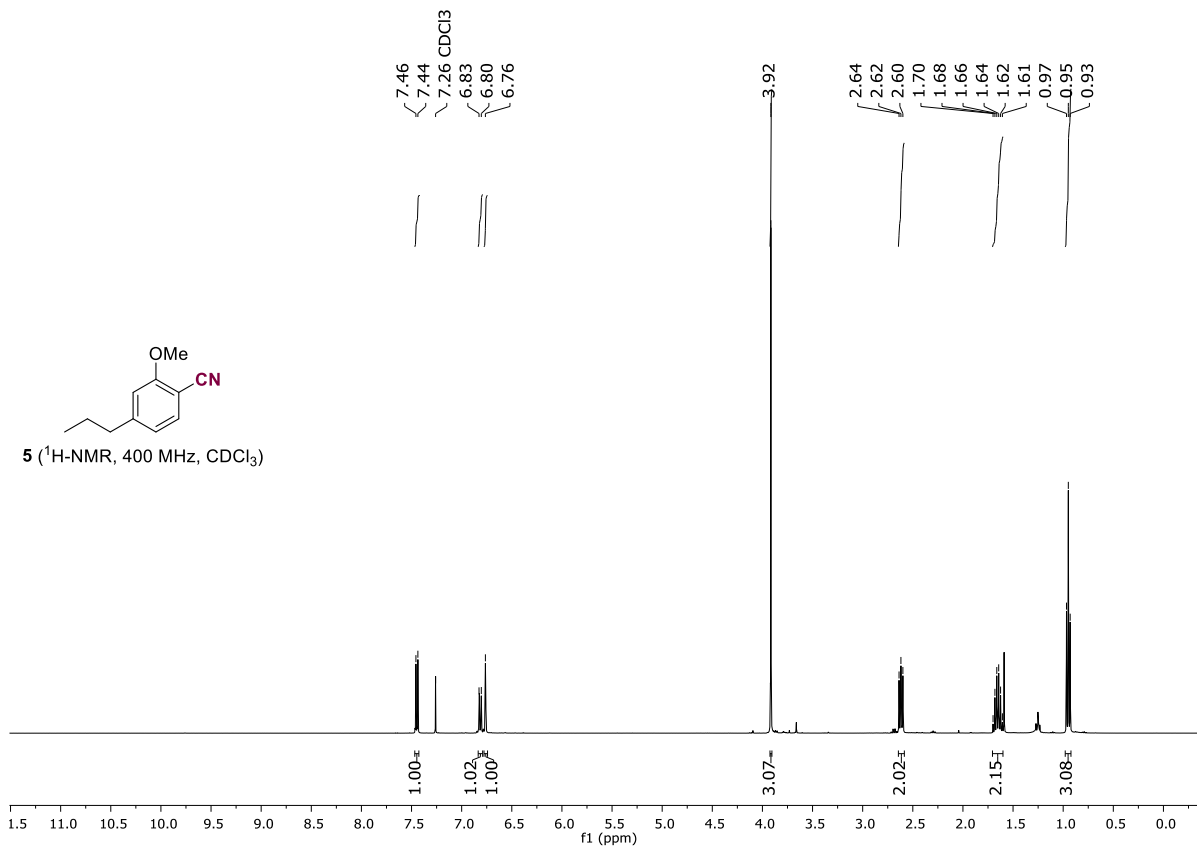


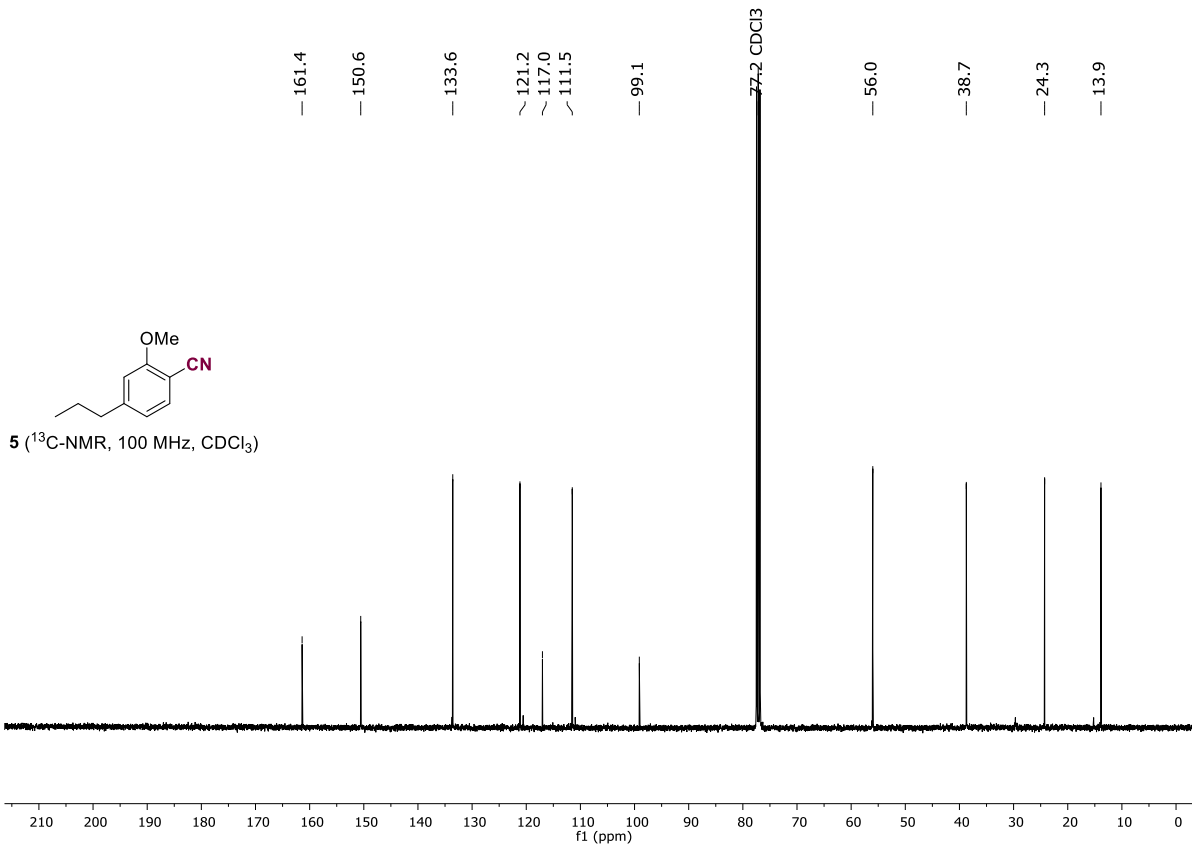
**2-methoxy-4-propylbenzonitrile from Norway Spruce sawdust ( $^1\text{H-NMR}$  and  $^{13}\text{C-NMR}$ )**



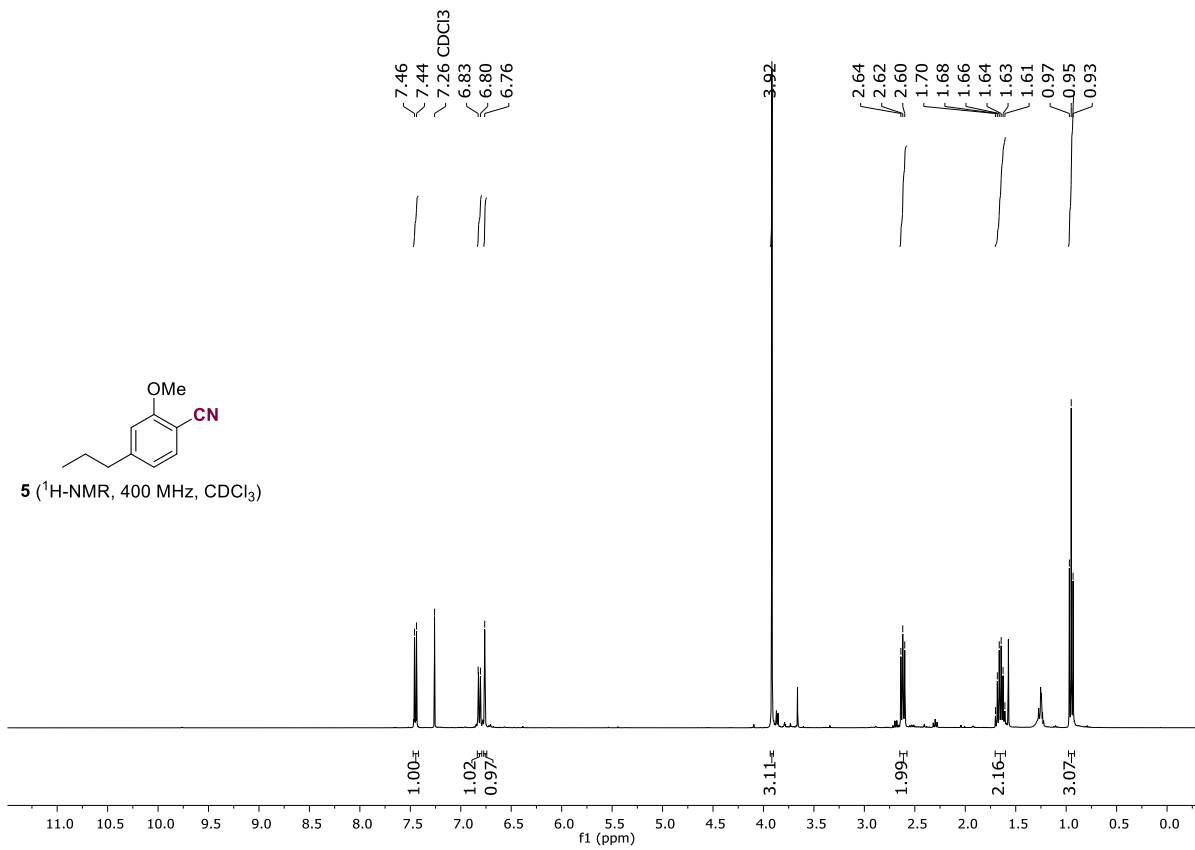


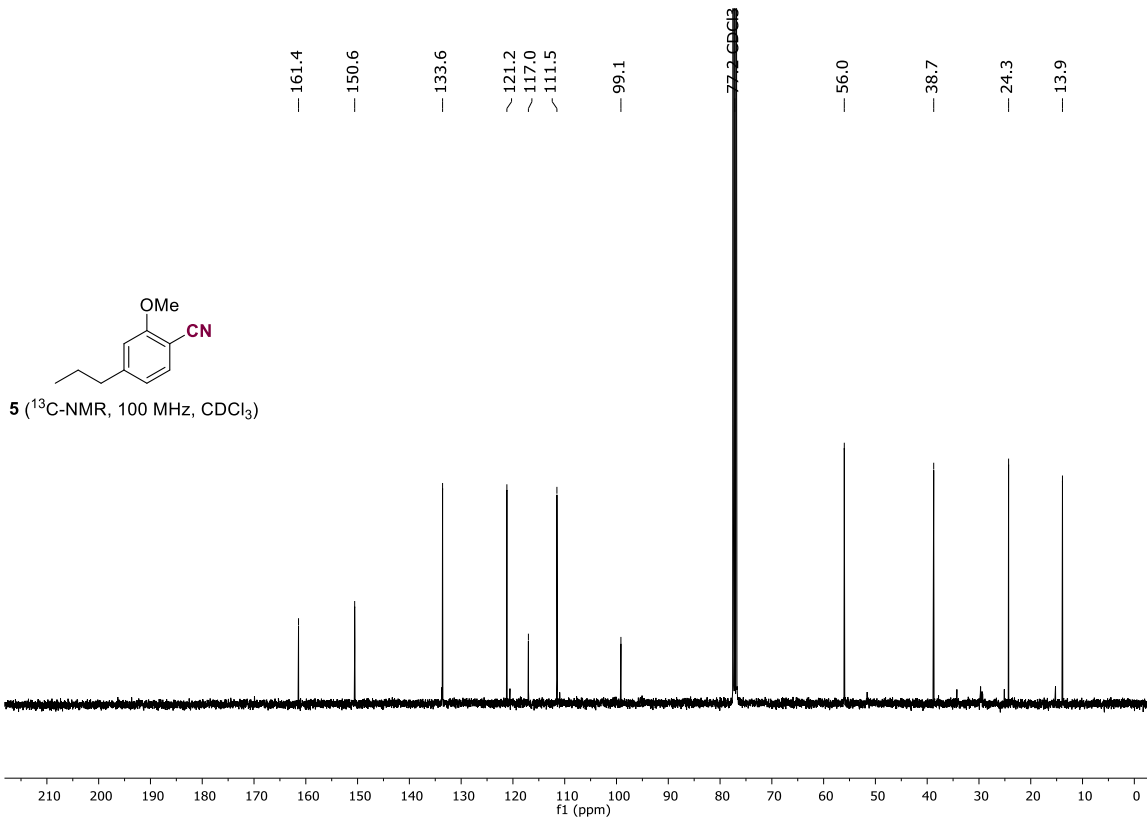
**2-methoxy-4-propylbenzonitrile from Grandis fir sawdust (<sup>1</sup>H-NMR and <sup>13</sup>C-NMR)**



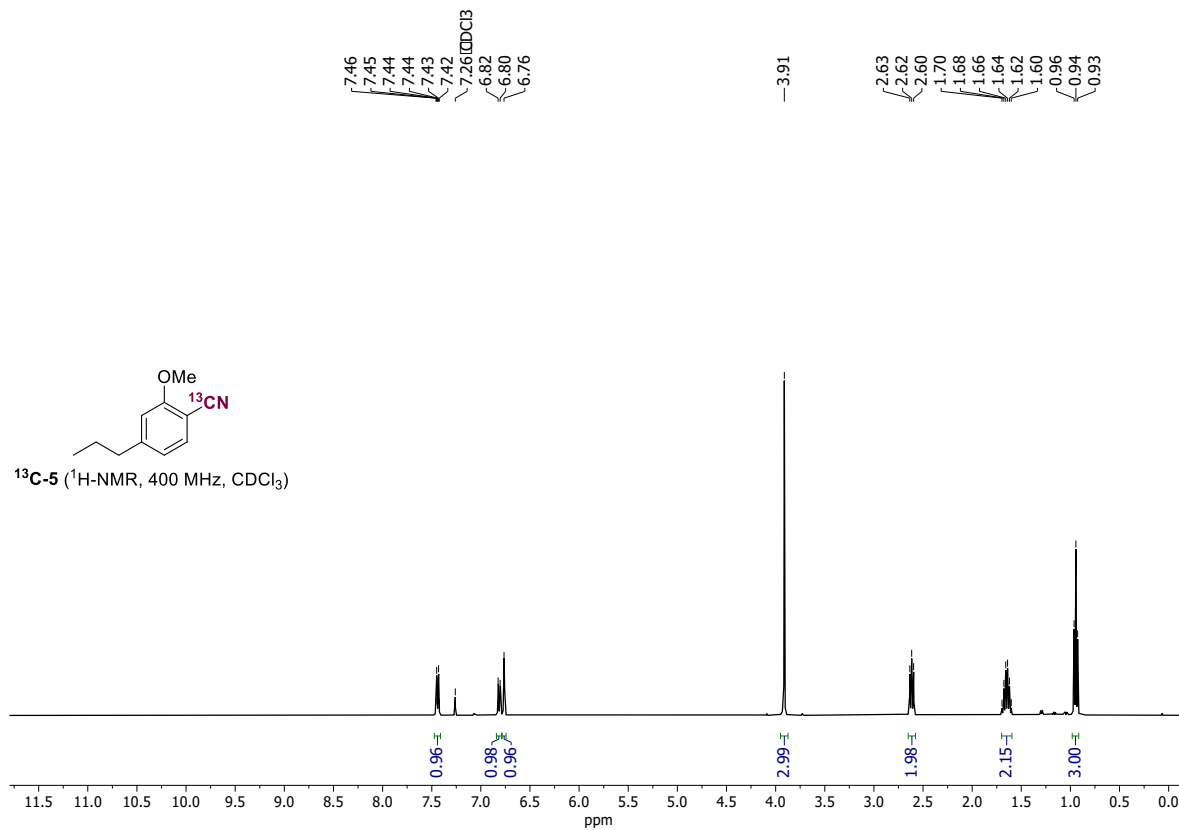


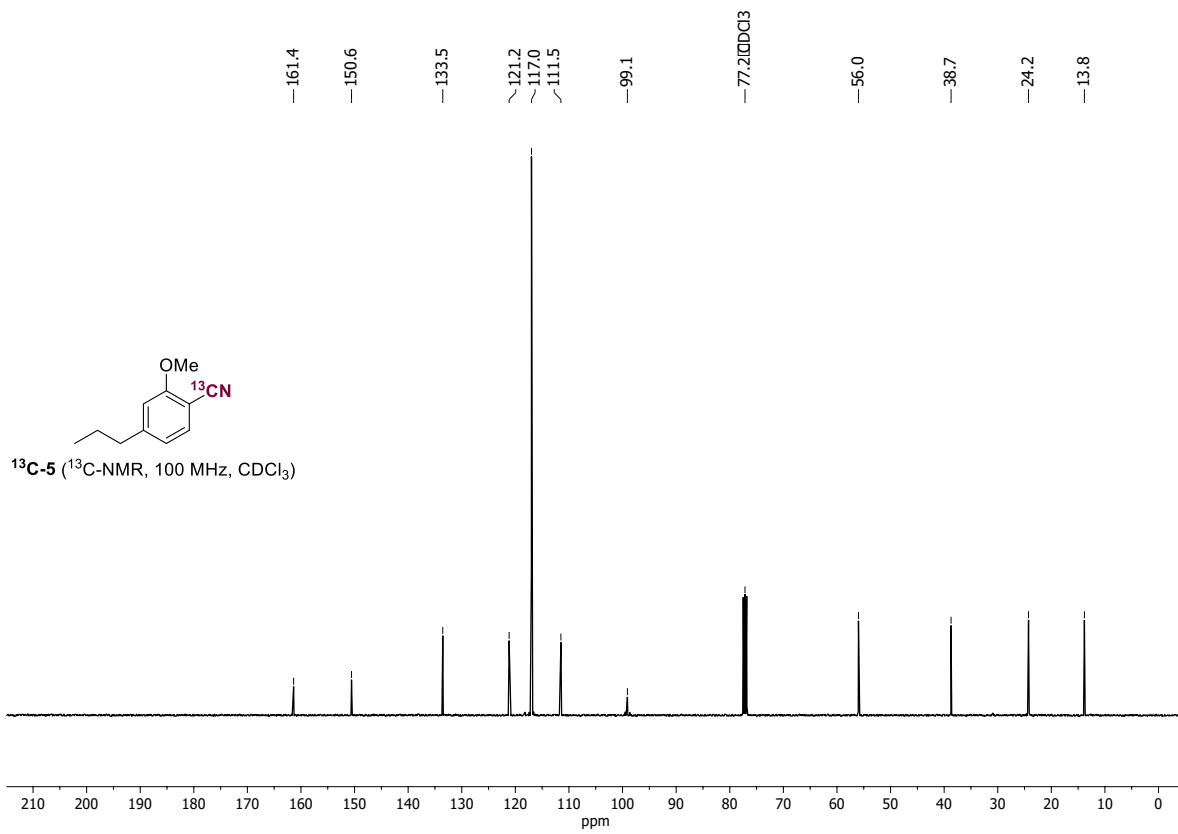
**2-methoxy-4-propylbenzonitrile from Noble fir sawdust (<sup>1</sup>H-NMR and <sup>13</sup>C-NMR)**



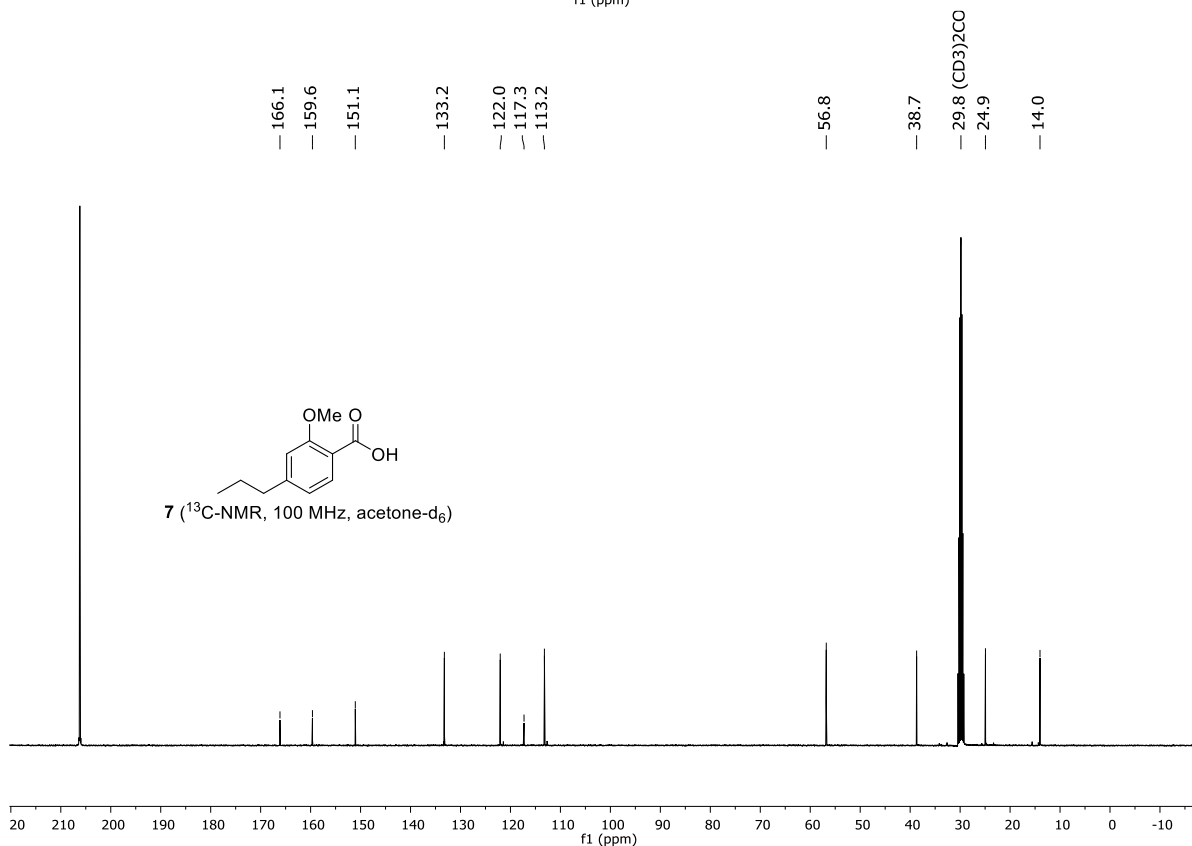
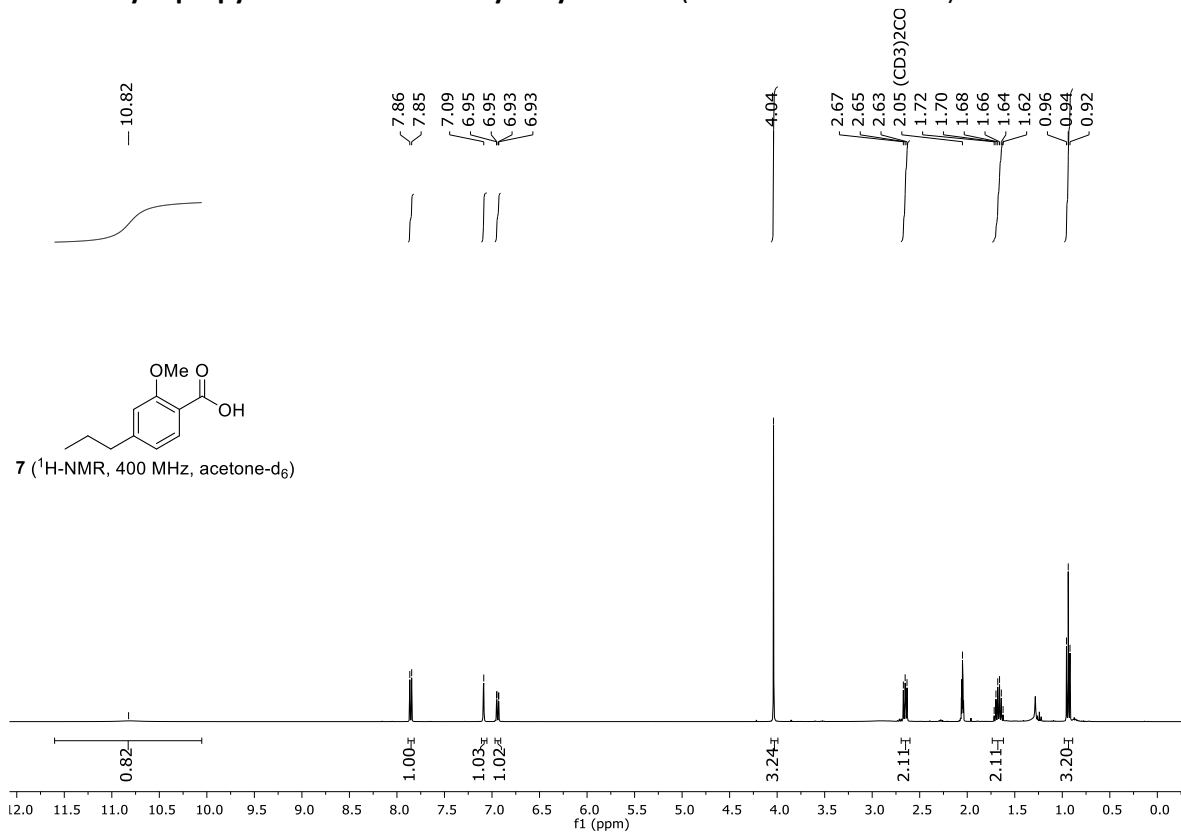


$^{13}\text{C}$ -2-methoxy-4-propylbenzonitrile ( $^1\text{H}$ -NMR and  $^{13}\text{C}$ -NMR)

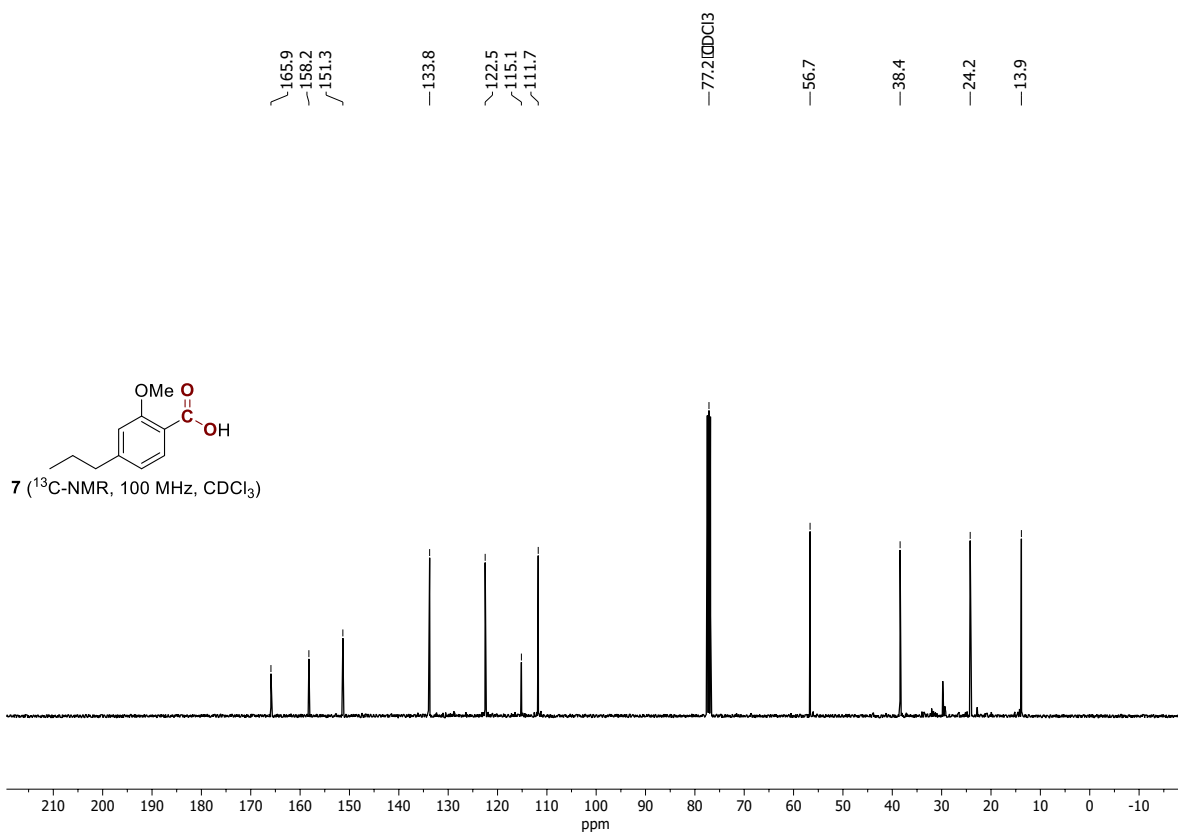
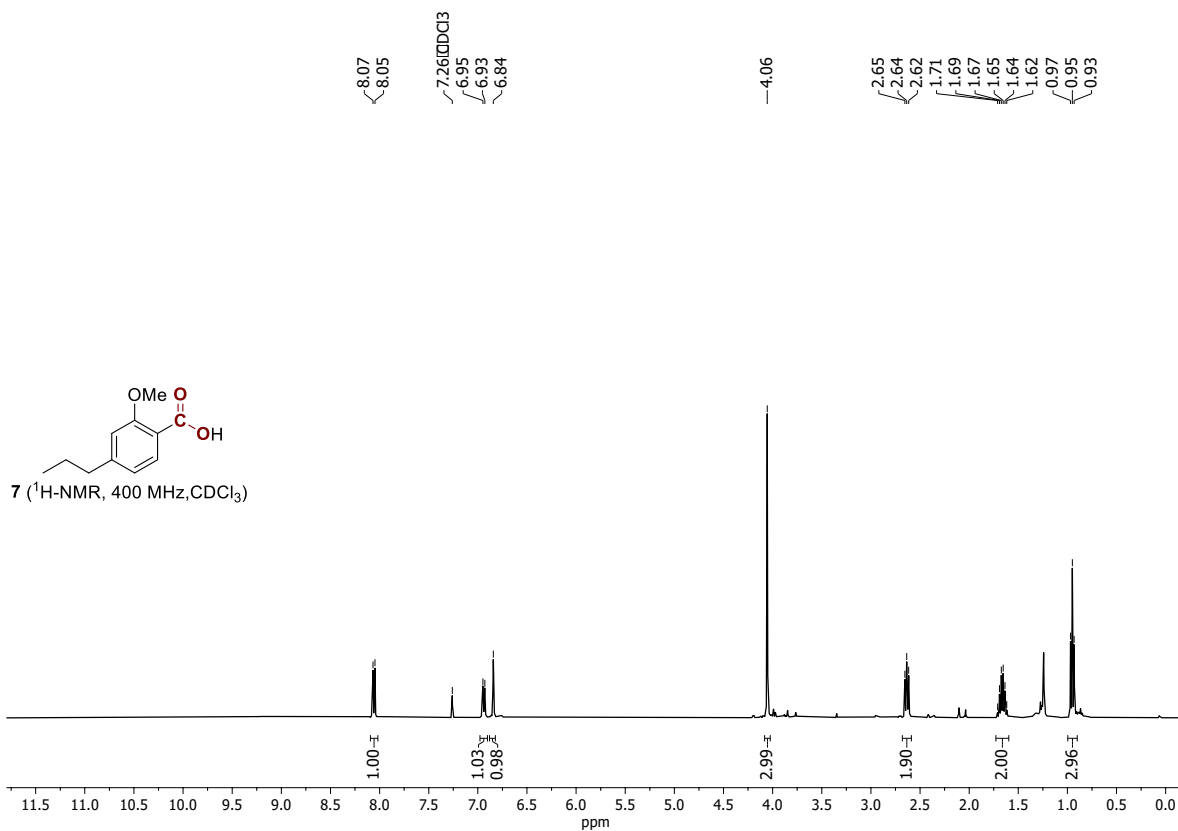




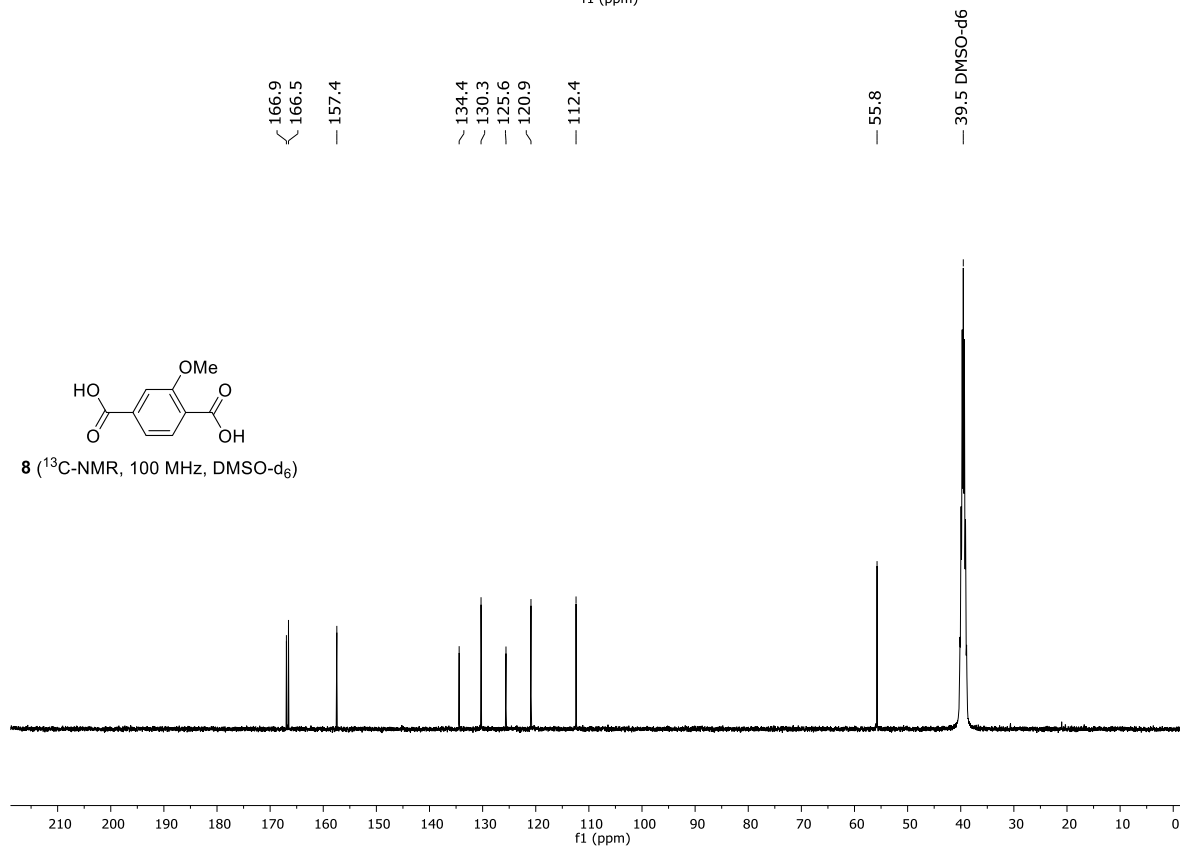
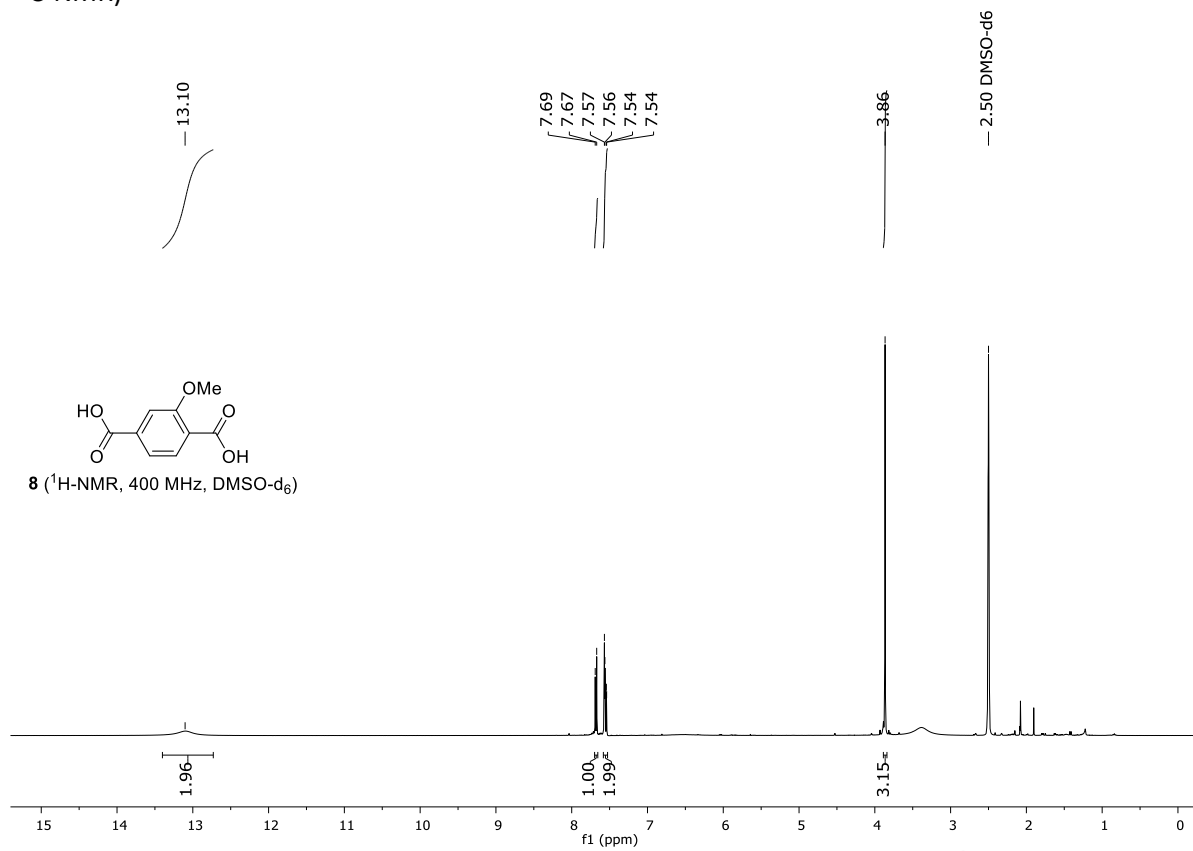
2-Methoxy-4-propylbenzoic acid from hydrolysis route (<sup>1</sup>H-NMR and <sup>13</sup>C-NMR)



2-Methoxy-4-propylbenzoic acid from carboxylation route with spruce sawdust ( $^1\text{H-NMR}$  and  $^{13}\text{C-NMR}$ )

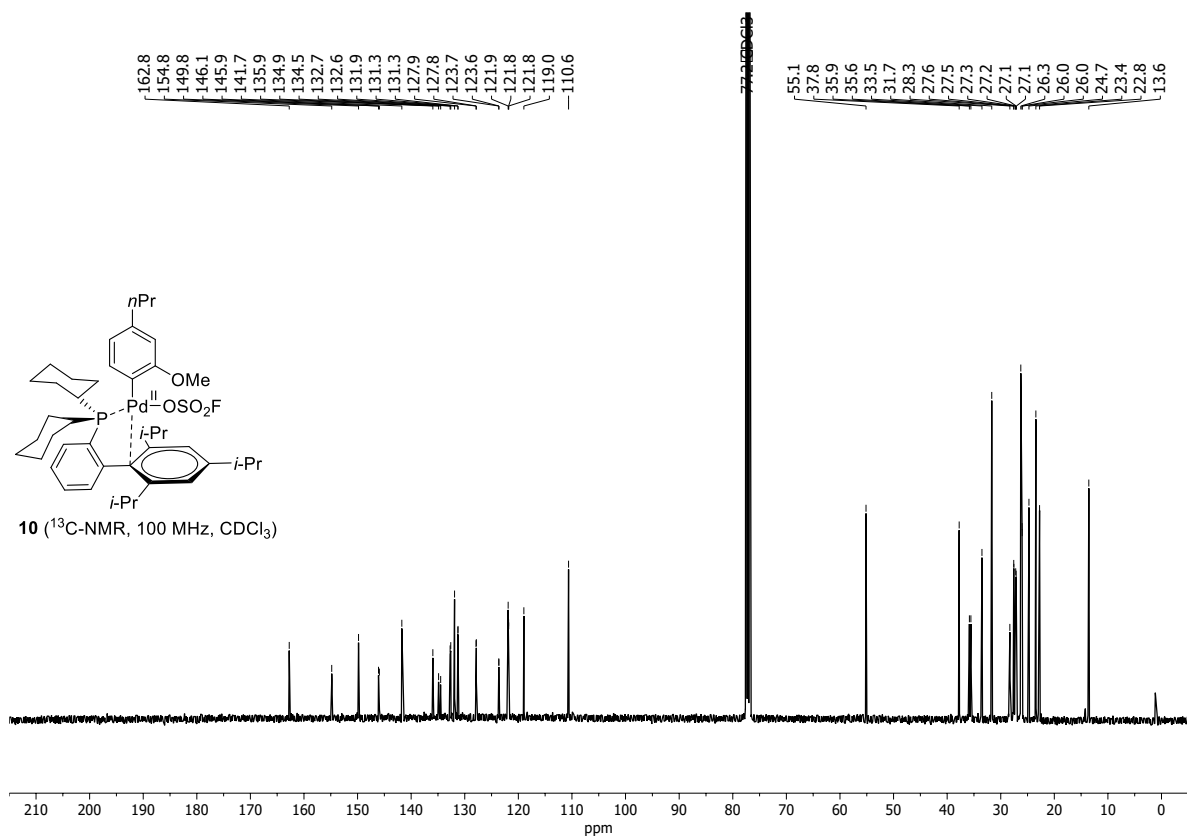
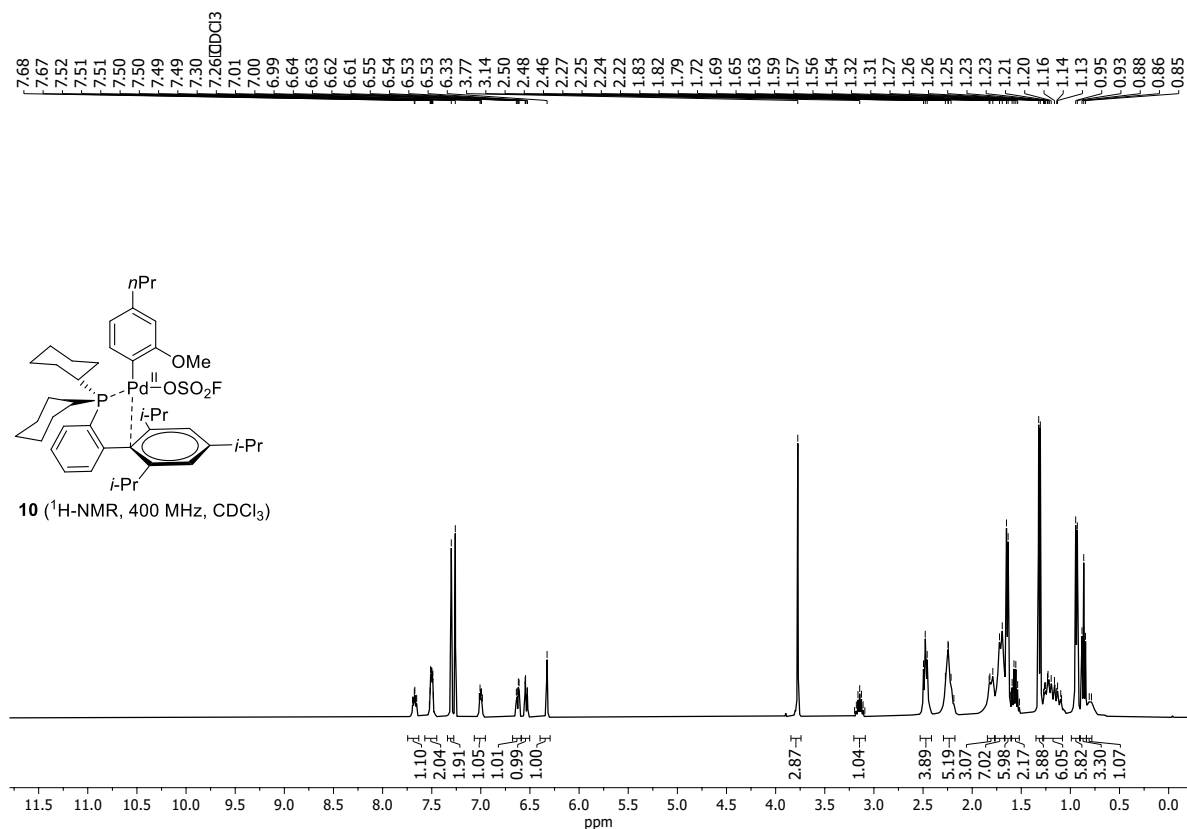


**2-Methoxyterephthalic acid from isolated 2-methoxy-4-propylbenzoic acid from sawdusts (<sup>1</sup>H-NMR and <sup>13</sup>C-NMR)**

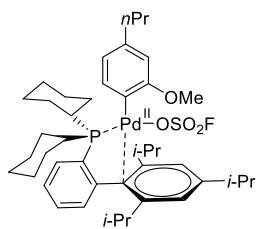




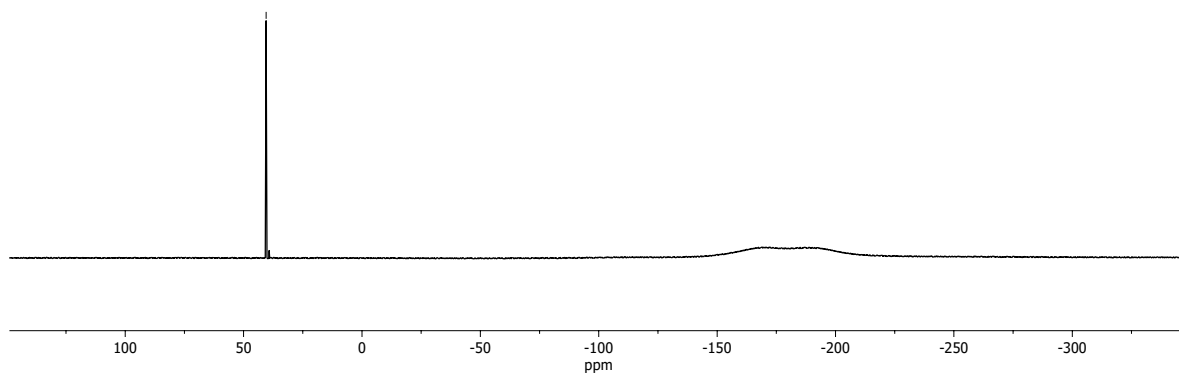
Oxidative addition complex **10** ( $^1\text{H-NMR}$ ,  $^{13}\text{C-NMR}$ ,  $^{19}\text{F-NMR}$  and  $^{31}\text{P-NMR}$ )



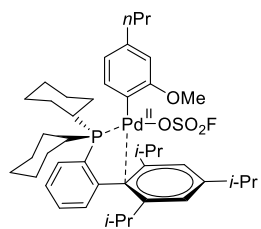
-40.5



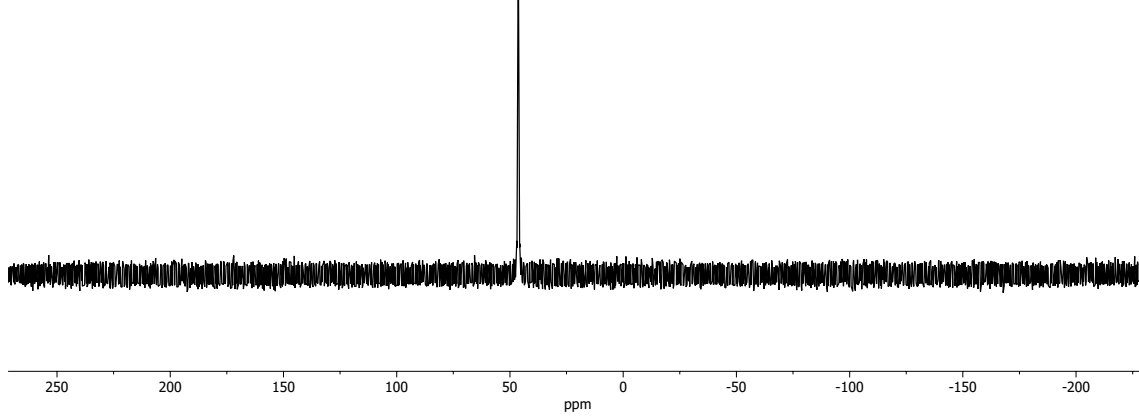
**10** (<sup>19</sup>F-NMR, 367 MHz, CDCl<sub>3</sub>)



-46.3



**10** (<sup>31</sup>P-NMR, 167 MHz, CDCl<sub>3</sub>)



Oxidative addition complex **11** ( $^1\text{H-NMR}$ ,  $^{13}\text{C-NMR}$ ,  $^{19}\text{F-NMR}$  and  $^{31}\text{P-NMR}$ )

